

Alma Mater Studiorum - Università di Bologna

**DOTTORATO DI RICERCA in
Ingegneria Chimica dell'Ambiente e della Sicurezza**

Ciclo XXVIII

Settore Concorsuale di afferenza: 09/D3 – Impianti e processi industriali chimici

Settore Scientifico disciplinare: ING-IND/25 – Impianti Chimici

**ANALISI DI PROCESSI DI VALORIZZAZIONE ENERGETICA DI
BIOMASSE**

-

ANALYSIS OF BIOMASS TO ENERGY PROCESSES

Presentata da: LUCIA BASILE

**Coordinatore Dottorato
Prof.ssa Ing. Serena Bandini**

**Relatore
Prof. Ing. Valerio Cozzani**

Esame finale anno 2016

TABLE OF CONTENTS

I. Introduction.....	1
1 World energy scenario and sustainable energy future.....	1
2 Energy from biomass.....	2
3 Biomass.....	3
3.1 Biomass Properties.....	3
3.2 Biomass Composition: Macrocomponents.....	7
4 Biomass Conversion Technology.....	11
4.1 Combustion.....	11
4.2 Gasification.....	12
4.3 Fermentation.....	12
4.4 Anaerobic Digestion.....	13
4.5 Pyrolysis.....	13
4.6 Liquefaction.....	14
5 The Bio-Refinery Concept.....	14
6 Outline of the Present Study.....	16
II. Approaching the biomass pyrolysis process.....	18
1 Biomass Pyrolysis.....	18
1.1 Principles.....	18
1.2 Mechanism and Kinetics.....	19

1.3	Type of Reactor.....	21
2	Yields and Energy Distribution in Pyrolysis Process.....	26
2.1	Influence of Process Conditions	26
2.2	Pyrolysis Products.....	29
3	Heat Transfer.....	30
3.1	Heat of Reaction.....	31
3.2	Energy Balances in the Pyrolysis Process	33
III.	Experimental Deviad Procedures.....	35
1	Thermogravimetric Analyzer.....	35
1.1	Instrument Characteristics	35
1.2	Instrument calibration.....	36
1.3	Experimental Procedures.....	36
2	Differential Scanning Calorimeter at atmospheric pressure.....	37
2.1	Instrument Characteristics	37
2.2	Instrument calibration.....	39
2.3	Experimental Procedures.....	40
3	Differential Scanning Calorimeter In pressure	41
3.1	Instrument Characteristics	41
3.2	Instrument calibration.....	42
3.3	Setup Design and Installation	42
3.4	Experimental Procedures.....	43
4	Method for the assessment of heat of pyrolysis.....	43
5	Fixed-bed reactor	45
6	Analytical equipment	47
6.1	Elemental analyzer (EA)	47
6.2	Karl Fisher (KF).....	47
6.3	Micro Carbon Test Residue (MCRT).....	47
6.4	Molecular weight distribution (GPC).....	47

6.5	Viscometer	48
6.6	Gas chromatograph – Mass spectrometer (GC-MS)	48
6.7	Micro – Gas chromatograph (GC)	48
7	Materials for Calorimetric Analysis	48
8	Materials for Liquefaction Experiment	50
IV.	Overall heat demand of the biomass pyrolysis process.....	52
1	Biomass characterization by thermogravimetric analysis	52
2	Weight loss analysis	55
2.1	Building blocks decomposition.....	55
2.2	Initial sample weight influence	55
3	Heat transport phenomena	57
3.1	Characteristic time of thermal diffusion	57
3.2	Sample thickness influence	58
4	Heat demand analysis	60
4.1	Pressure influence	61
4.2	Phenomenological Model.....	64
4.3	Initial sample weight influence	67
4.4	Mass transfer limitations influence.....	70
4.5	Purge gas flow rate influence.....	74
5	Empirical Model Correlation for Heat of Reaction with Char Yield.....	75
5.1	Apparent parallel reaction process	76
5.2	Apparent consecutive reaction process.....	77
5.3	Validation of the model with experimental data	80
V.	Macro-components summative approach for the overall heat demand	83
1	Biomass Composition: Macrocomponents	83
2	Weight Loss Analysis	84
3	Heat Demand Analysis	86

4	Influence of pressure on the heat of pyrolysis of biomass macrocomponents.....	90
5	Comparison between biomass and biomass macrocomponents.....	95
6	Analysis of mixture of biomass macrocomponents.....	98
7	Additive correlation for biomass heat demand.....	100
VI.	Liquefaction of lignin in its produced oil: process parameters screening.	102
1	Lignin Liquefaction: State of Art.....	102
2	Lignin Liquefaction experiments and validation	103
2.1	Influence of temperature and residence time	106
2.2	Influence of Lignin Loading	107
3	Lignin Liquefaction in Recycled Oil.....	110
4	Upgrading of Lignin Liquefaction Oil: Hydrotreatment	112
VII.	Conclusions	113
	References	116

CHAPTER I

INTRODUCTION

1 WORLD ENERGY SCENARIO AND SUSTAINABLE ENERGY FUTURE

The world energy consumption is about 560 EJ/year [1], presently mostly provided by fossil sources (>80%) [2] and supposed to grow in the coming years [1]. This can for a large part be ascribed to the expected increase of population (+40% in 2050) and to the increasing energy consumption in upcoming economies as China and India [3]. Fossil fuels are now the more widely used source for energy production, but they are not renewable nor CO₂ neutral. It is almost universally accepted that the release of CO₂ into the atmosphere coming from these fuels is at least in part responsible for the climate change [4].

A primary concern is now the availability of such sources. Fossil fuels are being consumed without replacement, creating a volatile market with ever increasing prices. The consumption of fossil fuels caused gradual depletion of world's accessible oil reservoirs. Companies are failing to find new reserves of oil sufficient to meet the future needs. Most oil producers are investing in more capital-intensive projects, needing to drill in remote places and deeper to obtain oil. The extensive use of fossil fuels and related chemicals introduces greenhouse gases, such as, CO₂, chlorofluorocarbons (CFCs) and methane into the atmosphere causing the "greenhouse gas effect". This second problem of global warming effect of CO₂ and other greenhouse gases on the environment has generated a lot of public and political concern.

Besides the concerns about global warming and finite fossil fuel reserves, the security of supply and its associated politics are an important factor determining the energy scenarios [4]. Since a large amount of the fossil fuels is coming from political less stable countries, the security of fossil fuel supply is not always straightforward. This stimulates countries to develop local alternative energy programs from unconventional sources. The supply of renewable energy is one of the main challenges that mankind will face over the coming decades. Climate change, demographic developments coupled with increasing wealth, political issues and ending fossil fuel reserves drive governments to stimulate the usage of renewable resources like wind, hydro, solar and biomass for the energy supply.

Renewable energy resources can be one of the potential alternative solutions to fossil fuels and their derivatives. They have become a large focus of research as energy sources due to their reduced environmental risks and pollution. In addition to their sustainable favorability, renewable energy resources

are, in general, more evenly distributed over earth's surface than fossil fuels and may be exploited using less capital-intensive technologies. Renewable energy sources have the advantage to diversify and decentralize the energy supplies and to achieve energy self-sufficiency at a local, regional, and national level [5].

Biomass, sun (e.g. photovoltaic solar cells and solar heat collectors), wind (e.g. wind turbines), water (e.g. hydropower, tidal energy) and geothermal resources are all sources of renewable energy, but biomass is the only renewable resource of carbon for the production of chemicals, materials and fuels. In this context the development of biomass-related clean energies has become an important working area.

2 ENERGY FROM BIOMASS

Biomass represents stored solar energy and is therefore the only renewable energy resource that consists of actual matter (predominantly C,H,O,N) [6]. The transformation of biomass into fuels and chemicals becomes increasingly important to mitigate global warming and diversify energy resources. The current usage of biomass accounts for 13% of the total energy produced, but almost all this energy is used in developing countries for heating and cooking [1]. The energy scenario of Shell predicts an increase of 2.5-3 times the current biomass usage in 2050 [3].

In the past 10 years, there has been renewed interest, world-wide, in biomass as an energy source. Wood and other forms of biomass including energy crops and agricultural and forestry wastes are some of the main renewable energy resources available. These can provide the only source of renewable liquid, gaseous and solid fuels. Biomass is considered the renewable energy source with the highest potential to contribute to the energy needs of modern society for both the developed and developing economies world-wide [7], [8]. Energy from biomass based on short rotation forestry and other energy crops can contribute significantly towards the objectives of the Kyoto Agreement in reducing the green-house gases emissions and to the problems related to climate change [9]. Biomass fuels and residues can be converted to energy via thermal, biological and physical processes.

Biomass is the sole resource available for fast introduction of renewable fuels and chemicals into the market. There are several reasons for this situation. Firstly, technological developments relating to the conversion, crop production, etc. promise the application of biomass at lower cost and with higher conversion efficiency than was possible previously. For example, when low cost biomass residues are used for fuel, the cost of electricity is already now often competitive with fossil fuel-based power generation. More advanced options to produce electricity are looking promising and allow a cost-effective use of energy crops e.g. production of methanol and hydrogen by means of gasification processes. The second main stimulus is the agricultural sector in Western Europe and in the US, which is producing food surpluses. This situation has led to a policy in which land is set aside in order to reduce surpluses. Related problems, such as the de-population of rural areas and payment of significant subsidies to keep land fallow, makes the introduction of alternative, non-food crops desirable. Demand for energy will provide an almost infinite market for energy crops grown on such (potentially) surplus land. Thirdly, the potential threat posed by climate change, due to high emission levels of greenhouse gases (CO₂ being the most important one), has become a major stimulus for renewable energy sources in general. When produced

by sustainable means, biomass emits roughly the same amount of carbon during conversion as is taken up during plant growth. The use of biomass therefore does not contribute to a buildup of CO₂ in the atmosphere [10].

3 BIOMASS

Biomass is a term for all organic material produced by green plants converting sunlight into plant material through photosynthesis and includes all land- and water-based vegetation, as well as all organic wastes. The biomass resource can be considered as organic matter, in which the energy of sunlight is stored in chemical bonds. When the bonds between adjacent carbon, hydrogen and oxygen molecules are broken by digestion, combustion, or decomposition, these substances release their stored, chemical energy. If biomass is processed efficiently, either chemically or biologically, by extracting the energy stored in the chemical bonds and the subsequent 'energy' product combined with oxygen, the carbon is oxidized to produce CO₂ and water. The process is cyclical, as the CO₂ is then available to produce new biomass.

The value of a particular type of biomass depends on the chemical and physical properties of the large molecules from which it is made. Man for millennia has exploited the energy stored in these chemical bonds, by burning biomass as a fuel and by eating plants for the nutritional content of their sugar and starch. More recently, fossilized biomass has been exploited as coal and oil. However, since it takes millions of years to convert biomass into fossil fuels, these are not renewable within a time-scale mankind can use. Burning fossil fuels uses "old" biomass and converts it into "new" CO₂; which contributes to the "greenhouse" effect and depletes a non-renewable resource. Burning new biomass contributes no new carbon dioxide to the atmosphere, because replanting harvested biomass ensures that CO₂ is absorbed and returned for a cycle of new growth [10].

Biomass has always been a major source of energy for mankind and is presently estimated to contribute of the order 10-14% of the world's energy supply [10]. Biofuels can in principal be produced from any source of biomass like wood and wood waste, agricultural residues, forestry residues and waste from the food industry. Wood based biomass is mainly studied in this thesis. Wood has a well-known composition and has a low ash content, making it an ideal feed for pyrolysis research. In addition, the majority of the pyrolysis research is focused on wood, making the comparison of experimental results more straightforward. Wood can generally be classified in two groups namely hardwood and softwood [6]. The softwoods are also known as coniferous woods like pine and spruces, whereas hardwoods include for example beech, oak and maple [6]. Lignocellulose, the major component of woody biomass, consists mainly out of three types of polymers namely cellulose, hemicellulose and lignin. The weight fractions of cellulose, hemicellulose and lignin varies for the different biomass species [11]. Commercially interesting second generation biomass feedstocks are for example straw, bagasse and rice husk.

3.1 BIOMASS PROPERTIES

Biomass is similar to other fuel types. In the need for standardized methods of analysis leading to accurate and consistent evaluations of fuel properties, there are several methods frequently used to

assess major properties of biomass fuels. They are summarized in Table 1. Some of these methods were developed for other fuels, such as coal, but are more generally applicable and have been found to be adequate for biomass as well [12].

Table 1. Methods of biomass fuel analysis

Property	Analytical method
Heating value	ASTM ABBE
Particle size distribution	ASTM E828
Bulk density	ASTM E873
<i>Proximate composition</i>	
Moisture	ASTM E871
Ash	ASTM E830 (575°C), ASTM D1102 (600°C)
Volatiles	ASTM E872/E897
Fixed carbon	by difference
<i>Ultimate Elemental</i>	
C, H	ASTM E777
N	ASTM E778
S	ASTM E775
Cl	ASTM E776
Ash elemental	ASTM D3682, ASTM D2795, ASTM D4278
Ash fusibility	ASTM E953/D1857
Metals	ASTM E885

The inherent properties of the biomass source determine both the choice of conversion process and any subsequent processing difficulties that may arise. The choice of the biomass source is influenced by the form in which the energy is required and it is the interplay between these two aspects that enables flexibility to be introduced into the use of biomass as an energy source. Depending on the energy conversion process selected, particular material properties become important during processing [10]. The categories of biomass examined in most biomass research activities and considered for exploitation are woody and herbaceous species.

3.1.1 MOISTURE CONTENT

The high moisture content in biomass is one of the major disadvantages. This content normally varies in the interval of 3-63% and it can become as high as 91% [13]. Two forms of moisture content are of interest in biomass: intrinsic moisture and extrinsic moisture. The first is the moisture content of the material without the influence of weather effects, the second is influenced by prevailing weather conditions

during harvesting on the overall biomass moisture content. In practical terms, it is the extrinsic moisture content that is of concern, as the intrinsic moisture content is usually only achieved, or applicable, under laboratory conditions. Also of importance in respect of the prevailing weather conditions at the time of harvesting, is the potential contamination of the harvested biomass by soil and other detritus, which can in turn have a significant deleterious impact during subsequent treatment or processing. The parameters of interest that are affected by such contamination are the ash and alkali metal content of the material. The relationship between biomass moisture content and appropriate bio-conversion technology is essentially straightforward, in that thermal conversion requires low moisture content feedstock (typically <50%), while bio-conversion can utilize high moisture content feedstocks. Thermal conversion technologies can also use feedstocks with high moisture content but the overall energy balance for the conversion process is adversely impacted. On this basis, woody and low moisture content herbaceous plant species are the most efficient biomass sources for thermal conversion to liquid fuels, such as methanol. For the production of ethanol by biochemical (fermentation) conversion, high moisture herbaceous plant species, such as sugarcane, are more suited: such species can also be fermented via another biochemical process, anaerobic digestion, to produce methane [10].

3.1.2 CALORIFIC VALUE

The calorific value (CV) of a material is an expression of the energy content, or heat value, released when burnt in air. The CV is usually measured in terms of the energy content per unit mass, or volume. The CV of a fuel can be expressed in two forms, the gross or higher heating value (HHV) and the net or lower heating value (LHV).

The HHV is the total energy content released when the fuel is burnt in air, including the latent heat contained in the water vapor and therefore represents the maximum amount of energy potentially recoverable from a given biomass source. In practical terms, the latent heat contained in the water vapor cannot be used effectively and therefore, the LHV is the appropriate value to use for the energy available for subsequent use [10]. The actual amount of energy recovered will vary with the conversion technology.

3.1.3 ELEMENTAL ANALYSIS

The composition of biomass is highly variable because each biomass variety has specific origin and formation conditions, which can cause enrichment or depletion of different elements and phases. The elemental composition of biomass may potentially include the entire periodic table. As a general trend most of the elements determined in biomass are C, Ca, Cl, H, K, Mg, N, Na, O, P and S. On the other hand, most of the elements detected in ash are Al, Ca, Cl, Fe, K, Mg, Mn, Na, O, P, Rb, S, Si, Sr and Zn [14]. Elemental analysis of a fuel, presented as C, N, H, O and S together with the ash content, is termed the ultimate analysis of a fuel. The principal constituent of biomass is carbon, making up from 30 to 60% wt. of dry matter depending on ash content. Typically, 30 to 40% wt. of the dry matter in biomass is oxygen. Of the organic component, hydrogen is the third major constituent, comprising typically 5 to 6% wt. dry matter. Nitrogen, sulfur, and chlorine can also be found in quantity, usually less than 1% dry matter but occasionally well above this [12].

The significance of the O:C and H:C ratios on the calorific value of solid fuels can be illustrated using a Van Krevelen diagram (Figure 1). A useful means of comparing biomass and fossil fuels is in terms of their O:C and H:C ratios. The lower the respective ratios the greater the energy content of the material. Comparison of biofuels with fossil fuels, such as coal, shows clearly that the higher proportion of oxygen and hydrogen, compared with carbon, reduces the energy value of a fuel, due to the lower energy contained in carbon–oxygen and carbon–hydrogen bonds, than in carbon–carbon bonds [7].

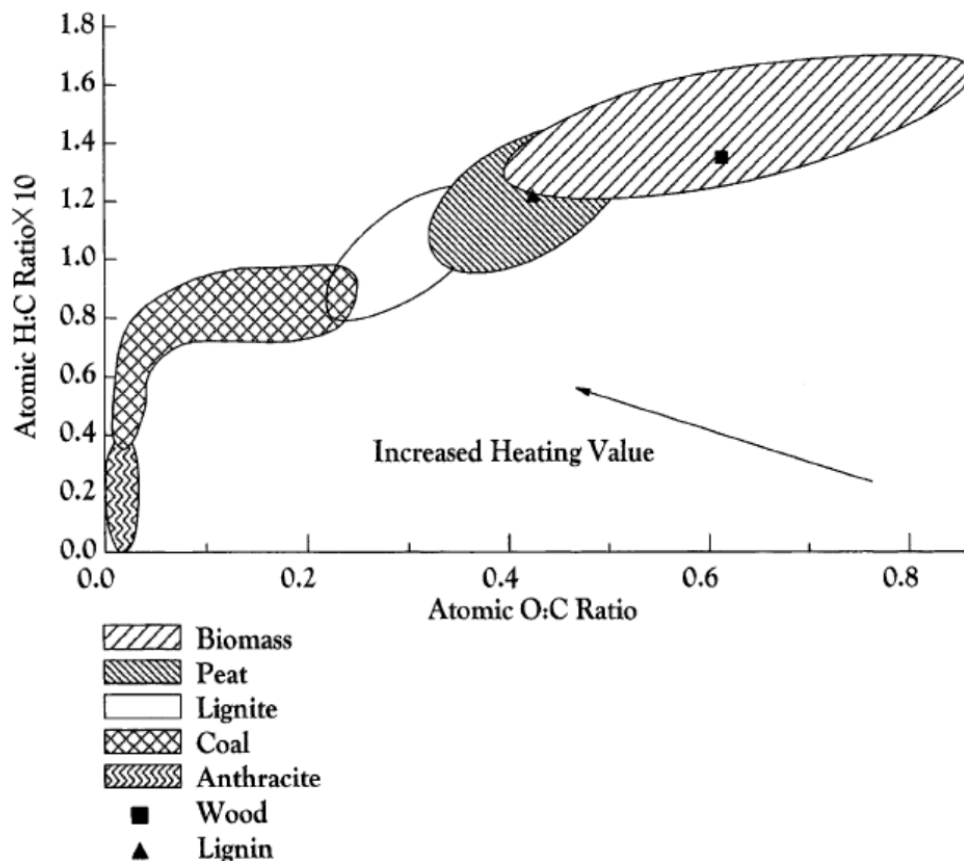


Figure 1. Van Krevelen diagram for various solid fuels

3.1.4 ALKALI METAL CONTENT

The alkali metal content of biomass i.e. Na, K, Mg, P and Ca, is especially important for any thermochemical conversion processes. The reaction of alkali metals with silica present in the ash produces a sticky, mobile liquid phase, which can lead to blockages of airways in the furnace and boiler plant. It should be noted that while the intrinsic silica content of a biomass source may be low, contamination with soil introduced during harvesting can increase the total silica content significantly, such that while the content of intrinsic silica in the material may not be a cause for concern, the increased total silica content may lead to operational difficulties [10].

3.1.5 PROPORTION OF FIXED CARBON AND VOLATILE MATTER

Fuel analysis has been developed based on solid fuels, such as coal, which consists of chemical energy stored in two forms, fixed carbon and volatiles: the volatiles content, or volatile matter (VM) of a solid fuel, is that portion driven-off as a gas (including moisture) by heating (to 950 °C for 7 min); the fixed carbon content (FC), is the mass remaining after the releases of volatiles, excluding the ash and moisture contents. Laboratory tests are used to determine the VM and FC contents of the biomass fuel. Fuel analysis based upon the VM content, ash and moisture, with the FC determined by difference, is termed the proximate analysis of a fuel. The significance of the VM and FC contents is that they provide a measure of the ease with which the biomass can be ignited and subsequently gasified, or oxidized, depending on how the biomass is to be utilized as an energy source. This type of fuel analysis is of value for biological conversion processes only once the fuel is produced, enabling a comparison of different fuels to be undertaken.

3.1.6 BULK DENSITY

An important characteristic of biomass materials is their bulk density, or volume, both as-produced and as-subsequently processed. The importance of the as-produced, bulk density is in relation to transport and storage costs. The density of the processed product impacts on fuel storage requirements, the sizing of the materials handling system and how the material is likely to behave during subsequent thermo-chemical/biological processing as a fuel/feed- stock. As an example, taking wood as a reference material for transport and storage costs at about 20 £/m³, for straw to be competitive on the same density basis, it needs either to be baled, or processed into a cubed/pelleted form, with a concomitant increase in costs [10]. The low energy density (both low bulk density and heating value) of biomass is a significant disadvantage for biomass conversion. For example, the energy density of biomass is only 10-40% of that of most fossil fuels and biomass heating values generally are slightly over half that of coal. Furthermore, the biomass particle densities are about half that of coal, whereas the biomass bulk densities are about one fifth that of coal. The lower energy density of biomass requires a biomass resource close to the processing facility, high storage cost and minimal storage time because the weathering and bacteria can lower the energy quality of the biomass [13].

3.2 BIOMASS COMPOSITION: MACROCOMPONENTS

Biomass contains varying amounts of cellulose, hemicellulose, lignin and a small amount of other extractives. Cellulose is a long chain glucose polymer. Hemicellulose is a heterogeneous branched polysaccharide that binds tightly to the surface of each cellulose micro-fibril. Lignin can be regarded as a group of amorphous, high molecular-weight, chemically related compounds (Figure 2). Cellulose is generally the largest fraction, representing about 40–50% of the biomass by weight; the hemicellulose portion represents 20–40% of the material by weight [10]. The chemical composition of biomass is very different from that of coal. The presence of large amounts of oxygen in plant carbohydrate polymers means the pyrolytic chemistry differs sharply from these of other fossil feeds.

The weight percent of cellulose, hemicellulose, and lignin varies in different biomass species of wood. Woody plant species are typically characterized by slow growth and are composed of tightly bound fibers,

giving a hard external surface, while herbaceous plants are usually perennial, with more loosely bound fibers, indicating a lower proportion of lignin, which binds together the cellulosic fibers [6]. The relative proportions of cellulose and lignin is one of the determining factors in identifying the suitability of plant species for subsequent processing as energy crops.

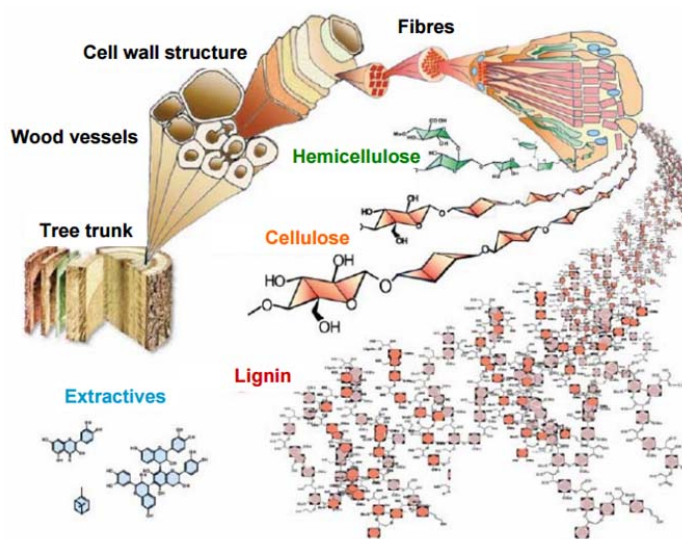


Figure 2. Structure of lignocellulosic biomass

The proportions of cellulose and lignin in biomass are important in biochemical conversion processes. The biodegradability of cellulose is greater than that of lignin, hence the overall conversion of the carbon-containing plant material present as cellulose is greater than for plants with a higher proportion of lignin, a determining factor when selecting biomass plant species for biochemical processing. For the production of ethanol, a biomass feedstock with a high, cellulose/hemi-cellulose content is needed to provide a high yield. While the lignin content represents a potentially large energy source, current techniques involving hydrolysis/enzymatic systems cannot convert the lignin to syngas [10]. Table 2 gives the proportions of cellulose/hemicellulose/lignin for softwoods and hardwoods and for comparison, wheat straw and switchgrass.

Table 2. Cellulose/lignin content of selected biomass (wt.%)

Biomass	Lignin %	Cellulose %	Hemicellulose %
Softwood	27-30	35-40	35-30
Hardwood	20-25	45-50	20-25
Wheat straw	15-20	33-40	20-25
Switchgrass	5-20	30-50	10-40

3.2.1 CELLULOSE

Cellulose consists of high molecular weight (10^6 Da or more) linear polymers of glucose that are held rigidly together as bundles of fibers to provide material strength. The cellulose typically accounts for some 40-50 wt% of dry wood.

Cellulose is insoluble and crystalline. The crystalline structure resists thermal decomposition better than hemicelluloses. Amorphous regions in cellulose exist and contain waters of hydration, and free water present within the wood. This water, when rapidly heated, disrupts the structure by a steam explosion-like process prior to chemical dehydration of the cellulose molecules [6].

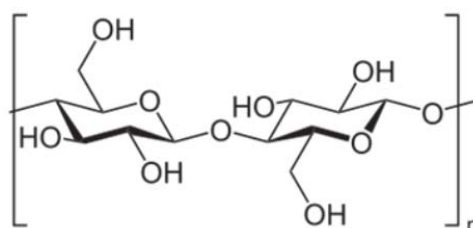


Figure 3. Repeating cellulose unit [14]

3.2.2 HEMICELLULOSE

The second major wood chemical constituent is hemicellulose. It consists of shorter polymers of various sugars that glue the cellulose bundles together. It usually accounts for some 25-35 wt% of the mass of dry wood, 28% in softwoods, and 35% in hardwoods. Hemicelluloses exhibit lower molecular weights than cellulose. The number of repeating saccharide monomers is only ~ 150 , compared to the number in cellulose (5000-10000). Cellulose has only glucose in its structure, whereas hemicellulose has a mixture of various monosaccharides (average molecular weight < 30000 Da) such as glucose, mannose, galactose, xylose, arabinose, and some contains short side-chain "branches" pendent along the main polymeric chain [6].

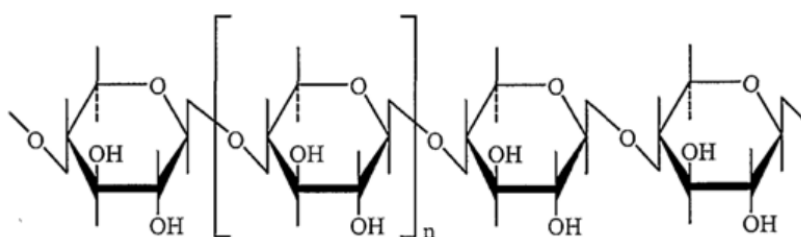


Figure 4. Xylan with no side chain[14]

3.2.3 LIGNIN

The third major component of wood is lignin, which consists of a tri-dimensional polymer of propyl-phenol that is imbedded in and bound to the hemicellulose. It provides rigidity to the structure. It accounts for 23%-33% of the mass of softwoods and 16%-25% of the mass of hardwoods. It is an amorphous cross-linked resin with no exact structure. It is the main binder for the agglomeration of fibrous cellulosic

components while also providing a shield against the rapid microbial or fungal destruction of the cellulosic fibers.

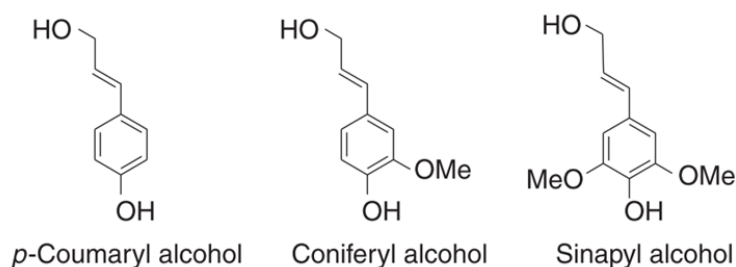


Figure 5. Alcoholic monomers in lignin structure [15]

The building blocks of lignin are hydroxyl-phenylpropane units issued from three monomers p-coumaryl, coniferyl and sinapyl alcohols (Figure 5) differently distributed depending on the vegetal material (softwood, hardwood or grass). In lignin biosynthesis, these units undergo radical dimerization and further oligomerization, and they eventually polymerize and cross-link. The guaiacol lignin which is derived from the polymerization of coniferyl phenylpropane unit is found predominately in softwoods materials. The sinapyl unit is in hardwoods higher than that in softwoods [16]. Lignin has an amorphous structure, which leads to a large number of possible interlinkages between individual units, because the radical reactions are nonselective random condensations. Ether bonds predominate between lignin units, unlike the acetal functions found in cellulose and hemicellulose, but carbon-to-carbon linkages also exist. Covalent linking also exists between lignin and polysaccharides, which strongly enhances the adhesive bond strength between cellulose fibers and its lignin “potting matrix”.

3.2.4 ASH

The chemical breakdown of a biomass fuel, by either thermo-chemical or bio-chemical processes, produces a solid residue. When produced by combustion in air, this solid residue is called ‘ash’ and forms a standard measurement parameter for solid and liquid fuels. The ash content of biomass affects both the handling and processing costs of the overall, biomass energy conversion cost. Dependent on the magnitude of the ash content, the available energy of the fuel is reduced proportionately. In a thermo-chemical conversion process, the chemical composition of the ash can present significant operational problems. This is especially true for combustion processes, where the ash can react to form a ‘slag’, a liquid phase formed at elevated temperatures, which can reduce plant throughput and result in increased operating costs [10]. During biochemical conversion, the percentage of solid residue will be greater than the ash content formed during combustion of the same material. For a biochemical conversion process, the solid residue represents the quantity of non-biodegradable carbon present in the biomass. This residue will be greater than the ash content because it represents the recalcitrant carbon which cannot be degraded further biologically but which could be burnt during thermo-chemical conversion.

4 BIOMASS CONVERSION TECHNOLOGY

Biomass can be converted into useful forms of energy using a number of different processes. Factors that influence the choice of conversion process are: the type and quantity of biomass feedstock; the desired form of the energy, i.e. end-use requirements; environmental standards; economic conditions; and project specific factors. In many situations it is the form in which the energy is required that determines the process route, followed by the available types and quantities of biomass.

Conversion of biomass to energy is undertaken using two main process technologies: thermo-chemical and bio-chemical/biological. Within thermo-chemical conversion four process options are available: combustion, pyrolysis, gasification and liquefaction. Bio-chemical conversion encompasses two process options: digestion (production of biogas, a mixture of mainly methane and carbon dioxide) and fermentation (production of ethanol). A distinction can be made between the energy carriers produced from biomass by their ability to provide heat, electricity and engine fuels. While biological processing is usually very selective and produces a small number of discrete products in high yield using biological catalysts, thermal conversion often gives multiple and often complex products, in very short reaction times with inorganic catalysts often used to improve the product quality or spectrum [17]. The major conversion technologies and processes are discussed in the following sections.

4.1 COMBUSTION

Combustion of biomass and related materials is widely practiced commercially to provide heat and power. The technology is commercially available and presents minimum risk to investors. The product is heat, which must be used immediately and/or for power generation. Overall efficiencies to power tend to be rather low at typically 15% for small plants up to 30% for larger and newer plants. Costs are only currently competitive when wastes are used as feed material such as from pulp and paper, and agriculture. Emissions and ash handling remain technical problems. The technology is, however, widely available commercially and there are many successful working examples throughout North America and Europe, frequently utilizing forestry, agricultural and industrial wastes [18].

Combustion occurs both in the gas phase with the burning of volatile materials released through pyrolysis of the fuel upon heating, and heterogeneously in the solid phase as char oxidation. The burning of volatiles is generally quite rapid and follows as fast as volatiles are released, the oxidation of the char occurs much more slowly. The residence time of the particle in the furnace and the environment of the particle are therefore important to the total conversion attained through combustion, as well as the emissions from the combustor [12].

The burning of biomass in air is used over a wide range of process equipment, e.g. stoves, furnaces, boilers, steam turbines, turbo-generators, etc. Combustion of biomass produces hot gases at temperatures around 800-1000°C. It is possible to burn any type of biomass but in practice combustion is feasible only for biomass with a moisture content <50%, unless the biomass is pre-dried. High moisture content biomass is better suited to biological conversion processes. The scale of combustion plant ranges from very small scale (e.g. for domestic heating) up to large-scale industrial plants in the range 100-3000 MW. Co-combustion of biomass in coal-fired power plants is an especially attractive option because of the high conversion efficiency of these plants. Net bio-energy conversion efficiencies for biomass combustion

power plants range from 20% to 40%. The higher efficiencies are obtained with systems over 100 MWe or when the biomass is co-combusted in coal-fired power plants [19].

Fuel moisture is a limiting factor in biomass combustion due to its effect on heating value. The combustion reaction is exothermic, the evaporation of water strongly endothermic. The auto-thermal limit self-supporting combustion for most biomass fuels is around 65% wt. on wet basis. Above this point, insufficient energy is liberated by combustion to satisfy evaporation and product heating. Practically, most combustors require a supplemental fuel, such as natural gas, when burning biomass in excess of 50 to 55% moisture on wet basis, and CO and other products of incomplete combustion may be emitted in greater quantities depending on combustor design [12].

4.2 GASIFICATION

Gasification is the conversion of biomass into a combustible gas mixture by the partial oxidation of biomass at high temperatures, typically in the range 800–900°C with a controlled amount of oxygen and/or steam. Gasification occurs in a number of sequential steps: (i) drying to evaporate moisture, (ii) pyrolysis to give gas, vaporized tars or oils and a solid char residue, (iii) gasification or partial oxidation of the solid char, tars and gases [18]. Pyrolysis is the first step of gasification, occurring at 350-800°C as a consequence of the heating up of the biomass. Gas, vaporized tars and a solid char residue are produced at those temperatures. The relative yields of gas, liquid and char depend mostly on the rate of heating and the final temperature [20]. Volatile materials and char react with an oxidant agent, usually steam to give CO, CO₂, H₂ and less amounts of hydrocarbons. The gas composition is influenced by many other factors such as feed composition, water content, reaction temperature, and the extent of oxidation of the pyrolysis product [18].

The gas is very costly to be stored or transported so it has to be used immediately. The low calorific value gas produced (about 4–6 MJ/Nm³) can be burnt directly or used as a fuel for gas engines and gas turbines. The product gas can be used as a feedstock (syngas) in the production of chemicals (e.g. methanol). One promising concept is the biomass integrated gasification/combined cycle, where gas turbines convert the gaseous fuel to electricity with a high overall conversion efficiency. The integration of gasification and combustion/heat recovery ensures a high conversion efficiency, producing net efficiencies of 40-50% (based on the lower heating value of the incoming gas) for a plant of 30-60 MW capacity [19]. The fuel gas quality requirements, for turbines in particular, are very high. Nevertheless, not all the tar produced in the pyrolysis step is completely converted due to physical or geometrical limitations of the reactor and to chemical limitations of the reactions involved. As a consequence, syngas results to be contaminated by tar, which is to be removed by thermal, catalytic or physical processes. This aspect of tar cracking or removal in gas clean-up is one of the most important technical barriers which limits the implementation of gasification technologies [18].

4.3 FERMENTATION

Fermentation is used commercially on a large scale in various countries to produce ethanol from sugar crops (e.g. sugar cane, sugar beet) and starch crops (e.g. maize, wheat). The biomass is ground down and the starch converted by enzymes to sugars, with yeast then converting the sugars to ethanol.

Purification of ethanol by distillation is an energy-intensive step, with about 450 lt. of ethanol being produced per ton of dry corn [21]. The solid residue from the fermentation process can be used as cattle-feed and in the case of sugar cane, the bagasse can be used as a fuel for boilers or for subsequent gasification [21]. Ethanol is generally mixed with gasoline, which, at low percentages, can be done without adaptations to the current vehicle fleet. Ethanol has the advantage to lower NO_x and dust emissions to some extent, if compared with straight gasoline. However, ethanol production from food crops as maize and cereals is not economically competitive with gasoline and diesel [22].

The conversion of lignocellulosic biomass (such as wood and grasses) is more complex, due to the presence of longer-chain polysaccharide molecules and requires acid or enzymatic hydrolysis before the resulting sugars can be fermented to ethanol. Such hydrolysis techniques are currently at the pilot stage [19]. Lignocellulosic biomass requires pretreatment to clean and size the biomass, and destroy its cell structure to make it more accessible to further chemical or biological treatment. Also, the lignin part of the biomass is removed, and the hemicellulose is hydrolyzed to monomeric and oligomeric sugars. The cellulose can then be hydrolyzed to glucose. The sugars are fermented to ethanol, which needs to be purified and dehydrated [22].

4.4 ANAEROBIC DIGESTION

Anaerobic digestion is the conversion of organic material directly to a gas, termed biogas, a mixture of mainly methane and carbon dioxide with small quantities of other gases such as hydrogen sulphide. The biomass is converted by bacteria in an anaerobic environment, producing a gas with an energy content of about 20-40% of the lower heating value of the feedstock. Anaerobic digestion of biomass has been demonstrated and applied commercially with success to a multitude of situations and for a variety of feedstock such as organic domestic waste, organic industrial wastes, manure, sludge, etc. It is particularly suited for treating high moisture content organic wastes, i.e. 80-90% moisture. Biogas can be used directly in gas engines and gas turbines and can be upgraded to higher quality natural gas, by the removal of CO₂. Used as a fuel to produce electricity only, the overall conversion efficiency from biomass to electricity is about 10-16% [19].

A specific source of biogas is landfilling. The production of methane rich landfill gas from landfill sites makes a significant contribution to atmospheric methane emissions. In many situations the collection of landfill gas and production of electricity by converting this gas engines is profitable and the application of such systems has become widespread. The benefits are obvious: useful energy carriers are produced from gas that would otherwise contribute to increase methane in the atmosphere (which has stronger GHG impact than the CO₂ emitted from the power) [22].

4.5 PYROLYSIS

Pyrolysis is the conversion of biomass to liquid (termed bio-oil or bio-crude), solid and gaseous fractions, by heating the biomass in the absence of air [12]. Pyrolysis has a long history in the upgrading of biomass. Today's processes can be tuned to form char, oil and/or gas, depending on the temperature and reaction time, from ~300°C and hours, to 400–500°C and minutes or seconds, on to >700°C and fractions of a second [23]. The relative proportions of the pyrolysis products depends very much on the pyrolysis

method, the characteristics of the biomass and the reaction temperature. The char produced by pyrolysis is typically light and porous. It has a high energy content (~30 GJ/t), which makes it a valuable fuel for industrial and consumer applications. The gases have a moderate energy content, and can be used for generating heat or electricity. The pyrolysis oil is a very complex and multiphase mixture of low and high molecular weight components, including water (~25%), a variety of organic oxygenates and polymeric carbohydrate and lignin fragments.

Pyrolysis has been applied for thousands of years for charcoal production but it is only on the last 30 years that fast pyrolysis at moderate temperatures of around 500°C and very short reaction times of up to 2 s has become of considerable interest. This is because the process directly gives high yields of liquids of up to 75 wt.% which can be used directly in a variety of applications [1] or used as an efficient energy carrier. Further details about the pyrolysis process are given in the following chapter.

4.6 LIQUEFACTION

A variation of the pyrolysis process for the production of bio-oil is the direct thermal liquefaction under liquid phase conditions and using milder temperatures of 250-370°C [23]. In the liquefaction, lignocellulosic biomass is converted directly into a liquid, unlike in pyrolysis, in which vapors are first formed and then condensed into liquid. Pyrolysis requires dry biomass, for wet biomass it may not be economical due to the high energy requirement to dry the biomass [24]. However, for the liquefaction process drying of biomass is not required. High pressure inside the reactor prevents water from evaporation and saves energy on latent heat of vaporization of water. Pyrolysis and heat thermal liquefaction are different with respect to their process parameters as summarized in Table 3.

Table 3. Fast pyrolysis vs. direct thermal liquefaction

Process	Temperature °C	Pressure MPa	Residence time	Drying	Carrier medium
Fast pyrolysis	370-700	0.1-0.5	<2 s	Required	Not required
Liquefaction	150-370	0.1-24	5-30 min	Not required	Water/Solvent

In principle, both pyrolysis and liquefaction processes can be integrated within an existing manufacturing complex such as an oil refinery, where the produced bio-oil/bio-crude can then be transported to a central location for further processing or for its direct use.

5 THE BIO-REFINERY CONCEPT

A bio-refinery is a facility that integrates biomass conversion processes and equipment to produce fuels, power and chemicals from biomass. The bio-refinery concept is analogous to today's petroleum refineries, which produce multiple fuels and products from petroleum. Industrial bio-refineries have been identified as the most promising route to the creation of a new bio-based industry.

For optimal use of the renewable resources, it is constructive to think in terms of a bio-refinery, where the raw material coming into the refinery is completely transformed into a number of different products. A bio-refinery can take advantage of the differences in biomass components and intermediates and maximize the value derived from the biomass feedstock. Sustainable use of biomass must include using all components of the raw material, not just the most easily convertible fractions. For wood, this would mean converting all parts of the raw material into value-added products, in this context preferably in the form of transport fuels.

Ethanol production from the carbohydrate fractions of wood is already applicable. However, the lignocellulosic raw material also contains other components. Thus, the use of the carbohydrate fractions leaves around one-third of the material as a low-value byproduct or waste. This is a significant drawback both for the efficiency of conversion and for the economy of the whole process. Altogether, the lignin should be considered as the second most abundant source of renewable and sustainable carbon next to cellulose and exploited as such. Within this concept, the lignin and extractives that are “left over” from ethanol production should be processed to give value-added products, rather than just being burned as a process energy source [25]. In Europe, a limited number of bio-refineries that use lignocellulosic biomass for the production of second-generation bioethanol are currently in operation (Table 4).

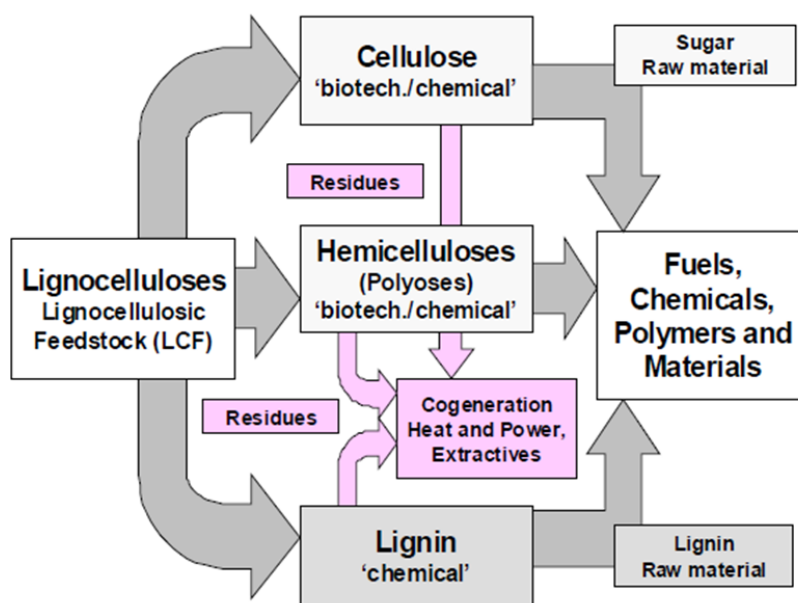


Figure 6. Basic design Lignocellulosic Feedstock Bio-refinery co-producing bioethanol, added-value chemicals and secondary energy carriers [26].

The main constituents hemicellulose, cellulose and lignin are strongly interconnected by a variety of physico-chemical bonds that makes it difficult to separate them as individual constituents in high yields. Consequently, efficient and cost-effective fractionation technology is a clear asset to open up the possibility to treat each constituent separately, using dedicated conversion technologies to obtain specific target chemicals. A bio-refinery in which the fractionation is combined/integrated with subsequent

processing steps, offers a solution for a cost-effective and environmentally sound valorization of biomass. Figure 6 presents a general scheme of such a bio-refinery.

Table 4. Examples of European lignocellulosic bio-refineries [27]

Company	Feedstock	Fractionation process	Main product
ABNT (Spain)	Wheat straw	Steam explosion	Bioethanol
Chempolis (Finland)	Agricultural residues	Organosolv	Bioethanol
Inbicon (Denmark)	Agricultural residues	Hydrothermal	Bioethanol
Beta Renewables (Italy)	Agricultural residues	Steam explosion	Bioethanol
CIMV (France)	Wheat straw	Organosolv	Cellulose, C5 sugars, lignin

Many pulp and paper mills have started to exploit new processes for cost-effective recycling methods, including wider usage of renewable sources. Usually, a pulp and paper mill produces only paper and recycles the chemicals used for pulping, producing energy for internal use. However, paper mills have a clear potential of becoming bio-refineries by utilizing a larger part of the organic components in the wood, e.g., hemicellulose and lignin. By isolating lignin from the black liquor, it can be used as a fuel in a lime kiln or be further upgraded. Consequently, it is prudent in the long run to recover as much of the fiber from biomass. Integrated systems of processing will enable the selection of materials to be processed into higher priority products, and those for energy and chemicals will be derived from the rejected materials [11].

6 OUTLINE OF THE PRESENT STUDY

The aim of the present study is the detailed investigation of the pyrolysis processes of lignocellulosic biomass. Pyrolysis conversion processes are an important technological option for biofuel production and energy recovery from biomass and wastes. Pyrolysis is also a first step in gasification and in other thermochemical conversion processes for the exploitation of energy from biomass. In such a wide horizon, two topics are investigated in detail: the thermal effects associated to the pyrolysis process, necessary to correctly assess the overall heat balances of thermochemical conversion processes, and the fate and conversion products of lignin during pyrolysis.

Knowledge of the thermal behavior and reactivity of biomass is essential for the effective design and operation of thermochemical conversion units. Thus, the investigation of the influence of operating conditions on the outcomes of the thermal conversion of biomass feedstock in pyrolysis processes is an important element to enhance the design and the optimization of new biomass-to-energy processes. Thermoanalytical techniques, such as thermogravimetric analysis (TG) and differential scanning calorimetry (DSC), provide this information in a straightforward manner.

Thinking in terms of a bio-refinery approach, lignin valorization is a key-issue for enhanced profitability of sustainable bio-based industries. The challenge, however, is that lignin is very difficult to decompose and

generates very high amounts of solid residue as compared to other components of lignocelluloses. For this reason, the lignin pyrolysis has been experimentally investigated. In particular, a variation of the pyrolysis process for the production of a bio-oil is the liquefaction using a solvent. Thus the investigation of process parameters during lignin liquefaction has been studied as a method to make the lignin pumpable and easier to handle as a high-value liquid feedstock.

Chapter 2 provides an overview of the biomass pyrolysis process principles and mechanism. It highlights state of the art of thermochemical conversion technologies in which pyrolysis plays the central role. Relevant historical and/or recent developments are reviewed as well.

Chapter 3 describes materials, experimental set-ups, general procedures and analytical equipment that are used in the present study. Experimental procedures are also presented, including the specific methods used for the experimental assessment of the heat of pyrolysis.

In Chapter 4 the influence of some key experimental parameters on the overall heat demand of the pyrolysis process have been investigated. Temperature, pressure, and particle size are the main operative factors which affect the heat and mass transfer phenomena during biomass pyrolysis, therefore having an important influence on the outcomes of the thermal decomposition process. The goal of this study is to establish the reaction enthalpy effects accompanying biomass pyrolysis.

Chapter 5 investigates the influence of process conditions on the thermal effects associated to biomass macrocomponents pyrolysis: cellulose, hemicellulose and lignin. The scope is to analyze the interactions among the components and to determine if they are significant to determine the biomass thermal behavior. For this purpose the thermal effects during pyrolysis of biomass macrocomponents mixtures have been analyzed and compared with those of single components or lignocellulosic biomass with the same composition.

Chapter 6 is intended to explore lignin liquefaction as process to convert lignin in a flowable bio-oil product with improved properties like lower oxygen content and molecular weight. Guaiacol has been chosen as solvent, because of its aromatic chemical structure similar to lignin and its pyrolysis/solvolytic products. A process parameters screening and simulation of a continuous recycle have been described. The study aims to show that bio-oil produced might be used as a source of aromatics in further upgrading process by the use of a cracking catalyst. In addition, knowledge is obtained on the thermal stability of lignin.

Chapter 7 summarizes the key learnings of this research, draws an overall conclusion and presents an outlook on the potential of the pyrolysis and liquefaction process and the further developments needed.

CHAPTER II

APPROACHING THE BIOMASS PYROLYSIS PROCESS

1 BIOMASS PYROLYSIS

1.1 PRINCIPLES

Mankind has used pyrolysis and related processes for thousands of years. The earliest known example is the use of charcoal, produced as an unintentional residue from cooking fires, for cave drawings by Cro-Magnon man some 38000 years ago [28]. Pyrolysis dates back to at least ancient Egyptian times, when tar for caulking boats and embalming agents were made by pyrolysis. In the Bronze Age charcoal was used for smelting metals. Pyrolysis processes have been used for thousands of years for coke and charcoal production. Before fossil fuels became the preferred feedstocks for chemical production, in the early part of the twentieth century, biomass pyrolysis reactors in industrialized countries consisted of various types of ovens and horizontal and vertical steel retorts, essentially all of which were operated in the batch mode. Provision was made for charcoal recovery, pyro-ligneous acid refining, by-product recovery and gas recovery and usage [29]. In the 1980s, researchers found that the pyrolysis liquid yield could be increased heating a biomass feedstock at a rapid rate and condensing rapidly the vapors produced [6].

Pyrolysis converts organics to solid, liquid, and gas by heating in the absence of oxygen. The distribution and the amount of products within each solid, liquid, and gas phase produced are strongly dependent on the process variables.

The aim of the slow pyrolysis process is to produce mainly charcoal, whereas the fast pyrolysis process should convert the biomass into a maximum quantity of liquid. In fast pyrolysis, biomass decomposes very quickly to generate mostly vapors and aerosols and some charcoal and gas. After cooling and condensation, a dark brown homogenous mobile liquid is formed which has a heating value about half that of conventional fuel oil. Both processes have in common that the energy in the biomass feedstock is concentrated in a smaller volume by which transport costs and storage space can be reduced. Also beneficial is that a more uniform, stable, and cleaner-burning product is obtained, that could serve as an intermediate energy carrier and feedstock for subsequent processing.

Virtually any form of biomass can be considered for pyrolysis. While most work has been carried out on wood because of its consistency and comparability between tests, over 100 different biomass types have been tested by many laboratories, ranging from agricultural wastes such as straw, olive pits and nut shells to energy crops such as miscanthus and sorghum, forestry wastes such as bark and solid wastes such as sewage sludge and leather wastes. In all cases, a commercial process comprises three main stages from feed reception to delivery of one or more useful products:

- Feed reception, storage, handling, preparation and pre-treatment;
- Conversion of biomass by pyrolysis to a more usable form of energy in liquid/solid form;
- Conversion of this primary product by processing, refining or clean-up to a marketable end-product such as electricity, heat, biofuels and/or chemicals.

1.2 MECHANISM AND KINETICS

The kinetics of thermal decomposition of biomass materials is complicated, as it involves a large number of reactions in parallel and series. Each of the structural constituents of biomass (hemicelluloses, cellulose, lignin, extractives) pyrolyze at different rates and by different mechanisms and pathways. The rate and extent of degradation of each of these components depend on the process parameters, reactor type, temperature, particle size, heating rate and pressure. The general changes that occur during pyrolysis are enumerated below [6]:

- i. Heat transfer from a heat source increases the temperature inside the fuel;
- ii. The initiation of primary pyrolysis reactions releases volatiles and forms char;
- iii. The flow of hot volatiles toward cooler solids results in heat transfer between hot volatiles and cooler un-pyrolyzed fuel;
- iv. Condensation of some of the volatiles in the cooler parts of the fuel, followed by secondary reactions, can produce tar;
- v. Autocatalytic secondary pyrolysis reactions proceed while primary pyrolytic reactions (item ii, above) simultaneously occur in competition;
- vi. Further thermal decomposition, reforming, water gas shift reactions, radicals recombination, and dehydrations can also occur, which are a function of the process's residence time/temperature/pressure profile.

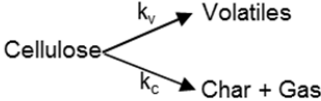

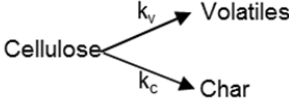
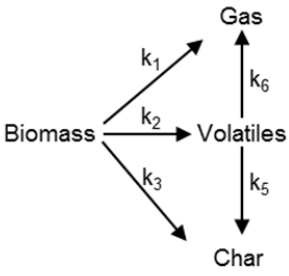
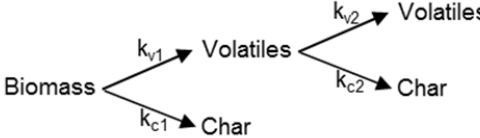
Over the past two decades, several types of biomass pyrolysis models have appeared in the literature. These models can be categorized into three categories. First category, where pyrolysis is described as a set of single step multiple reactions. In second class of models, thermal decomposition is expressed as a single first order irreversible reaction. These models are also known as "global decomposition models". In a third category of models, pyrolysis is described as a two-step process that exclusively account for the primary and secondary reactions. All of these models are summarized in Table 5.

Broido and Nelson (1975) [30] first proposed a single step-multiple reaction type mechanism for cellulose degradation based on the thermogravimetric study. According to this mechanism, cellulose preferentially produced char and low molecular weight volatiles at temperatures $<250^{\circ}\text{C}$. At higher temperatures ($>280^{\circ}\text{C}$), a competing reaction led to tar formation. This mechanism did not differentiate between char and gaseous compounds. It was later modified by Shafizadeh et al. (1979) [31] who proposed that cellulose first undergoes depolymerization to produce anhydro fragment, called as "active cellulose". The

active cellulose easily degraded into tar, char and gases through three single step reactions. They also speculated the secondary char formation from the re-polymerization of components of tar; however could not provide evidence based on the thermogravimetric data. This model is also known as Broido-Shafizadeh model (B-S model).

Mok and Antal (1983) [32] pointed out that both the above mentioned studies [30], [31] overlooked the fact that sufficiently large sample size (100-250 mg) was used, such that significant vapor-solid interactions could have incurred in the TGA. They coupled TGA with the Differential Scanning Calorimeter (DSC) and observed that at low sample size and high gas flow rates, very less amount of char was produced and reaction was endothermic. However, when larger sample size and lower flow rates were used, the char yield was 23% accompanied by the strongly exothermic reaction.

Table 5. Kinetic models proposed for biomass/cellulose pyrolysis

	Broido and Nelson (1975)
	Broido and Shafizadeh (B-S model) (1979)
	Suuberg and co-workers (1996)
	Modified B-S model (1979)
	Koufopoulos (1991)

Few years later, Suuberg and coworkers (1996) [33], [34] studied cellulose pyrolysis at various heating rates ranging between 0.1-60°C/min. They observed a transition in global decomposition kinetics at around 320°C from higher activation energy process (218 kJ/mol) to a lower activation energy process (140 kJ/mol). They explained these results on the basis of two single step competing reactions:

endothermic reaction of tar evaporation (538 J/g of volatiles) which is favored at higher heating rates and an exothermic reaction of char formation (2 kJ/g of char formed) which is favored at low heating rates.

All of the aforementioned models did not account for the secondary reactions that occur during pyrolysis. In order to exclusively account for these reactions, Shafizadeh et al. [35] proposed a modified version of B-S model, according to which, primary products (bio-oil, char and gases) were produced via three competing reactions from biomass and the bio-oil vapors further decomposed to produce secondary char and gases. Another model that accounted the secondary reactions was proposed by Koufopoulos et al. [36]. In this model, first stage consisted of two competing reactions producing primary volatiles and char. In a second stage, primary volatiles and char reacted to produce secondary volatiles and secondary char. Two research groups, Di Blasi et al. [37]–[39] and Babu et al. [40], [41] have presented elaborate models for biomass pyrolysis based on the original models proposed by Shafizadeh and Koufopoulos respectively. These models incorporate intra- and extra-particle heat transfer to simulate the pyrolysis behavior of single particle in a fluidized bed reactor, and are widely accepted today. An extended literature documents in details the radical reaction processes that take place during biomass pyrolysis, provided by Ranzi et al. [14], [42], [43].

1.3 TYPE OF REACTOR

The heart of a fast pyrolysis process is the reactor and considerable research development has focused on reactor types. Pyrolysis, perhaps more than any other conversion technology, has received considerable creativity and innovation in devising reactor systems.

Table 6. Fast pyrolysis reactors and heating methods[44]

Reactor type	Method of heating
Ablative coil	Reactor wall heating
Ablative mill	Reactor wall (disc) heating
Ablative plate	Reactor wall heating
Ablative vortex	Reactor wall heating
Circulating fluid bed	In-bed gasification of char to heat sand
Cyclone or vortex	Reactor wall heating
Entrained flow	Char combustion products Hot sand
Fluid bed	Heated recycle gas Hot inert gas Partial gasification Fire tubes
Horizontal bed	Fire tubes
Vacuum multiple hearth	Hearth heating
Rotating cone	Wall and sand heating
Stirred bed	Partial gasification of char
Transported bed	Recirculated hot sand heated by char combustion
Vacuum moving bed	Direct contact with hot surface

Table 7. Pyrolysis reactors types and characteristics*Bubbling fluid bed reactors*

- Simple construction and operation
- Good temperature control
- Very efficient heat transfer to biomass particles due to high solids density
- Easy scaling
- Well-understood technology
- Good and consistent performance with high liquid yields: of typically 70–75 wt.% from wood on a dry feed basis
- Small biomass particle sizes are needed to achieve high biomass heating rates of less than 2–3mm
- Residence time of solids and vapors is controlled by the fluidizing gas flow rate and is higher for char than vapors
- Char acts as an effective vapor cracking catalyst: good char separation is important

Circulating fluid bed and transported bed reactors

- Good temperature control
- Residence time for char is almost the same for vapor and gas: char is more attrited due to higher gas velocities
- Suitable for very large throughputs
- Well-understood technology
- Hydrodynamics more complex
- Closely integrated char combustion: more careful control requirements
- Heat transfer at large scale has to be proven

Ablative pyrolysis

- High pressure of particle on hot reactor wall, achieved due to centrifugal or mechanically force
- Large feeding size can be used
- High relative motion between particle and reactor wall
- Inert gas is not required: the processing equipment is smaller
- Reaction rates are limited by heat transfer to the reactor
- The reaction system is more intensive and complex
- The process is surface area controlled so scaling is more costly

Entrained flow

- Simple technology
- Poor heat transfer
- High gas flows give large plant and cause difficult liquid collection
- Good scale-up
- Lower liquid yields

Rotating cone

- Centrifugation (at around 10 Hz) drives hot sand and biomass up a rotating heated cone
- Carrier gas requirements are much less than for fluid bed and transported bed systems, however, gas is needed for char burn off and for sand transport
- Complex integrated operation of three subsystems is required: rotating cone pyrolyser, riser for sand recycling, and bubbling bed char combustor
- Liquid yields of 60–70% on dry feed are typically obtained

Vacuum pyrolysis

- Not a true fast pyrolysis process as solids residence time is very high
- It can process larger particles than most fast pyrolysis reactors
- There is less char in the liquid product due to lower gas velocities
- There is no requirement for a carrier gas
- Liquid yields of 35–50% on dry feed are typically obtained
- The process is relatively complicated mechanically

A variety of pyrolysis processes has been reported in the literature. The designs usually aim at satisfying three criteria: (1) a high temperature to enable cracking and decomposition reactions; (2) a large heat supply to drive them; and (3) a short residence time to minimize the condensation of volatile products [21].

As fast pyrolysis for liquids occurs in a few seconds or less, heat and mass transfer processes and phase transition phenomena, as well as chemical reaction kinetics, play important roles. The critical issue is to bring the reacting biomass particles to the optimum process temperature and minimize their exposure to the lower temperatures that favor formation of charcoal. One way this objective can be achieved is by using small particles, for example in the fluidized bed processes. Another possibility is to transfer heat very fast only to the particle surface that contacts the heat source which is used in ablative processes. In Table 6 the fast pyrolysis reactor and their relative heating methods are summarized.

During the last two decades, several different reactor designs have been explored that meet the rapid heat-transfer requirements. These reactor configurations have been shown to achieve liquid-product yields as high as 70%-80%, based on the starting dry biomass weight. Modern pyrolysis reactor configurations include fixed beds, moving beds, suspended beds, fluidized beds, entrained flow reactors, stationary vertical shaft reactors, horizontal shaft kilns, inclined rotating kilns, single and multi-hearth reactors and a host of other designs (Table 7). The most important configurations representative of biomass pyrolysis processes near commercialization can be classified within the following categories: bubbling fluidized-bed reactors; circulating fluidized-bed reactors; rotating cone reactors; ablative reactors, both cyclonic and plate type [6], [29], [44].

1.3.1 BUBBLING FLUIDIZED-BED REACTORS

A simple method for the rapid heating of biomass particles is to mix them with the moving sand particles of a high temperature fluid bed. High heat transfer rates can be achieved, as the bed usually contains small sand particles, generally about 250 μm . The heat required is generated by combustion of the pyrolysis gases, and/or char, and is eventually transferred to the fluid bed by heating coils (Figure 7). While the sand-to-biomass heat transfer is excellent, the heat transfer from the heating coils to the fluid bed is low, due to the resistance inside the coils, and the limiting driving force between the coils at 800-600°C and the fluid bed at 500-550°C. In an optimistic case, at least 10 to 20 m^2 surface area is required per ton/h of biomass fed [45].

Bubbling fluidized beds are usually referred to simply as fluidized beds, as opposed to circulating fluidized beds. Bubbling fluidized beds have the advantages of a well understood technology that is simple in construction and easy in operation [6], [17], [27]. Sand is often used as the solid phase of the bed. Bubbling fluidized beds produce good quality bio-oil with a high liquid product yield. Char does not accumulate in the fluidized bed, but it is rapidly eluted. The residence time of solids and vapors is controlled by the fluidizing gas flow rate. Char has a higher residence time than the vapors. The char acts as an effective vapor cracking catalyst at fast pyrolysis reaction temperatures. Therefore, rapid and effective char separation is important. This is usually achieved by ejection followed by separation in one or more cyclone separators. The byproduct char is typically about 15 wt.% of the products but about 25% of the energy of the biomass feed [17]. It can be used within the process to provide the process heat requirements by combustion or it can be separated and exported, in which case an alternative fuel is required. Depending on the reactor configuration and gas velocities, a large part of the char will be of a

comparable size and shape as the biomass fed. The fresh char is pyrophoric i.e. it spontaneously burns when exposed to air so careful handling and storage is required.

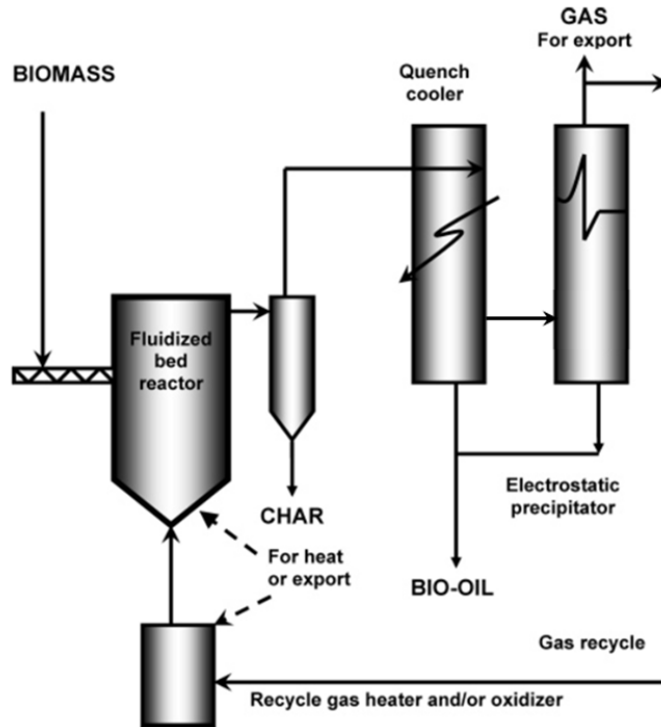


Figure 7. Bubbling fluidized bed reactor [6]

1.3.2 CIRCULATING FLUIDIZED-BEDS REACTORS

In a circulating fluidized bed (CFB), biomass is screwed into a reactor, where extensive contacting between inert particles (sand) and biomass takes place. Together with the char, sand is entrained out of the reactor, and sent to a combustor chamber where the char is burned. The main advantage of the CFB system compared to fluid bed is the direct heat supply to the biomass by recirculation of sand, reheated by combustion of pyrolysis char.

A typical layout is shown in Figure 8. Circulating fluidized bed and transported bed reactor systems have many of the features of bubbling beds, except that the residence time for the char is almost the same as that for the vapors. Furthermore, because of higher gas velocities, the char contents in the condensed bio-oil are higher, unless more extensive char removal are included [17]. An added advantage is that CFB is potentially suitable for larger throughputs even though the hydrodynamics are more complex as this technology is widely used at very high throughputs in the petroleum and petrochemical industry. Heat supply is usually from recirculation of heated sand from a secondary char combustor, which can be either a bubbling or circulating fluid bed. This leads to ash buildup in the circulating solids. Biomass ash is

known to be a cracking catalyst for the organic molecules in the volatile pyrolysis products. This causes a loss of volatiles from the bio-oil yield [6].

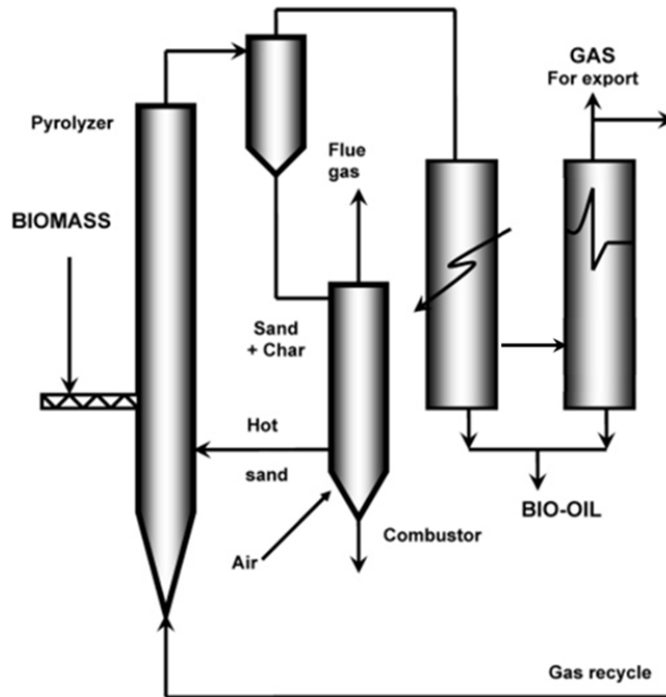


Figure 8. Circulating fluidized bed reactor [17]

1.3.3 ABLATIVE REACTORS

The surface, heated by hot flue gas, is rotating, and biomass is pressed onto the hot surface (approx. 600°C). The flue gas is produced by combustion of pyrolysis gases and/or of produced char.

In general the following limitations for this ablative technology can be expected: (i) limited heat transfer rates to the hot surface due to the indirect heating principle. This is caused by both a relatively small temperature difference between hot flue gas (likely around 800°C) and the pyrolysis reactor (around 500°C), and a low heat transfer coefficient. (ii) restrictions in feedstock morphology (particle shape, structure and density), the particle size and its free-flowing characteristics, because the material needs to be pressed against a hot surface.

1.3.4 ROTATING CONE REACTORS

In the rotating cone reactors, (Figure 9) biomass at ambient temperature is mixed with hot sand. Upon mixing with the hot sand of 550°C, biomass decomposes into condensable vapors, non condensable gases and char. An important characteristic of this reactor type is the absence of carrier gas, since it is the

rotating action of the cone which propels the solids from the reactor entrance to its exit. Because of the absence of carrier gas, the vapor products are not diluted and their flow is minimal. An undiluted and concentrated product flows from the reactor leads to small downstream equipment with related minimal investment costs. In mechanical terms, the reactor technology is remarkably simple and robust. The rotational speed of the cone is only 300 rpm and after more than 1000 h of operation signs of abrasion or wear are absent. Scaling-up of the reactor is possible by increasing its diameter. For capacities which require a cone diameter larger than 2m, stacking of multiple cones on a single axis leads to the lowest investment costs [29].

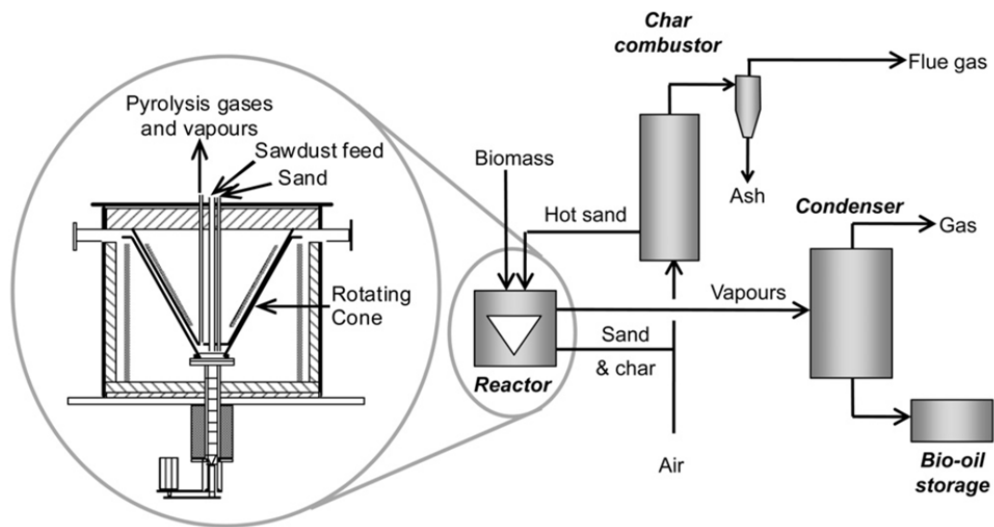


Figure 9. Rotating cone pyrolysis reactor and integrated process

2 YIELDS AND ENERGY DISTRIBUTION IN PYROLYSIS PROCESS

2.1 INFLUENCE OF PROCESS CONDITIONS

The relative proportions into the three product categories based on their physical state of existence: char (solid), bio-oil (liquid) and non-condensable gases (gas) significantly vary depending upon the process conditions. Temperature, pressure, heating rate, vapor residence time and particle size are the main operative factors which affect the heat and mass transfer phenomena and the kinetics during biomass pyrolysis, therefore having an important influence on the outcomes and yields of the thermal decomposition process.

The mainstream studies on the influence of process conditions on pyrolysis focused on the effect of heating rate and final pyrolysis temperature on product distribution, product composition and product energy content [36]. Lower process temperatures and longer vapor residence times favor the production of charcoal. High temperatures and longer residence times increase biomass conversion to gas, and moderate temperatures and short vapor residence time are optimum for producing liquids [17] (Figure 10).

In slow wood pyrolysis, biomass is heated to ~ 500 °C, with a heating rate of about 0.1 to 1 °C/s for a vapor residence time that varies from 5 min to 30 min [46]. Vapors do not escape as rapidly as they do in fast pyrolysis. Thus, components in the vapor phase continue to react with each other, as the solid char and any liquid are being formed [6]. In slow pyrolysis, lower heating rate and longer vapor residence time provides a suitable ambience and sufficient time for the secondary reactions to complete. Moreover, longer vapor residence time allows those vapors to be removed which are produced during the secondary reaction. This ultimately results in the formation of solid carbonaceous biochar [47].

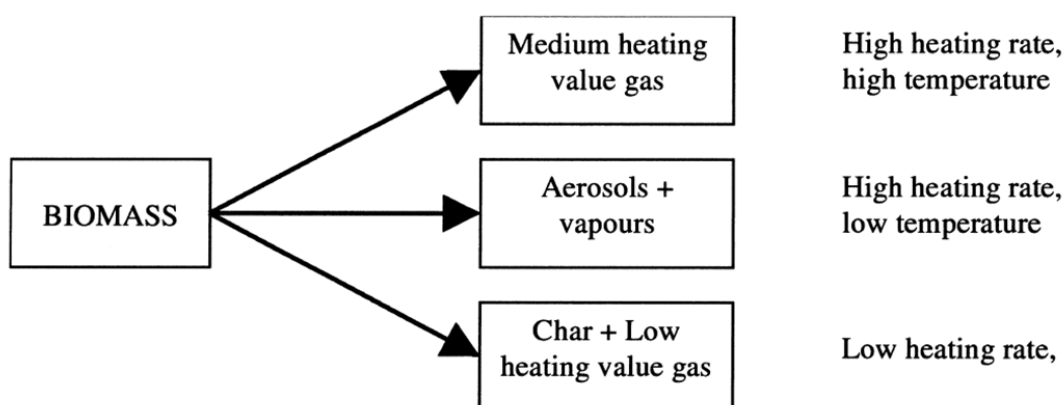


Figure 10. Biomass pyrolysis pathways [44]

Over the last two decades, fundamental research on fast or flash pyrolysis has shown that high yields of primary, non-equilibrium liquids and gases, including valuable chemicals, chemical intermediates, petrochemicals, and fuels, could be obtained from carbonaceous feedstocks. Thus, the lower value solid char from traditional slow pyrolysis can be replaced by higher-value fuel gas, fuel oil, or chemicals from fast pyrolysis [44].

In fast pyrolysis the main product, bio-oil, is obtained in yields of up to 75 wt.% on a dry-feed basis, together with by-product char and gas which can be used within the process to provide the process heat requirements so there are no waste streams other than flue gas and ash. There are four essential features of a fast pyrolysis process [18]. First, very high heating (1000°C/s) and heat transfer rates are used, which usually requires a finely ground biomass feed. Second, a carefully controlled pyrolysis reaction temperature is used, often in the 425-500 °C range. Third, short vapor residence times are used (typically <2 s). Fourth, pyrolysis vapors and aerosols are rapidly cooled to give bio-oil [6]. Liquid yield depends on biomass type, temperature, hot vapor residence time, char separation, and biomass ash content, the last two having a catalytic effect on vapor cracking. A fast pyrolysis process includes drying the feed to typically less than 10% water in order to minimize the water in the product liquid oil.

Table 8 and Figure 11 indicate the product distribution obtained from different modes of pyrolysis, showing the considerable flexibility achievable by changing process conditions. Reaction conditions are very important in the pyrolysis, since they affect not only the yields of pyrolysis products, but also their quality. Increasing the vapor residence time helps the re-polymerization of the biomass constituents by giving them sufficient time to react. Residence time not only affects the biochar yield but it also influences the

quality and characteristics of bio-char by promoting the development of micro- and macro-pores. Longer residence time has been reported to enhance the pore size in the char [47].

Table 8. Typical product weight yields (dry wood basis) obtained by different modes of pyrolysis of wood [17].

Mode	Conditions	Liquid	Solid	Gas
Fast	~500°C, short hot vapour residence time ~1 s	75%	12% char	13%
Intermediate	~500°C, hot vapour residence time ~10-30 s	50%	25% char	25%
Carbonization (slow)	~400°C, long vapour residence time hours-days	30%	35% char	35%
Torrefaction (slow)	~290°C, solids residence time ~10-60 min	0-5%	80% solid	20%

Particles size is a factor which should be also taken care in the pyrolysis process as it can control the rate at which the heat is transferred to the input biomass. On increasing the particle size the distance between the surface of the input biomass and its core increases which retards the rapid heat flow from the hot to cold end. This temperature gradient favors the char yield. Also on increasing the particle size the vapor formed during the thermal cracking of biomass has to cover more distance through the char layer causing more secondary reactions resulting in the formation of more amounts of char [47].

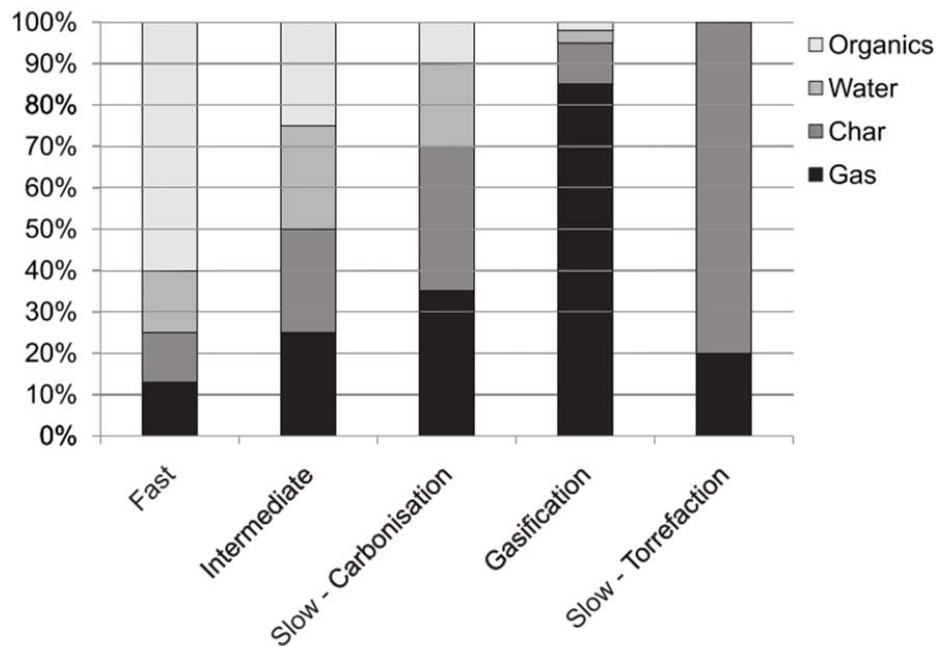


Figure 11. Product fraction distribution from pyrolysis [17]

Carrier gas flow rate is another parameter that influences the pyrolysis product distribution. Moderate to high amount of vapors are formed during the pyrolysis of biomass and if these vapors are not purged out

they can involve themselves in the secondary reactions and can change the nature and composition of the pyrolysis products.

2.2 PYROLYSIS PRODUCTS

The condensation of pyrolysis vapors and aerosols yields a dark brown colored liquid with a distinct smoky odor called as bio-oil. Non-condensable fraction of pyrolysis vapors usually consists of gaseous species such as carbon monoxide, carbon dioxide, methane and hydrogen. Solid residue obtained from pyrolysis is called as charcoal or char. It consists of dehydration, condensation and re-polymerization products of the non-volatile fragments of hemicellulose, cellulose and lignin that are produced during pyrolysis.

2.2.1 BIO-OIL

The liquid fraction of biomass pyrolysis is a complex mixture of water and organic chemicals. Water contents are typically in the range of 15-35% wt., although values outside this range have been reported. Organic components consist of acids, alcohols, aldehydes, ketones, esters, phenols, guaiacols, syringols, sugars, furans, alkenes, aromatics, nitrogen compounds and miscellaneous oxygenates. Their average molecular weight varies in the range of 300-1000 g/mol [29], [44]. The presence of water lowers the heating value and flame temperature; however, it reduces the viscosity and enhances the fluidity, which is good for bio-oil combustion in engines. The high oxygen content (35-40%) lowers the energy density and immiscibility with hydrocarbon fuels. Depending on the biomass feedstocks and pyrolytic processes, the viscosities of bio-oils vary in a large range (10-100 cP at 40°C). Aging studies have shown that viscosity and molecular weight increase together with time [29]. The storage stability of pyrolysis oil is rather poor. Bio-oil ages after it is first recovered, which is observed as a viscosity increase. Some phase separation may also occur. The instability is believed to result from a breakdown in the stabilized micro-emulsion and to chemical reactions, which continue to proceed in the oil. The carboxylic acids of bio-oil account for its acidic pH of 2–3. Acidity makes bio-oil very corrosive, requiring upgrading before use. The ash content of the pyrolysis oil has shown to be directly related to the char content of the oils. The lower heating value (LHV) of bio-oils is only 40–45% of that exhibited by hydrocarbon fuels. On a volume basis it is ~60% of the heating value of hydrocarbon oils, because of the high oxygen content, the presence of water and the higher density. A typical heating value of bio-oil is 17MJ/kg [29].

2.2.2 GAS

The pyrolysis gas contains carbon dioxide, carbon monoxide, methane, hydrogen, ethane, ethylene, minor amounts of higher gaseous organics and water vapor. Primary gases of fast pyrolysis (less than 5% wt. of the dry feed) contain about 53% wt. CO₂, 39% CO, 7% hydrocarbons (including methane) and <1 H₂. In practice, a part of the organic vapors is cracked to secondary gases, containing 9% wt. CO₂, 63% CO, 27% HC and 1.4% H₂. The LHV of these primary gases is 11MJ/m³ and that of pyrolysis gases formed, after severe secondary cracking of the organic vapors, is 20MJ/m³ [29].

2.2.3 CHAR

Char is the other major pyrolysis product. Depending on temperature, the char fraction contains inorganic materials, any unconverted organic solids and carbonaceous residues, produced on thermal decomposition of the organic components, in particularly lignin. The small particle size and high volatility of char, made in fast pyrolysis, cause it to be very flammable (auto-ignition temperature between 200 and 250°C), similar to powdered coal; hence, hot char must be properly handled. The ash content of the char is 6–8 times greater than in the original feed and as its alkali content is high it may cause slagging, deposition and corrosion problems in combustion. The LHV of chars have been reported to be about 32MJ/kg [29].

3 HEAT TRANSFER

There are two important requirements for heat transfer in a pyrolysis reactor: (i) to the reactor heat transfer medium (solid reactor wall in ablative and fixed bed reactors, gas and solid in fluid and transport bed reactors, gas in entrained flow reactors); (ii) from the heat transfer medium to the biomass.

The heat transfer rate that is necessary to heat the particles imposes a major design requirement. Each mode of heat transfer imposes certain limitations on the reactor operation and may increase its complexity. Two main ways of heating biomass particles can be considered: gas-solid heat transfer by primarily convection and solid-solid heat transfer with mostly conductive heat transfer. The penalties and interactions are summarized in Table 9.

Fluid bed pyrolysis utilizes the inherently good solids mixing to transfer approximately 90% of the heat to the biomass by solid-solid heat transfer with a probable small contribution from gas-solid convective heat transfer [44]. Circulating fluid bed and transport reactors also rely on both gas-solid convective heat transfer from the fluidizing gas and solid-solid heat transfer from the hot fluidizing solid although the latter may be less significant than fluid beds due to the lower solids bulk density. Some radiation effects occur in all reactors. The important feature of ablative heat transfer is that the contact of the biomass and the hot solid abrades the product char off the particle exposing fresh biomass for reaction. This removes particle size limitations in certain ablative reactors, but at the expense of producing micro-carbon which is difficult to remove from the vapor phase and reports to the liquid product.

Once the heat is transferred to the particle surface, the temperature inside the particle increases causing the removal of moisture that is present in the biomass particle and the starting of pyrolysis reactions [48]. Volatiles and gaseous products flow through the pores of the particle and participate in the heat transfer process. The pyrolysis reactions proceed with a rate depending upon the local temperature. During the pyrolysis process, the pores of the solid are enlarged, and the solid particle merely becomes more porous because the biomass converts into gases as discussed by Curtis and Miller [49]. According to Anthony and Howard [50], the enlarged pores of the pyrolyzing solid offer many reaction sites to the volatile and gaseous products of pyrolysis and favor their interaction with the hot solid. Inside the pyrolyzing particle, heat is transmitted by the following mechanisms: (a) conduction inside the solid particle, (b) convection inside the particle pores and (c) convection and radiation from the surface of the pellet.

Table 9. Reactor types and heat transfer [44]

Reactor type	Mode of heat transfer	Advantages/Disadvantages/Features
Ablative	95% Conduction 4% Convection 1% Radiation	Accepts large size Very high mechanical char abrasion from biomass Compact design Heat supply problematical Heat transfer gas not required Particulate transport gas not always required
Circulating fluid bed	80% Conduction 19% Convection 1% Radiation	High heat transfer rates High char abrasion and erosion leading to high char yield Char/solid heat carrier separation required Solids recycle required; Increased complexity of system Maximum particle sizes up to 6 mm Possible liquids cracking by hot solids Possible catalytic activity from hot char Greater reactor wear possible
Fluid bed	90% Conduction 9% Convection 1% Radiation	High heat transfer rates Heat supply to fluidising gas or to bed directly Limited char abrasion Very good solids mixing Particle size limit <2 mm in smallest dimension Simple reactor configuration
Entrained flow	4% Conduction 95% Convection 1% Radiation	Low heat transfer rates Particle size limit <2 mm Limited gas/solid mixing

According to these assumptions several researchers have developed formulation of energy conservation to model pyrolysis of a biomass particle. Mathematical models that are capable to describe pyrolysis phenomena can greatly assist the large scale development and optimization of pyrolysis processes [51]. In the field of biomass pyrolysis, there have been quite a number of works on modelling particle pyrolysis [34], [37], [38], [41], [47], [50], [51], [52], [53].

In modelling biomass particle pyrolysis, it is common to employ a kinetic model, whether it is a simple lumped kinetic model or a complex multiple reactions one, to form the base of the model for describing pyrolysis reactions. Afterwards, the consideration of the physical processes that involve physical changes, heat transfer and mass transfer comes in place. Furthermore, additional elements such as secondary reaction, particle shrinkage, heat of pyrolysis reaction, vapour residence time and interaction with the reactor environment are usually considered and studied.

3.1 HEAT OF REACTION

The paucity of reliable enthalpy of pyrolysis information is partly attributable to the fact that a simple calculative approach, based upon the enthalpies of formation of the starting material and of the products of the process, is still impractical. As it is the case with many pyrolysis processes, there is such a broad

range of products that the full accounting of products that would be necessary for obtaining a precise calculated value remains too difficult.

Literature review indicates a large scatter in the reported values for the heat of pyrolysis. A survey performed by Milosavljevic et al. [33] revealed that it may be in the range of -2100 to 2500 kJ/kg. The width of the range of results is due to variations in experimental method and in the conditions of pyrolysis [56]. Given the difficulty of measuring the pyrolysis heat, most of past researchers treated it as an adjustable parameter which would give reasonable agreement between the results of simulation and measurements. A pyrolysis heat of 418 kJ/kg was suggested by Chan et al. [57]; Gronli [58] assumed a heat of 150 kJ/kg for primary reactions; Park [53] estimated an endothermic heat of 64 kJ/kg for three parallel reactions. In contrast, there are limited studies which have intended to experimentally determine the pyrolysis heat, with no aid of parameter fitting in the simulating model. Havens et al. [59] showed that, based on experiments of differential scanning calorimetry (DSC), the heat of pyrolysis for pine and oak is 200 kJ/kg and 110 kJ/kg, respectively. In another effort to measure the pyrolysis heat of *Pinus Pinaster* thermal degradation using DSC, Bilbao et al. [60] reported an endothermic heat of 274 kJ/kg up to a conversion of 60%, whereas for the remaining conversion of the biomass, the process was observed to be exothermic with a heat of -353 kJ/kg. An extensive investigation to determine the heat of pyrolysis of dried cylindrical maple particles with 2 cm diameter and 8 cm length was conducted by Lee et al. [49] at two heat fluxes of 30 kW/m² and 84 kW/m². Their results showed that at a low heat flux the pyrolysis layer could be divided into three zones: an endothermic primary decomposition zone at temperatures up to 250°C, an exothermic partial char zone between 250°C and 340°C, and an endothermic surface char zone at 340°C < T < 520°C. The overall mass weighted heat of reaction was endothermic to the extent of 610 kJ/kg. In contrast, the overall heat of reaction at the higher heat flux was exothermic, being greater for perpendicular heating (in the range of -1090 to -1720 kJ/kg) than for parallel heating (in the range of -105 to -395 kJ/kg). The authors concluded that the heat of pyrolysis depends upon the external heating rate, total heating time and properties of biomass and char relative to the internal flow of heat and gas.

Milosavljevic et al. [33] studied the thermo-chemistry of cellulose pyrolysis by a combination of DSC and thermogravimetric analysis. They found that the main thermal degradation pathway was endothermic in the absence of mass transfer limitations that promoted char formation. They concluded that the endothermicity, which was estimated to be about 538 kJ/kg of volatiles evolved, was mainly due to latent heat requirement for vaporizing the primary tar decomposition products. It was also reported that the pyrolysis could be driven in the exothermic direction by char forming processes that would compete with tar forming processes. The formation of char, which was favored at low heating rates, was estimated to be exothermic to the extent of 2000 kJ/kg of char formed. The authors arrived at an interesting conclusion that the heat of pyrolysis could be correlated with the char yield at the end of pyrolysis, a result which was somewhat consistent with findings of Mok and Antal [32], who also observed a linear decrease in the endothermic heat of pyrolysis as the char yield increased. Hence, it was concluded that the char yield was the main factor determining whether the overall pyrolysis process is endothermic or exothermic. Table 10 summarizes the above discussed values of the pyrolysis heat which have been obtained by different researchers either through a fitting procedure or based on measurements.

Table 10. Values of heat of pyrolysis reported in literature

Heat of pyrolysis (kJ/kg)	Method	Reference
418	Fitting with experiments	Chan et al. [57]
150	Fitting with experiments	Gronli [56]
64	Fitting with experiments	Park [51]
255	Fitting with experiments	Koufopoulos et al. [61]
-20	Fitting with experiments	Koufopoulos et al. [61]
200	Measured	Havens et al. [57]
110	Measured	Havens et al. [57]
274	Measured	Bilbao et al. [58]
-353	Measured	Bilbao et al. [58]
610	Measured	Lee et al. [47]
-1090 to -1720	Measured	Lee et al. [47]
-105 to -395	Measured	Lee et al. [47]
0 to -420	Measured	Roberts [62]
500	Measured	Sibulkin [63]
1464 to -301	Measured	Curtis and Miller [49]
0	Measured	Atreya et al. [53]
570 to 710	Measured	Stenseng [64]
-2000	Measured	Milosavljevic I [34]

From these studies, it can be now understood why a wide range of values for the pyrolysis heat has been reported in the literature. How critical the accurate knowledge of the enthalpy of pyrolysis is depends upon the particular application. One application involves modeling fire phenomena: the pyrolytic behavior of cellulose is of interest in the context of fire and combustion research because this material serves as a good model of a charring solid and it is also obviously important in its own right [33]. In such analyses, an accurate heat of cellulose pyrolysis reactions is not the key to correctly modeling the thermal process occurring by the solid. Rather, for the purpose of simulating thermal degradation of a biomass particle, it is of importance that the pyrolysis heat must be chosen from similar heating and comparable measurement conditions (such as similar char yield) if it is taken from a referred source. Alternatively, it should be carefully correlated by comparing the simulation results with measurements, otherwise the predicted parameters of the pyrolysis model may not be reliable.

Furthermore the heat of pyrolysis is a useful concept for modelling not only pyrolysis process but also combustion and gasification process and its value cannot be determined from the thermodynamics properties alone. Pyrolysis is always also the first step in combustion and gasification processes where it is followed by total or partial oxidation of the primary products. The thermal characteristics of the pyrolysis process as one of the unavoidable steps during thermal decomposition of a biomass particle need to be carefully investigated.

3.2 ENERGY BALANCES IN THE PYROLYSIS PROCESS

The thermal effects of the pyrolysis process are of utmost importance for the selection and design of thermal conversion routes for biomass. The design of the system may vary with respect to heat transfer issues or sizing of the reactor on the basis of the energy required to carry out the pyrolysis. Energy contributions required to run the pyrolysis process are mainly:

- Transportation
- Chopping/Grinding
- Drying
- Heating to pyrolysis temperature
- Enthalpy of reaction
- Driving the equipment.

In theory, all this can be supplied by recycle from the products, once the process has been started-up, with the effect that the product quantities available for use downstream of the pyrolysis process are reduced.

Energy use in biomass transportation has been estimated for tractors, trucks, electric trains and boats for coastal shipping [65]. Delivered feedstock typically requires pretreatment prior to being fed into a pyrolysis reactor to avoid penalties that reduce yields and increase heat requirements. Mechanical particle-size reduction and drying are commonly used in thermochemical processes. Grinding biomass is an expensive and energy-intensive process. Grinding costs can add up to 11 \$/Mt of biomass [66]. Specific energy requirements can vary based on equipment and feedstock conditions. Feedstock drying is very important for thermochemical processes. Moisture embedded in the feed consumes process heat and contributes to lower process yields. For reasonable pyrolysis performance, moisture content of less than 7% is recommended [67]. Biomass drying typically requires about 50% more energy than the theoretical minimum of 2442 kJ per kg of moisture evaporated [68].

Enthalpy of pyrolysis is defined as the energy required to raise biomass from room temperature to the reaction temperature and convert the solid biomass into the reaction products of gas, liquids, and char. It is the total energy consumed by the biomass during pyrolysis, including contributions to both sensible enthalpy and enthalpy of reaction for the pyrolysis of biomass [68]. The sensible enthalpy refers to the energy absorbed by the biomass to raise its temperature only. The enthalpy of reaction is the energy required to drive the pyrolysis reactions. A standard enthalpy approach, at first glance, would seem suitable in quantifying the energy consumed in pyrolysis. This approach requires that the enthalpy of the products and reactants be referenced to a standard temperature. However, the products of pyrolysis are complex in nature with respect to their composition. Also, the sensible enthalpy or specific heat data corresponding to the products and reactants is many times difficult to determine. These contributions will be well explained and analyzed in the following chapters (Chapter IV and Chapter V) and a method for assessment the enthalpy of reaction will be introduced.

Table 10 shows the wide variety of reaction enthalpies assumed by various authors who have modeled pyrolysis and/or combustion processes in cellulosic biomass (especially wood). It may be noted that in no case the reaction enthalpy has a very large value. For example, if one uses as a crude approximation a constant solid heat capacity of around 2 J/g,K, then the process of heating the sample up to a typical degradation temperature of 350°C would involve a sensible enthalpy increase of about 650 J/g, comparable to the highest reported endothermic pyrolysis enthalpies [33]. Then, if the exotherm from the main reaction exceeds this value, enough energy is released to heat the sample [69]. As it will be clear in the Chapter IV and Chapter V, the process conditions influence at a big extent the exothermicity of the process.

CHAPTER III

EXPERIMENTAL DEVICES AND PROCEDURES

1 THERMOGRAVIMETRIC ANALYZER

1.1 INSTRUMENT CHARACTERISTICS

The Thermogravimetric Analyzer (TGA) is a thermal weight-change analysis instrument. It measures the amount and rate of weight change in a material, either as a function of increasing temperature, or isothermally as a function of time, in a controlled atmosphere. It can be used to characterize any material that exhibits a weight change and to detect phase changes due to decomposition, oxidation, or dehydration. A TGA consists of a sample pan that is supported by a precision balance. That pan resides in a furnace and is heated during the experiment, while purge gas controls the sample environment. The gas may be inert or a reactive gas that flows over the sample and exits through an exhaust. The mass of the sample is monitored during the experiment.



Figure 12. Thermogravimetric analyzer used in this study (TGA Q500)

The model used in the current study is a TGA Q500 from the TA Instruments Company (Figure 12). The TGA components are:

- The balance, which provides precise measurement of sample weight.
- The sample platform, which loads and unloads the sample to and from the balance.
- The furnace, which controls the sample atmosphere and temperature.
- The cabinet, where the system electronics and mechanics are housed.
- The heat exchanger, which dissipates heat from the furnace.
- The two mass flow controllers, which control the purge gas to the balance and furnace.

The TGA Q500 operates in the temperature range from ambient to 1000°C, and has an isothermal temperature accuracy of $\pm 1^\circ\text{C}$ and isothermal temperature precision of $\pm 0.1^\circ\text{C}$. It has a weighing capacity of 1.0 g, a sensitivity of 0.1 μg and a precision of $\pm 0.01\%$ (Table 11).

Table 11. TGA Q500 technical specifications

Temperature range	Ambient +5°C to 1000°C
Thermocouple	Platinel II
Heating rate	0.1 to 50°C/min

1.2 INSTRUMENT CALIBRATION

1.2.1 TEMPERATURE CALIBRATION

Temperature calibration is useful for TGA experiments in which precise transition temperatures are essential. To calibrate the TGA, three high-purity magnetic standards have been used: isotherm, nichel and trafoperm, with a curie temperature of respectively 142.5°C , 357.0°C and 749.0°C. The observed and correct temperatures correspond to the experimental and theoretical curie transition temperatures of the calibrant.

1.2.2 WEIGHT CALIBRATION

The weight calibration procedure calibrates both the 200 mg and 1 g weight ranges. The calibration parameters are stored internally in the instrument. It's essential to determine the exact weight of the calibration weights before they are used to calibrate the instrument.

1.3 EXPERIMENTAL PROCEDURES

All of TGA experiments have the following general outline:

- Selecting the pan type and material.
- Taring the empty sample pan.

- Loading the sample into the pan.
- Entering experiment information through the TA controller, this includes both sample and instrument information.
- Creating or selecting the experimental procedure using the instrument control software.
- Attaching and setting up external accessories as required such as the purge gas.
- Starting the experiment.

Samples used in TG runs were previously dried at 105 °C under a nitrogen flux of 60 ml/min for 10 min. Constant heating rate runs were carried out on the dry samples using a pure nitrogen purge gas flow rate of 60 ml/min, a heating rate of 10 °C/min and a final temperature of 950 °C. The purge gas was then switched to air (60 ml/min for 10 min) in order to allow detecting the ash content of the sample. The thermal program used for the experiments is summarized in Table 12.

Table 12. Operating parameters in TGA experiments

Sample Weight	3 – 20 mg
Final Temperature	950°C
Operating Pressure	Atmospheric
Purge gas flow	60 ml/min
Heating rate	10°C/min

2 DIFFERENTIAL SCANNING CALORIMETER AT ATMOSPHERIC PRESSURE

2.1 INSTRUMENT CHARACTERISTICS

The Differential Scanning Calorimeter (DSC) determines the temperature and heat flow associated with material transitions as a function of time and temperature. It also provides quantitative and qualitative data on endothermic (heat absorption) and exothermic (heat evolution) processes of materials during physical transitions that are caused by phase changes, melting, oxidation, and other heat-related changes.

The model used in the current study is a DSCQ2000 from the TA Instruments Company (Figure 13). A DSC system has three major components: the instrument itself, which contains the system electronics; the cell, which monitors differential heat flow and temperature; and a finned air cooling system which allows operation from ambient to 725°C, using flowing air as coolant (Table 13).

In a "heat flux" DSC, the sample material encapsulated in a pan, and the empty reference pan are sat on a thermoelectric disk surrounded by a furnace. As the temperature of the furnace is changed (usually by heating at a linear rate), heat is transferred to the sample and reference through the thermoelectric disk. The differential heat flow to the sample and reference is measured by area thermocouples using the thermal equivalent of Ohm's Law (Eq. (1)).

$$q = \frac{\Delta T}{R} \quad (1)$$

where q is the sample heat flow, ΔT is the temperature difference between sample and reference, R is the resistance of the thermoelectric disk.

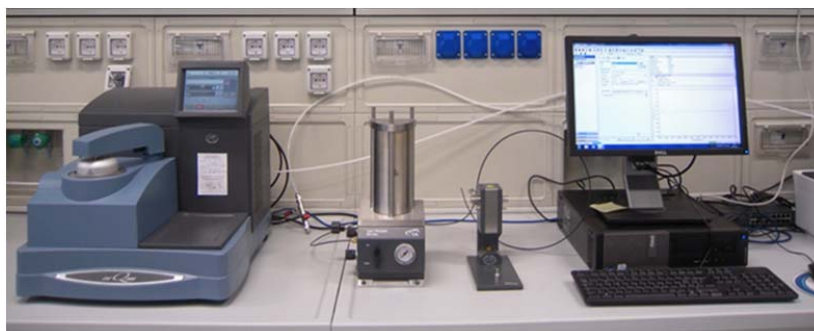


Figure 13. Differential scanning calorimeter at atmospheric pressure used in this study (DSC Q2000)

This simple relationship, however, does not take into account extraneous heat flow within the sensor or between the sensor and sample pan. The TA Instruments Q Series DSC's are specifically designed to account for those latter heat flows. The cell sensor consists of a constantan body with separate raised platforms to hold the sample and reference. The platforms are connected to the heating block (base) by thin-walled tubes that create thermal resistances between the platforms and the base. Area detectors (thermocouples) on the underside of each platform measure the temperature of the sample and reference. A third thermocouple measures the temperature at the base. The equation (2) below shows the thermal network model which represents this cell arrangement, and the resultant heat flow expression that describes this cell arrangement is:

$$q = -\frac{\Delta T}{R_r} + \Delta T_0 \left(\frac{R_r - R_s}{R_r R_s} \right) + (C_r - C_s) \frac{dT_s}{dt} - C_r \frac{d\Delta T}{dt} \quad (2)$$

where ΔT is the measured sample temperature (T_s) minus measured reference temperature (T_r); ΔT_0 is the measured base temperature of sensor (T_0) minus measured sample temperature (T_s); R_r is the reference sensor thermal resistance; R_s is the sample sensor thermal resistance; C_r is the reference sensor heat capacity and C_s is the sensor heat capacity.

The first term in this expression is the equivalent of the conventional single-term DSC heat flow expression. The second and third terms account for differences between the sample and reference resistances and capacitances respectively. These terms have their largest impact during regions of the thermal curve where the heat capacity of the sample is the predominant contributor to heat flow. The fourth term accounts for the difference in heating rate between the sample and reference. This term has its largest impact during enthalpic events (e.g., melting).

Table 13. DSC Q2000 technical specifications

Temperature range	Room temperature to 725°C
Sample size	0.5 to 100 mg (nominal)
Sample volume	10 mm ³ in hermetic pans
Sample pans	Various open or hermetically sealed
Purge gases	Recommended: air, argon, helium, nitrogen, oxygen
Typical purge flow rate	50 ml/min
Cell volume	3.4 ml

2.2 INSTRUMENT CALIBRATION

2.2.1 TZERO CALIBRATION

The DSC Tzero calibration requires two experiments. The first experiment is done without samples or pans; the second is performed with sapphire disks (approximately 95 mg) on both the sample and reference positions without pans. Both experiments use the same method: first the cell is preheated, it follows an equilibration at the initial temperature, holding isothermal for five minutes, heating at constant rate to a final temperature and holding isothermal for 5 minutes. The range of temperatures should be at least as broad as the desired experimental range. Tzero calibration should be done at relatively high heating rates such as 20°C/min in order to obtain the most accurate calibration of the sensor thermal capacitance and resistance values. Rates of less than 10°C/min are not recommended for Tzero calibration.

2.2.2 ENTHALPY CELL CONSTANT CALIBRATION

This calibration is based on a run in which a standard metal (e.g. indium) is heated through its melting transition. The calculated heat of fusion is compared to the theoretical value. The cell constant is the ratio between these two values. The onset slope, or thermal resistance, is a measure of the suppression of temperature rise that occurs in a melting sample in relation to the thermocouple. Theoretically, a standard sample should melt at a constant temperature. As it melts and draws more heat, a temperature difference develops between the sample and the sample thermocouple. The thermal resistance between these two points is calculated as the onset slope of the heat flow versus temperature curve on the front of the melting peak. The onset value is used for kinetic and purity calculations to correct for this thermal resistance.

2.2.3 TEMPERATURE CALIBRATION

Temperature calibration is based on a run in which a temperature standard (e.g. indium) is heated through its melting transition. The extrapolated onset of the recorded melting point of this standard is compared to the known melting point, and the difference is calculated for temperature calibration.

2.2.4 HEAT CAPACITY CALIBRATION

Heat capacity calibration is required if it is desirable to measure the absolute value of the sample's heat capacity. The calibration uses a standard material (e.g. sapphire) with a known heat capacity at a specific

temperature of interest. Calibration is typically done at a heating or cooling rate of 10 to 20 °C/min. At the end of the experiment the heat capacity calibration constant is calculated by dividing the theoretical value of heat capacity by the measured value at a specific temperature. The calculated constant is then manually entered into the instrument control software, where it is automatically applied to future experiments.

2.3 EXPERIMENTAL PROCEDURES

All of DSC experiments have the following general outline. The majority of these steps are performed using the instrument control software.

- Calibrating the instrument
- Selecting the pan type and material
- Preparing the sample
- Creating or choosing the test procedure and entering sample and instrument information through the TA Instrument control software
- Setting the purge gas flow rate
- Loading the sample and closing the cell lid
- Starting the experiment.

In the DSC-Q2000 atmospheric tests, typical sample weights between 3 and 20 mg and aluminum crucibles ($d = 5.1$ mm) were used. The sample cell was conditioned by a constant nitrogen purge flow (50 ml/min) at atmospheric pressure. The thermal program used for the experiments is summarized in Table 14. The crucibles were used with and without lid to analyze the difference in mass transfer during the separation of volatiles from the solid substrate. Samples used in DSC runs were previously dried at 105°C and all DSC runs were started at 105°C. A constant heating rate of 10°C/min, was used up to the final temperature, set at 550°C. At the end of each run, the furnace was cooled down to 30°C under nitrogen purge gas flow and a second run was performed on the char sample using the same temperature–time program. At the end of the DSC runs the char residue was weighed, and the yields in char and volatile products were estimated. The set-up of the DSC devices used for experimental runs do not allow the separate determination of the yields in gaseous and liquid products among volatile species.

Table 14. Operating parameters in DSC Q2000 experiments

Sample Weight	3 – 20 mg
Final Temperature	550°C
Operating Pressure	Atmospheric
Purge gas flow	50 ml/min
Heating rate	10°C/min

3 DIFFERENTIAL SCANNING CALORIMETER IN PRESSURE

3.1 INSTRUMENT CHARACTERISTICS

The Pressure DSC (PDSC) cell is a DSC cell enclosed in a steel cylinder that can be pressurized up to 7 MPa. This ability to vary pressure as well as temperature provides the following:

- Resolution of overlapping peaks
- Determination of heats of vaporization and vapor pressure
- Reaction rates in controlled atmospheres
- Studies of pressure-sensitive reactions

The model used in the current study is a DSCQ20P from the TA Instruments Company (Figure 14). The PDSC cell has two gas flow control valves, a three-way valve, a pressure gauge, a pressure release valve, and gas pressure fittings on the side. The pressure relief valve has a set at 8.3 MPa gauge. A pressure transducer continuously measures actual sample pressure and stores it in the data file.

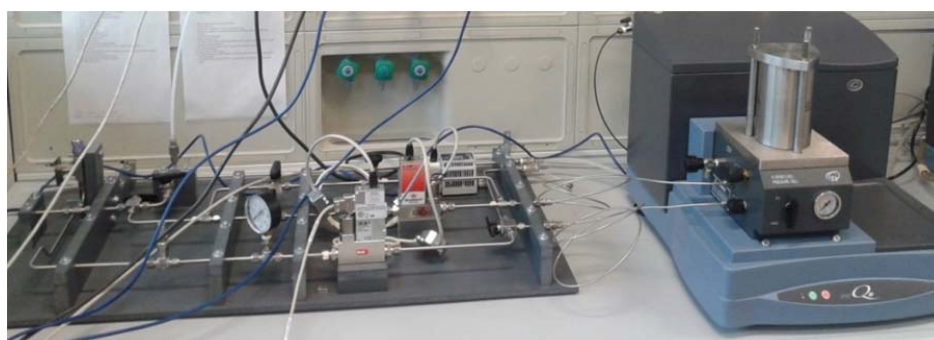


Figure 14. Differential scanning calorimeter in pressure used in this study (DSC Q20P)

The PDSC uses a constantan (thermoelectric) disc as a primary heat transfer element. A silver heating block, capped with a vented silver lid, encloses the constantan disc. The selected sample and an inert reference are placed in pans that sit on raised portions of the disc. Heat is transferred through the constantan disc to both the sample and the reference pans. Differential heat flow to the sample and reference are monitored by the constantan area thermocouples. Purge gas is preheated by circulation before entering the sample chamber. Gas exits through the vent hole in the silver lid.

Table 15. DSC Q20P technical specifications

Temperature range	Room temperature to 725°C
Pressure	-100 kPa gauge to 7 MPa gauge
Purge gases	Air, argon, helium, nitrogen, oxygen, hydrogen, carbon monoxide, carbon dioxide

3.2 INSTRUMENT CALIBRATION

3.2.1 BASELINE SLOPE AND OFFSET CALIBRATION

The baseline slope and offset calibration involves heating an empty cell through the entire temperature range expected in subsequent experiments, holding isothermal at the temperature limits. The calibration program is used to calculate the slope and offset values needed to flatten the baseline and zero the heat flow signal.

3.2.2 ENTHALPY CELL CONSTANT CALIBRATION

See Section 2.2.2.

3.2.3 TEMPERATURE CALIBRATION

See Section 2.2.3

3.2.4 PRESSURE CALIBRATION

Pressure calibration is an optional calibration procedure for the Pressure DSC cells. It is based on comparing the pressure reading at two points, typically one atmosphere and another pressure selected by you, to the pressure reading on an external pressure gauge.

3.3 SETUP DESIGN AND INSTALLATION

A specific gas circuit was built to allow DSC runs under pressure in the presence of a constant purge gas flow. Figure 15 shows the experimental set-up. A control loop was realized to pressurize the test cell up to the selected operating pressure and to keep a constant pressure and a constant purge gas flow during the test. An EL-PRESS P-702CV pressure controller and an EL-FLOW F-201CV mass flow controller, both by Bronkhorst (The Netherlands) were used for pressure and gas flow control.

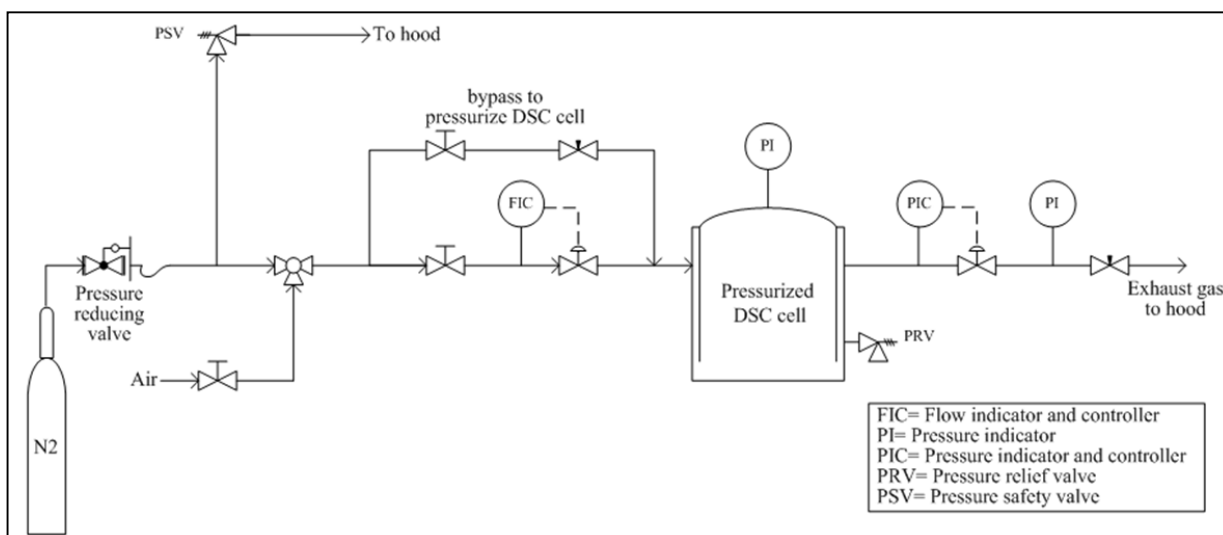


Figure 15. Simplified scheme of the experimental set up used for DSC runs under pressure

3.4 EXPERIMENTAL PROCEDURES

Runs were carried out at the following operating pressures: 0.1, 0.5, 1, 2, and 4 MPa. In a first set of runs, the inlet nitrogen flow rate was fixed to 0.050 Nl/min, corresponding to an outlet flow rate of 50 ml/min, in order to obtain a constant heat capacity of the gas flow during experimental runs. In a second set of runs, the influence of the flow rate was investigated and the flow rate was varied between 5-50 ml/min. Gas residence time in the DSC is affected by temperature and pressure, but it was always comprised between about 0.1 and 0.9 s, well below the time scale of DSC measurements.

The DSC runs were performed using 5 mm diameter aluminum crucibles. The crucibles were used with and without lid to analyze the difference in mass transfer during the separation of volatiles from the solid substrate. The thermal program and the experimental procedure were the same of the DSC Q2000 (Table 16).

Table 16. Operating parameters in DSC Q10P experiments

Sample Weight	3 – 20 mg
Final Temperature	550°C
Operating Pressure	0.1- 4 MPa
Purge gas flow	5 - 50 ml/min
Heating rate	10°C/min

4 METHOD FOR THE ASSESSMENT OF HEAT OF PYROLYSIS

In order to assess the heat of pyrolysis, it is necessary to obtain quantitative data for the from the raw DSC curves. In particular, it is necessary to separate the contribution of the pyrolysis reaction process from other thermal effects recorded by the DSC device.

Actually the experimental curves obtained in a DSC analysis result from several contributes, some depending on the thermal behavior of the sample (heat capacity of the sample, latent heat of evaporation of volatile components, heat of primary pyrolysis, heat of secondary reactions) and some due to the experimental setup (asymmetric radiative heat exchange between the sample and the DSC cell due to the change in the surface emissivity of the biomass) [70]. The approach of Rath et al. [71], briefly summarized in the following, was used to obtain quantitative data for the heat of reaction from the DSC curves.

The effect of heat capacity of the sample (Q_{sh}) can be isolated by calculating a theoretical heat flow curve for sample heating from the data on the specific heat of biomass and char available in the literature [41], [72], [73]:

$$Q_{sh} = (1 - X(T))m_0c_{p,bio} \frac{dT}{dt} + X(T)m_{char}c_{p,char} \frac{dT}{dt} \quad (3)$$

where m_0 and $c_{p,bio}$ are respectively the initial sample weight and heat capacity, m_{char} and $c_{p,char}$ are respectively the final weight and heat capacity of the final solid residue (called “char” in the following discussion), T is the temperature, dT/dt is the heating rate, and $X(T)$ is a dimensionless sample conversion defined as:

$$X(T) = \frac{m_0 - m_T}{m_0 - m_{char}} \quad (4)$$

where m_T is the sample weight at temperature T . The values of $c_{p,bio}$ and $c_{p,char}$ can be experimentally measured or derived from generic correlations. In the present study the correlations proposed by Koufopoulos et al. [36] were used in the calculations (Table 17). The contribution of asymmetric radiative heat exchange was evaluated from the DSC run. Since the experimental heat flow of the second run carried out on char (Q_{char}) can be considered the sum of the sensible heat of the char and of the asymmetric radiative heat exchange [71], it is possible to calculate the radiative heat flow (Q_{rad}) as the difference between the experimental DSC curve obtained from the char after the pyrolysis run and the heat flow needed to heat the char, calculated on the basis of char specific heat [70].

Table 17. Specific heat of wood and char

Substance	Specific heat, $J\ kg^{-1}\ ^\circ C^{-1}$
Wood	$c_p = 1112.0 + 4.85T$
Char	$c_p = 1003.2 + 2.09T$

The contribution of asymmetric radiative heat exchange can be evaluated by a DSC tests on the char after pyrolysis run, as described above. Since the experimental heat flow of the second char test (Q_{char}) can be considered the sum of the sensitive heat of the char and of the asymmetric radiative heat exchange [4], it is possible to calculate the radiative heat flow (Q_{rad}) as the difference between the experimental and the calculated heat flow of the residual char:

$$Q_{rad} = Q_{char} - m_{char}c_{p,char} \frac{dT}{dt} \quad (5)$$

The heat flow due to the pyrolysis process (Q_r) may thus be obtained subtracting the radiation effect (Q_{rad}) and the contribution of heat capacity (Q_{sh}) from the experimental heat flow curve recorded for the biomass sample (Q_{exp}):

$$Q_r = Q_{exp} - Q_{rad} - Q_{sh} \quad (6)$$

The total heat requirement associated to the pyrolysis process is then calculated by numerical integration as:

$$H_p = \frac{1}{m_0} \int_{T_i}^{T_f} Q_r dT \quad (7)$$

where T_i and T_f are the initial and final temperatures of the decomposition process. The values of these temperatures depend on the biomass type and were evaluated from the dTG curve as the endpoints of

the temperature interval for which the dTG value equals $-0.5\%/min$. Reproducibility of heat flow data obtained by this procedure evidenced that maximum error in the final heat flow values was always lower than 10%.

5 FIXED-BED REACTOR

Lignin liquefaction experiments have been carried out using an in-house made stirred autoclave with an internal volume of 45 ml. For safety reasons, the set-up is placed inside a high pressure room and controlled from outside during the high temperature/pressure part of the experiment. A schematic diagram of the setup is shown in Figure 16. The reactor has a hollow shaft stirrer (0-48 Hz), that is expected to mix the reactor content and to improve mass transfer. The reactor lid contains two orifices, one for a thermocouple and one to connect it to a line with a pressure reader and a gate valve.

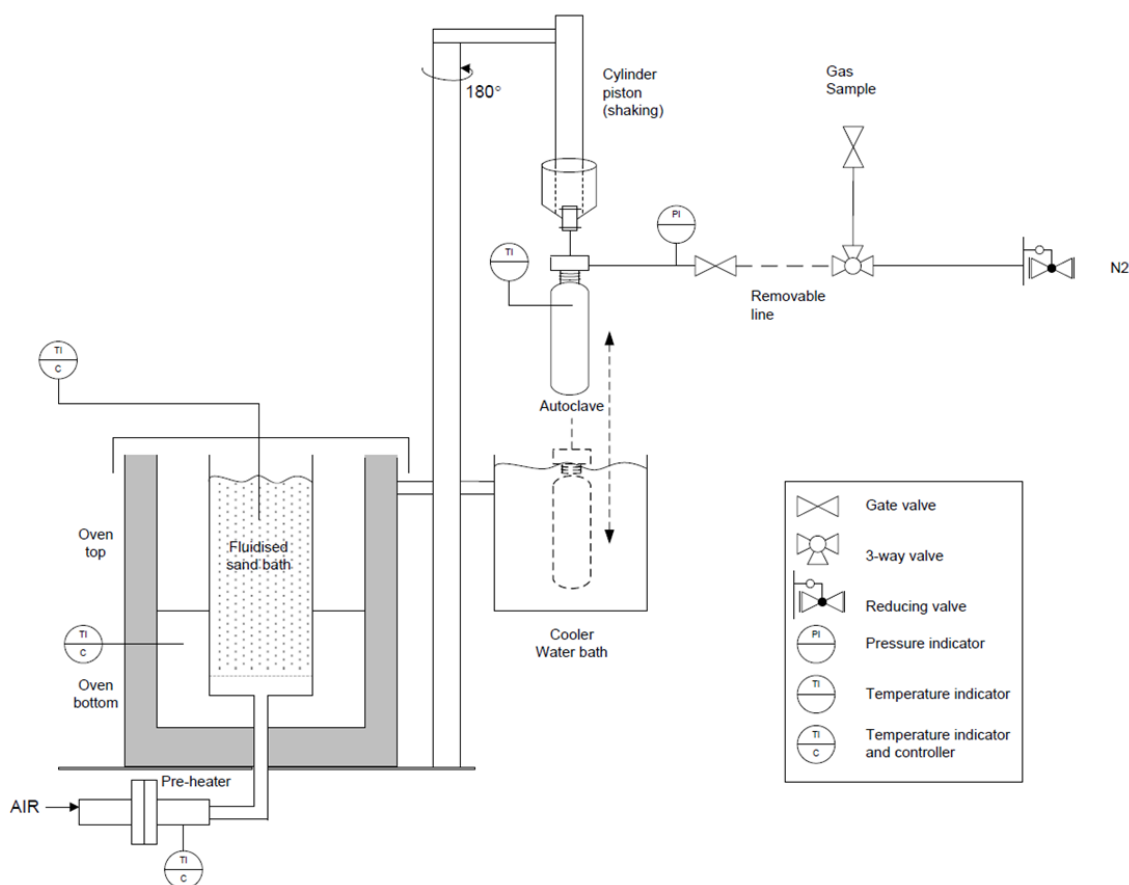


Figure 16. Schematic drawing of the fixed bed reactor used for lignin liquefaction experimental runs

The reactor is fixed to a pneumatic arm, that allowed the reactor to be immersed in a fluidized sand bed and a cooling bath to obtain fast heating and cooling, respectively. The fluidized sand bed is heated by two electric ovens with independent temperature controllers. The fluidization gas is pre-heated by a separate heating element. By means of the pneumatic arm, the autoclave is heated by immersion in a fluidized sand bed after the desired reaction time, it is lifted and quenched by immersion in the water bath. This method is adopted to minimize, as much as possible, the effects of heating and cooling on the final composition.

At the start of the experiment, the pneumatic arm is moved to the position over the sand bed and then immersed in the bed. The reactor temperature has been varied between 300 and 450°C, and the heating rate to achieve the desired set-point is 5 min approximately. The temperature and the pressure of the reactor are recorded during the run. After the desired reaction time (from 1 to 25 min excluding the heating time), the reactor is lifted from the hot sand bed, and immersed in the water bath to rapidly cool down at 20°C, with a cooling rate of 200 s approximately.

In a typical experiment, the reactor is filled with the desired amount (total 20 g) of guaiacol or recycled oil and lignin at a concentration of 20-60% wt. depending on the experiment. The reactor is then closed tightly and attached to the moving arm. After leaking test with nitrogen, the reactor is purged and filled with 5 bar of nitrogen, then the gas line is detached.

After the reactor is cooled to room temperature, pressure is noted and a gas sample is taken for analysis. With the gas composition and the final pressure and temperature inside the reactor, it was possible to calculate the amount of each gas produced. After complete depressurization, the autoclave is disconnected from the arm and opened. The liquid sample is collected in a glass vial (called as bio-oil 1) and the reactor is rinsed with acetone to remove leftover liquid and solid deposits if any. The obtained acetone wash (called as bio-oil 2) is evaporated in a rotavapor and weighed to close the material balance. Typically bio-oil 2 varies between 2 and 40% wt. of the total oil. For some of the experiments the produced oil is recycled as a liquid solvent for the subsequent run. In this case the reactor is filled with 4 g of fresh lignin and 16 g of produced oil. In recycle experiments, a nominal lignin content has been defined as the sum of fresh lignin and lignin introduced with produced oil. Lignin present in produced has been considering unreacted. With this iteration procedure, 4 refill runs of the lignin liquefaction product has been proven, reaching a nominal lignin content of 60wt%.

An hydrotreatment experiment has been performed on the liquefaction oil containing 60 % wt. of lignin liquefaction product and thus 40 % wt. guaiacol. The liquefaction oil was produced at 300°C and a residence time of 25 minutes. In this case the reactor is loaded with 20 g of this oil feedstock together with 5 % wt. Ru/C and 120 bar of initial hydrogen pressure. The heating rate is of approximately 60-90°C/min. The reactor temperature was 300°C. The duration of the hydrotreatment experiment was 2 hours. The product collection and mass balance closure is similar to the procedure of the liquefaction experiments. The only difference is that the oil product is filtered, to remove the catalyst, prior to analysis. The hydrotreated oil product has been collected from the reactor as a single batch (bio-oil 1) as it was light and completely free flowing.

6 ANALYTICAL EQUIPMENT

6.1 ELEMENTAL ANALYZER (EA)

The elemental composition is determined using a Fisons Instruments 1108 EA CHN. The method uses flash combustion of dried, ground samples which have been weighed into tin capsules. The sample material is weighed in a tin capsule (2 to 5 mg of materials are required). The sample is placed in the autosampler, purged with helium. When the autosampler rotates, the samples are dropped into a vertical quartz tube, the combustion reactor, which is kept at a temperature of 1070 °C. When a sample is dropped, a pulse of O₂ is injected and the tin capsule containing the sample undergoes flash combustion. The helium carrier gas takes the gases produced from the flash combustion through the combustion reactor which contains the oxidation catalysts copper (II) oxide and platinumised alumina. All the carbon in the sample is oxidized to CO₂, and all the nitrogen is oxidized to nitrogen oxides (NO_x). The helium carrier gas then takes the gases into the quartz reduction column containing copper wire which acts as a reduction catalyst. The reduction column reduces the nitrogen oxides to N₂ gas. The resulting mixture of analytically detectable gases CO₂, H₂O and N₂ are carried by the helium carrier gas through a chromatographic column. The separated gases are detected by a thermal conductivity detector (TCD). Oxygen is determined by difference.

6.2 KARL FISHER (KF)

A 787 KF Titrino is used to quantify the water content of the pyrolysis oil and the produced liquid phases (aqueous and oil). The moisture determination of water by the Karl Fischer method depends on the reaction that takes place quantitatively between water and a reagent very sensitive to water. The reaction is carried out in a suitable solvent. In our equipment the titrant used is Hydranal Composite 5 (Riedel-deHaën) and the solvent is a solution of methanol (Aldrich) and dichloromethane (Aldrich) (volumetric ratio 3:1).

6.3 MICRO CARBON TEST RESIDUE (MCRT)

Micro-carbon residue tests (MCRT) were performed following the ASTM D4530 standard in a Tanaka AMC-3 micro-carbon residue tester. A quantity of sample is weighed, placed in a glass vial, and heated to 500°C. Heating is performed in a controlled manner, for a specific period of time, and under an inert (nitrogen) atmosphere. The volatiles formed are swept away by the nitrogen. The carbonaceous residue remaining is reported as a mass percent of the original sample, and noted as "carbon residue (micro)."

6.4 MOLECULAR WEIGHT DISTRIBUTION (GPC)

Gel Permeation Chromatography (GPC) is a type of Size-Exclusion Chromatography (SEC). It separates molecules by size. Average molecular weights and molecular weight distributions are calculated based on the elution behavior in a size exclusion column set. The column is filled with porous particles which usually have pore size distribution close to the hydrodynamic volumes of molecules to be analyzed. Molecules in solution are separated by their size. Small molecule that can penetrate most pores will travel a longer

distance and come out the column later, in contrast a large molecule that cannot penetrate into any pores will travel a shorter distance and come out earlier.

Using a polystyrene calibration, this separation is translated into a molecular weight distribution. Because there is no uniform relationship between molecular size and weight, GPC analysis only gives an indication of the molecular weight distribution. The system used to carry out these analyses has been an Agilent 1200 series HPLC system, using GPC PLgel3 μ meter MIXED-E columns; the flow was 1 ml/min at 40 °C column temperature. The solvent used was tetrahydrofuran (THF). Apparent molecular weights were determined by calibration with a solutions of polystyrene with molecular weight ranging from 162 to 30230 Da.

6.5 VISCOMETER

Viscosity was measured using a rotational viscosity meter (Brookfield DV-E). It measures viscosity by measuring the force required to rotate a spindle in the fluid to be analyzed. The spindle is immersed in the fluid and driven at a constant rotational frequency. The viscosity is related to the torque generated by the fluid resistance to the induced movement and is hence determined by measuring the tightening of the spiral spring attached to the spindle.

6.6 GAS CHROMATOGRAPH – MASS SPECTROMETER (GC-MS)

Low-molecular weight components present in the liquid are identified by using Gas Chromatography-Mass Spectrometry (GC-MS) with an Agilent GC-MS (GC 7890A MS 5975C). GC-MS uses two techniques that are combined into a single method for analyzing mixtures of chemicals. Gas chromatography separates the components of a mixture, and mass spectroscopy characterizes each of the components individually. Combining the two techniques helps to analyze the samples both qualitatively and quantitatively. The standards used to calibrate the instrument in order to be detected and quantified as substance in the liquid are: guaiacol, eugenol and phenol.

6.7 MICRO – GAS CHROMATOGRAPH (GC)

Gas samples were analyzed with an off-line gas chromatography (Varian Micro GC CP-4900) with two analytical columns, 10m Molsieve 5 Angstrom and 10m PPQ, using Helium as carrier gas. The gas detected are N₂, CO, CO₂, CH₄, C₂H₄, C₂H₆, C₃H₆, C₃H₈.

7 MATERIALS FOR CALORIMETRIC ANALYSIS

For the study on the thermal effects of the pyrolysis process and on the assessment of the heat of pyrolysis, it has been analyzed some kind of lignocellulosic biomass and some forms of biomass macrocomponents isolated from biomass.

As lignocellulosic biomass, four different biomass samples were analyzed: corn stalks, poplar, and two cultivar of switchgrass: "Trailblazer" and "Alamo". The biomass feedstock was provided by the Department of Agro-Environmental Science and Technology of the University of Bologna (Italy).

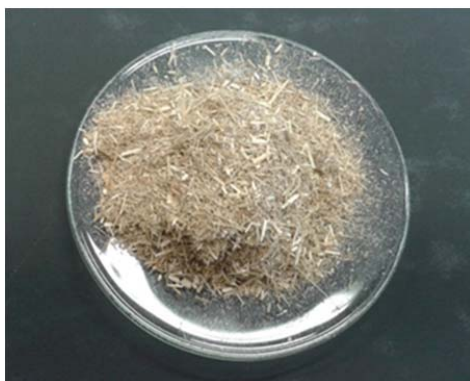


Figure 17. Corn stalks as received



Figure 18. Pressed discs of corn stalks

The material was farmed and harvested in Ozzano and Cadriano (Bologna, Italy), dried overnight (15 h at 105°C) and ground up to a particle size lower than 1mm. Samples for TG and DSC runs were obtained pressing and punching the biomass particles to compact discs (about 5mm diameter and 0.4 to 0.7 mm height depending on the desired sample weight) that fitted the crucibles used in DSC analysis. Table 18 summarized the proximate and ultimate analysis of the lignocellulosic biomass used in this study.

Table 18. Properties of the lignocellulosic biomass used in this study

Properties	Corn stalks	Poplar	Switchgrass Alamo	Switchgrass Trailblazer
<i>Proximate analysis</i>				
Volatiles	77.7	81.8	79.3	64.1
Fixed Carbon	16.0	14.8	12.1	8.6
Ash	6.3	3.4	6.7	27.3
<i>Ultimate analysis</i>				
C	45.5	47.8	46.8	52.1
H	5.8	5.9	5.9	6.7
N	1	0.5	0.5	0.6
O*	47.7	45.8	46.8	40.6

*by difference

As representative of biomass components, three kind of isolated forms were chosen from Sigma Aldrich. Except for cellulose, hemicellulose and lignin are present in different forms in real biomasses. For example, hemicellulose can exist in form of xylans, xyloglucans, mannans and mixed linkage β -glucans while the content of p-coumaryl, coniferyl and sinapyl alcohol in lignin is dependent on the source

feedstock. Moreover, hemicellulose and lignin present in the raw biomass can be modified on dependence of the extraction method from the biomass matrix [74], [75]. In this work cellulose powder, xylan from beechwood and lignin alkali (Sigma Aldrich) have been chosen as model compounds given the robustness of the knowledge of their behavior in a wide variety of pyrolysis conditions [76], [77]. Table 19 reports the proximate analysis of the biomass samples on dry basis.

Table 19. Properties of the biomass macro-components used in this study

Properties	Cellulose	Hemicellulose	Lignin
<i>Proximate analysis</i>			
Volatiles	94.8	73.9	55.7
Fixed Carbon	4.9	21.8	40.5
Ash	0.3	4.2	3.7
<i>Ultimate analysis</i>			
C	42.2	43.3	63.4
H	6.3	6.1	5.8
N	0	0	0.7
O*	51.5	50.6	30.1

*by difference

It has to be underlined that, the physical and chemical properties of lignins differ, depending on the extraction or isolation technology used to isolate them. Because lignin is inevitably modified and partially degraded during isolation, thermal decomposition studies on separated lignin will not necessarily match the pyrolysis behavior of this component when it is present in the original biomass.

8 MATERIALS FOR LIQUEFACTION EXPERIMENT

In the liquefaction experiments, it has been analyzed the softwood lignin as biomass and the Guaiacol as solvent. The softwood lignin supplied by Innventia (Drottning Kristinas väg 61 Stockholm, Sweden) was derived from paper industry and has been isolated by pulping process. The Guaiacol supplied by Sigma Aldrich has been analyzed because it can be considered the model compound of lignin and it can be considered as a product of lignin liquefaction itself.

All other solvents used for the product analysis were obtained from Sigma-Aldrich and had a purity >98%. Ru/C catalyst was used in the hydrotreatment experiment and had a metal loading of 5 wt.% and a particle size of approximately 14 μm . The BET surface area of the catalyst is $810 \pm 11 \text{ m}^2/\text{g}$. Hydrogen was purchased from the High pressure Laboratory ring system and had a purity >99.99%.



Figure 19. Softwood Lignin

Table 20. Properties of the lignin used in the dissolution experiments

Properties	Softwood Lignin
Moisture, % wt.	9.4
C, % wt. d.b.	59.3
H, % wt. d.b.	5.4
N, % wt. d.b.	0.1
O, % wt. d.b.	35.2
Ca, % wt d.b.	0.0037
K, % wt d.b.	0.0016
Mg, % wt d.b.	0.2349
Na, % wt d.b.	0.3380
Total Alkali metals, % wt. d.b.	0.338
Ash, % wt. d.b.	0.59
Av. Molecular weight, g/mol	2314
MCRT residue @ 550°C, % wt. d.b.	50.8

Table 21. Properties of solvent used in the dissolution experiments

Properties	Guaiacol
C, % wt. d.b.	67.8
H, % wt. d.b.	6.4
O, % wt. d.b.	25.8
Av. Molecular weight, g/mol.	124

CHAPTER IV

OVERALL HEAT DEMAND OF THE BIOMASS PYROLYSIS PROCESS

1 BIOMASS CHARACTERIZATION BY THERMOGRAVIMETRIC ANALYSIS

TG analyses are based on the volatilization rate of biomass. Pyrolysis tests were performed in a TGA in order to record the sample weight loss and rate of weight loss as a function of time or temperature under dynamic conditions, in the range of 25-950 °C. The experiments were carried out at atmospheric pressure, under a nitrogen atmosphere, with a flow rate of 60 ml/min, at a linear heating rate of 10 °C/min.

Table 22. Proximate analysis of biomass feedstocks

	dry basis %			wet basis %			
	Volatiles	Fixed Carbon	Ash	Moisture	Volatiles	Fixed Carbon	Ash
Corn stalks	77.7	16.0	6.3	3.3	75.2	15.4	6.1
Poplar	81.8	14.8	3.4	2.2	80.0	14.4	3.3
Switchgrass Alamo	79.3	12.1	6.7	3.0	77.0	11.8	8.3
Switchgrass Trailblazer	64.1	8.6	27.3	3.4	61.9	8.3	26.4

A preliminary analysis has been performed in order to determine the volatiles, fixed carbon and ash content and characterize the biomass. For this purpose, the samples were conditioned at 30°C under nitrogen flow, in order to provide a consistent and common starting point for all the measurements. The samples were heated in the TGA furnace with a rate of 10°C/min to 105°C, in order to remove the moisture. After an isotherm of 10 min, the dry basis mass of the sample was measured. The temperature was further increased, still at the heating rate of 10°C/min, up to 950°C and held constant at this value for 10 min. Next, purge gas was switched to air (60 ml/min), in order to burn the organic content. The volatile matter reported in Table 22 has been determined by the weight difference at 105°C and 950°C under nitrogen flow. The fixed carbon content has been determined by weight difference after the combustion of the sample at 950°C in air. The ash is the residue mass after combustion [20]. In order to ensure the

reproducibility of the analysis there were repeated at least three times. The proximate analysis have been calculated on wet basis, referring to the sample weight after the stabilization at 30°C, and on dry basis, referring to the sample weight after the stabilization at 105°C.

Mass loss (TG) and differential mass loss (DTG) curves from TGA experiments with a rate of 10°C/min till 550°C are presented in Figure 20. for the four type of biomass studied. The samples were conditioned at 105°C under nitrogen flow, in order to remove moisture and provide a consistent and common starting point for all the measurements All the curves show a limited weight loss up to 200°C, confirming that the condition process at 105°C was effective in removing moisture and volatile compounds [51]. Above 200°C thermal decomposition starts, with an increasing rate as the temperature is further raised. The major loss weight zone is observed between 230 and 390°C, followed by a flat tailing zone up to about 550°C, after which the devolatilization is essentially completed [78].

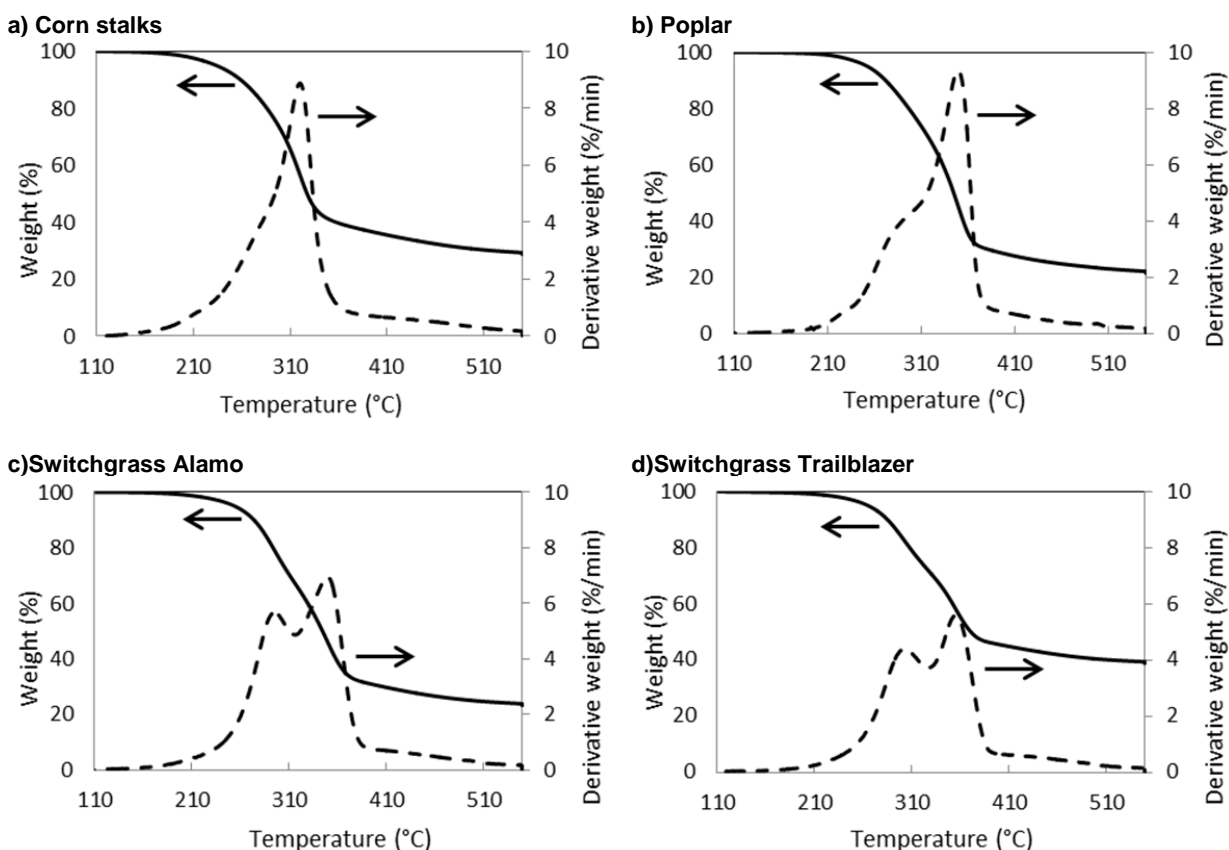


Figure 20. TG and DTG curves for corn stalks (a), poplar (b), switchgrass “Alamo” (c) and switchgrass “Trailblazer” (d). Reference Initial sample mass at 105°C 7mg.

Figure 21 compares the TGA curves for the analyzed materials referred to the sole organic fraction of the material. The contribution of ashes to the sample weight was numerically eliminated by the following rescaling operation:

$$\%wt_{daf} = \frac{\%wt_{dry} - \%wt_{ash}}{100\% - \%wt_{ash}} \quad (8)$$

where $\%w_{daf}$ is the dry and ash-free percent weight of the sample at temperature T , $\%w_{dry}$ is the percent weight on dry basis from TGA experiment at the same T , and $\%w_{ash}$ is the ash percent weight on the initial sample (dry basis). Figure 21 clearly shows that the different behaviour of the two cultivars of switchgrass in the TG tests of Figure 20 is mainly due to different content of ashes.

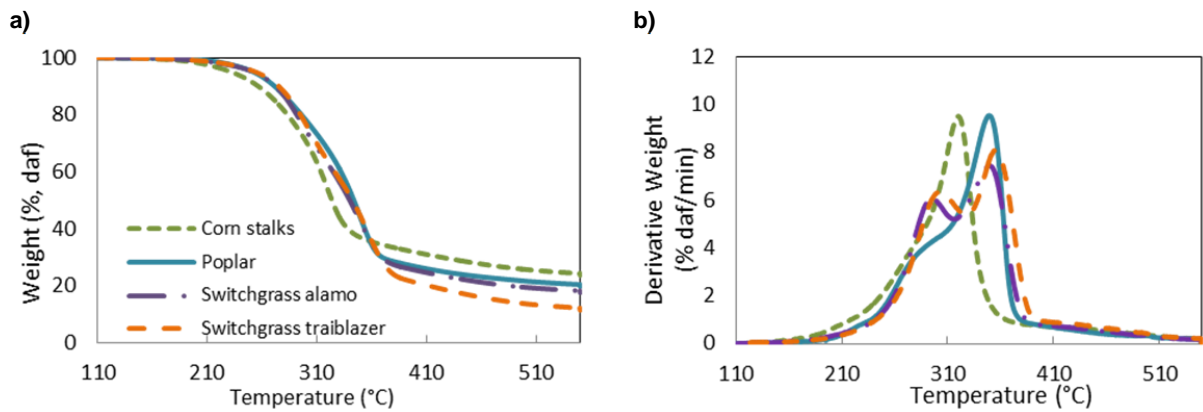


Figure 21. TG (a) and DTG (b) profiles for biomass materials; the curves are calculated for the ash-free mass of the samples.

Table 23 summarizes the yields and characteristic temperatures of the pyrolysis process for the analyzed samples. Char yield is defined as:

$$\eta_{dry} = \frac{m_{char}}{m_0} \quad (9)$$

$$\eta_{daf} = \frac{m_{char} - m_{ash}}{m_0 - m_{ash}} \quad (10)$$

where η_{dry} and η_{daf} are the char yields defined on the initial dry mass and ash-free mass, respectively. Corn stalks evidence the greater char yield and the earliest onset of reactivity. Poplar and switchgrass Alamo yield similar quantities of char.

Table 23. Pyrolysis parameters of the biomass materials as for TGA results. Reference Initial sample mass at 105°C 7mg.

	Char yield at 550°C (% wt. daf)	Max decomposition rate (10 ² min ⁻¹)	Temperature at max decomposition rate (°C)
Corn stalks	23.8	8.9	320
Poplar	19.8	9.4	349
Switchgrass Alamo	17.6	7.0	349
Switchgrass Trailblazer	11.5	5.6	355

In a DTG diagram (Figure 21.b) the reactivity of a material is directly proportional to peak height and inversely proportional to peak temperature [79]. If analyzed on an ash-free basis, the four samples presents similar overall reactivity. However, a different temperature and shape of the decomposition velocity peaks is observed.

2 WEIGHT LOSS ANALYSIS

2.1 BUILDING BLOCKS DECOMPOSITION

Biomass pyrolysis can be related to the thermal decomposition behavior of the three macro-components of lignocellulosic biomass: hemicellulose, cellulose and lignin [80]. These macro-components in general cover respectively 20-40 %wt., 40-60 %wt., and 10-25 %wt. of the biomass material [10].

Gasparovic et al., studying the pyrolysis of wood and main wood compounds by thermogravimetric techniques, showed that decomposition of hemicellulose and cellulose takes place in the temperature from 200 to 380°C with a velocity peak around 290°C and 250 to 380°C with a velocity peak around 350°C, respectively. Whereas lignin is decomposed in range from 180 to 900°C without a pronounced peak [80]. The major weight loss of the materials analyzed in current study occurs at temperatures compatible with hemicellulose and cellulose degradation. The two corresponding peaks are quite evident in both switchgrass samples, while the peak corresponding to the decomposition of hemicellulose is present as a shoulder on the main peak for the poplar sample. For the corn stalks a single peak is observed, probably due to overlapping. In any sample, the tailing zone corresponds to the decomposition of lignin, which is the least reactive component.

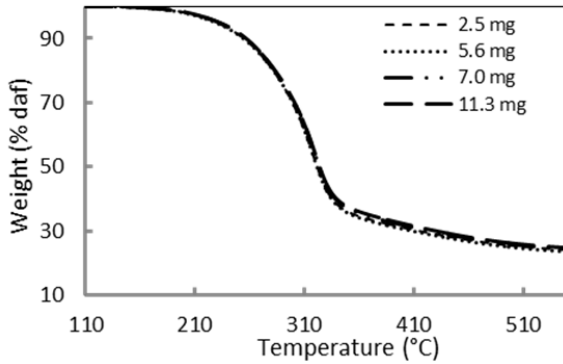
2.2 INITIAL SAMPLE WEIGHT INFLUENCE

The effect of sample size on TG profiles has been investigated on the four type of biomass. TG curves are expected to change depending on sample weight. Figure 22 shows the effect of initial sample weight on the thermal degradation, as obtained by TGA tests (heating rate of 10°C/min in nitrogen flow up to 550°C). The general tendency is of increasing in the char yield when the initial sample weight increases. It indicates that a higher resistance to the flow of the volatile pyrolysis products from the sample to the bulk gas phase leads to a higher char yield.

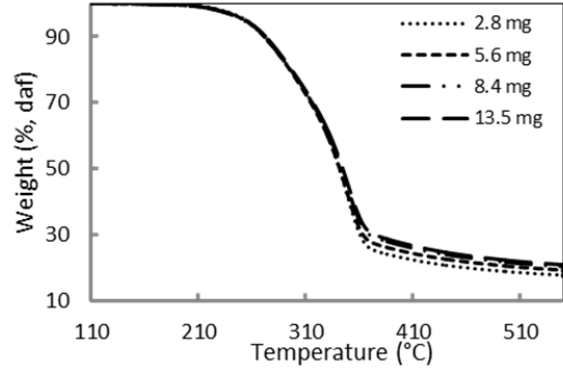
A possible account is that as the sample size increases, the mass transfer barrier becomes more significant and this provides a longer residence time in the sample for volatiles products from primary reactions. Hence, the volatiles products are encouraged to further react with solid phase (secondary reactions), enhancing char formation. Koufopoulos et al. [61] suggested that secondary reactions would enrich the carbon content of the final residue. When interacting with the carbonaceous solid, primary products reform into char and secondary volatile products. Ahuja et al. [52] pointed out that secondary vapor-solid interactions may actually be the main source of char formed from biomass pyrolysis. During the pyrolysis process, the pores of the solid are enlarged, and the solid particle merely becomes more porous because the biomass converts into gases as discussed by Curtis and Miller [49]. According to

Anthony and Howard [81], the enlarged pores of the pyrolyzing solid offer many reaction sites to the volatile and gaseous products of pyrolysis and favor their interaction with the hot solid.

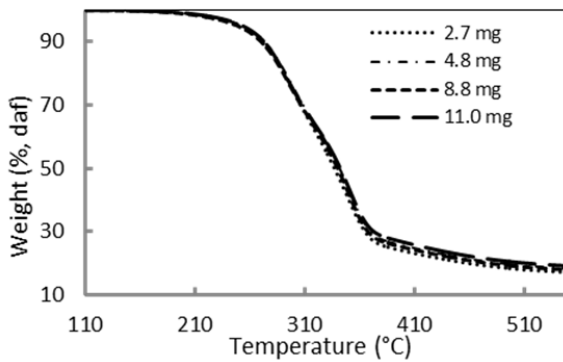
a) Corn stalks



b) Poplar



c) Switchgrass Alamo



d) Switchgrass Trailblazer

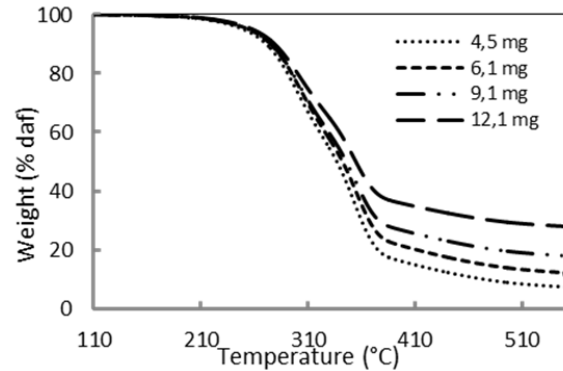


Figure 22. TG profiles of corn stalks (a), poplar (b), switchgrass “Alamo” (c) and switchgrass “Trailblazer” (d) with different initial weight

Table 24. Char yield at 550°C detected in TG runs (10°C/min, pure nitrogen) for samples having different initial weights.

Corn stalks		Poplar		Switchgrass Alamo		Switchgrass Trailblazer	
Initial weight (mg)	Char yield (% daf)	Initial weight (mg)	Char yield (% daf)	Initial weight (mg)	Char yield (% daf)	Initial weight (mg)	Char yield (% daf)
3.6	17.0	3.6	13.2	4.8	13.8	4.2	7.6
4.4	19.1	5.4	15.1	6.2	14.1	6.3	8.5
6.0	21.3	7.7	18.4	7.9	15.2	7.1	15.2
7.2	22.8	8.4	19.1	10.1	15.3	9.1	14.2
11.7	23.0	13.5	19.5	11.0	17.6	10.8	17.7

In Table 24, the influence of the initial sample weight on the char yield at atmospheric pressure up to a final temperature of 550°C is summarized. As shown in the table, high differences in the final char yield are observed, depending on the initial sample mass.

This could be due to differences in the main pyrolysis process. Curtis and Miller [49] remarked that the increase in the mass-transfer resistance results in the decrease of the condensable product fraction, because a longer vapour residence time in the reacting region induces more severe secondary reaction of the hot pyrolysis products with the decomposing solid, leading to the formation of secondary char [51]. These char-forming secondary reactions, dependent on the vapor residence time, were considered in several studies addressing the modeling of the biomass pyrolysis process [37], [52], [53], [55], [82]–[84].

3 HEAT TRANSPORT PHENOMENA

3.1 CHARACTERISTIC TIME OF THERMAL DIFFUSION

In order to explore heat transport phenomena inside the particle, a set of experiments with different sample size were done. In the TG and DSC the transport phenomena inside the tested material are controlled by the thickness of the compressed disk sample used in the test. Increasing the disk thickness will increase the residence time for evolved gases, therefore promoting further reactions. However a practical limit exist to the maximum thickness, since also heat transfer is altered by this dimension and the correct interpretation of the results asks for a quasi-isothermal behavior of the sample.

According to dimensional analysis of the local heat transfer equation, the characteristic time of thermal diffusion across the sample ($t_{diff.}$) can be evaluated as:

$$t_{diff.} = \frac{L^2}{\alpha} = \frac{L^2 \rho_{app} c_p}{k} \quad (11)$$

where L is the characteristic length of the sample (i.e. thickness) and α is the thermal diffusivity. The thermal diffusivity can be calculated from the values of apparent density (ρ_{app}), specific heat (c_p) and thermal conductivity (k) of the sample. The physically measurable parameters used are those proposed by the correlation of Koufopoulos et al. [61], and developed and modified by Babu and Chaurasia [41] and reported in Table 25:

Table 25. Physical properties correlation used for biomass and char

Properties	Correlation	Ref.
Specific heat capacity [$\text{J/kg}^{-1} \text{ }^\circ\text{C}^{-1}$]	$c_p = 1112.0 + 4.85T$	[61]
Thermal conductivity [$\text{W/m}^{-1} \text{ }^\circ\text{C}^{-1}$]	$k = 0.13 + 0.0003T$	[41]
Apparent density [kg/m^3]	$\rho_{app} = 650$	[61]

Using the values reported in Table 25, the characteristic time of thermal diffusion can be calculated for a number of sample thickness for the materials of interest. The results are reported in Table 26. As evident

from the table, disks up to 12 mg have characteristic times no larger than 3.5s. Considering the external heat solicitation (temperature ramp 10°C/min), this may correspond to temperature differences up to 0.6°C, which are reasonably acceptable in the current tests.

Table 26. Characteristic time of thermal diffusion of the 5.1 mm diameter sample disk for different biomasses. The values of sample thickness for each mass are the result of direct measurements on the compressed disks.

Biomass	Initial mass (mg)	Sample thickness (mm)	Characteristic time of thermal diffusion (s)	Thermal conductivity (m ² /s)
Corn stalks	3	0.2	0.2	$1.22 \cdot 10^{-7}$
	6	0.3	0.8	$1.22 \cdot 10^{-7}$
	9	0.5	1.9	$1.22 \cdot 10^{-7}$
	12	0.6	3.4	$1.22 \cdot 10^{-7}$
Poplar	3	0.1	0.2	$1.07 \cdot 10^{-7}$
	6	0.3	0.7	$1.07 \cdot 10^{-7}$
	9	0.4	1.7	$1.07 \cdot 10^{-7}$
	12	0.6	3.0	$1.07 \cdot 10^{-7}$
Switchgrass Alamo	3	0.1	0.2	$1.16 \cdot 10^{-7}$
	6	0.3	0.8	$1.16 \cdot 10^{-7}$
	9	0.5	1.8	$1.16 \cdot 10^{-7}$
	12	0.6	3.2	$1.16 \cdot 10^{-7}$
Switchgrass Trailblazer	3	0.1	0.2	$1.02 \cdot 10^{-7}$
	6	0.3	0.7	$1.02 \cdot 10^{-7}$
	9	0.4	1.6	$1.02 \cdot 10^{-7}$
	12	0.5	2.8	$1.02 \cdot 10^{-7}$

A direct evaluation of the characteristic times of mass diffusion is not possible, since the apparent mass diffusivity of the samples is unknown. For similar values of thermal and mass diffusivity ($Le \approx 1$) similar characteristic times are expected. Typical mass diffusivity of light hydrocarbons in air are around 10-5 m²/s, which is a couple of order of magnitude higher than the values of thermal diffusivity. However accounting for the effects like diffusion in pores, vacuum fraction and tortuosity, characteristic times at least of the order of tenth of seconds are expected.

3.2 SAMPLE THICKNESS INFLUENCE

To study the heat transmission in the particle in a rigorous way a lot of models has been proposed in the literature. Inside the pyrolyzing particle, heat is transmitted by the following mechanisms: conduction inside the solid particle, convection inside the particle pores and convection and radiation from the surface of the pellet. For simplicity, it is assumed that heat is transmitted inside the solid by conduction only [40]. The energy balance of the sample disc is:

$$-k \frac{\partial^2 T}{\partial y^2} = \frac{\partial \rho c_p T}{\partial t} + \Delta H X(T) \frac{\partial \rho}{\partial t} \quad (12)$$

with the following boundary conditions:

$$\begin{cases} T = T_0 & \text{at } y = 0 \text{ for } t > 0 \\ -k \frac{\partial T}{\partial y} = h(T_s - T_\infty) + \sigma \varepsilon (T_\infty^4 - T_s^4) & \text{at } y = L \text{ for } t > 0 \end{cases} \quad (13)$$

where y is the axial dimension, ΔH is the overall heat of reaction and $X(T)$ is defined in equation (4), L is the height of the sample, T_0 is the temperature of the thermoelectric disk at the bottom of the crucible, T_s is the temperature at the surface of the sample, T_∞ is the bulk temperature of the gas in the DSC cell and h is the heat transfer coefficient for convection. The analytical solution of the above equation is very complicated and not operational. The equation is solved with a finite difference numerical backward implicit scheme by Jalan et al. [54]. However it's possible to study the different contribution making some assumption. To compare the external heat transfer with the internal heat transfer by conduction we can assume that the heat of reaction is negligible; with this assumption and with the following boundary conditions, the governing equation is:

$$-k \frac{\partial^2 T}{\partial y^2} = \frac{\partial \rho c_p T}{\partial t} \quad (14)$$

with the following boundary conditions:

$$\begin{cases} T = T_0 & \text{at } y = 0 \text{ for } t > 0 \\ -k \frac{\partial T}{\partial y} = h(T_s - T_\infty) + \sigma \varepsilon (T_\infty^4 - T_s^4) & \text{at } y = L \text{ for } t > 0 \end{cases} \quad (15)$$

To compare the external heat transfer with the heat of reaction we can assume that the internal heat transfer by conduction is negligible; with this assumption and with the following boundary conditions, the governing equation is:

$$-k \frac{\partial^2 T}{\partial y^2} = \Delta H X(T) \frac{\partial \rho}{\partial t} \quad (16)$$

with the following boundary conditions:

$$\begin{cases} T = T_0 & \text{at } y = 0 \text{ for } t > 0 \\ \frac{\partial T}{\partial y} = 0 & \text{at } y = L \text{ for } t > 0 \end{cases} \quad (17)$$

Assuming the constancy of density with time, the analytical solution is:

$$T = T_0 - \Delta H X(T) \frac{\rho}{k} \left(\frac{y^2}{2} - Ly \right) \quad (18)$$

Since the direction of the heat transfer is the axial, an interesting value of y is at the surface of the particle ($y=L$); with this value the equation (17) becomes:

$$T = T_0 - \Delta HX(T) \frac{L^2 \rho}{2k} \quad (19)$$

Since the height of the sample is not always a measured variable, it's more operational to express the (18) as a function of the initial sample weight:

$$T = T_0 - \Delta HX(T) \frac{m^2}{2k\rho\pi^2r^4} \quad (20)$$

where r is the radius of the disk. Using this relation it has been evaluated the temperature at the surface for every analysis. The temperature at the bottom and at the surface of the particle is found to be uniform. As expected, there is a very little difference between the two temperatures for the effect of the reaction.

4 HEAT DEMAND ANALYSIS

DSC is based on measurements of the energy change of the sample under a predetermined heat cycle [29]. Samples used in DSC runs were previously dried at 105°C under a nitrogen flux of 60 ml/min for 10 min. All DSC runs were started at 105°C. A constant heating rate of 10°C/min, was used up to the final temperature, set at 550°C. At the end of each run, the furnace was cooled down to 30°C under nitrogen purge gas flow and a second run was performed on the char sample using the same temperature-time program. At the end of the DSC runs the char residue was weighed, and the yields in char and volatile products were estimated. The set-up of the DSC devices used for experimental runs do not allow the separate determination of the yields in gaseous and liquid products among volatile species.

The effect of operating parameters plays an important role over mass transport phenomena, affecting the overall heat demand of the pyrolysis process. The consequent changes in the reaction heat, and thus the actual reaction temperatures are important also for the control of product quality [85]. For this reason the influence of some key experimental parameters on the overall heat demand of the pyrolysis process has been investigated, with particular attention on the parameters of limitations in the mass transfer of the volatiles from the decomposing solid to the gas phase:

- operating pressure
- initial sample weight
- gas flow rate
- sample conditions (pierced lid)

Runs were carried out at the following operating pressures: 0.1, 0.5, 1, 2, and 4 MPa. The inlet nitrogen flow rate was varied between 5 and 50 ml/min. Samples used were pressed and punched to form compact discs (about 5mm diameter and 0.4 - 0.7 mm height) that fitted the crucibles used in DSC analysis. Both open crucibles and crucibles with a pierced lid were used in experimental runs. A single pierce was realized on lids using a 0.5 mm diameter needle.

Figure 23 reports the weight loss (TG), the differential weight loss (dTG) and the raw heat flow curves from DSC experiments obtained using a pure nitrogen purge flow of 50 ml/min and a constant heating rate of 10°C/min at atmospheric pressure on a sample with an initial weight of about 8 mg. As expected, Figure

23 evidences that the main peaks of the dTG and DSC curves are almost at the same temperature and that thermal effects of the pyrolysis process at atmospheric pressure are endothermic, except those from corn stalks.

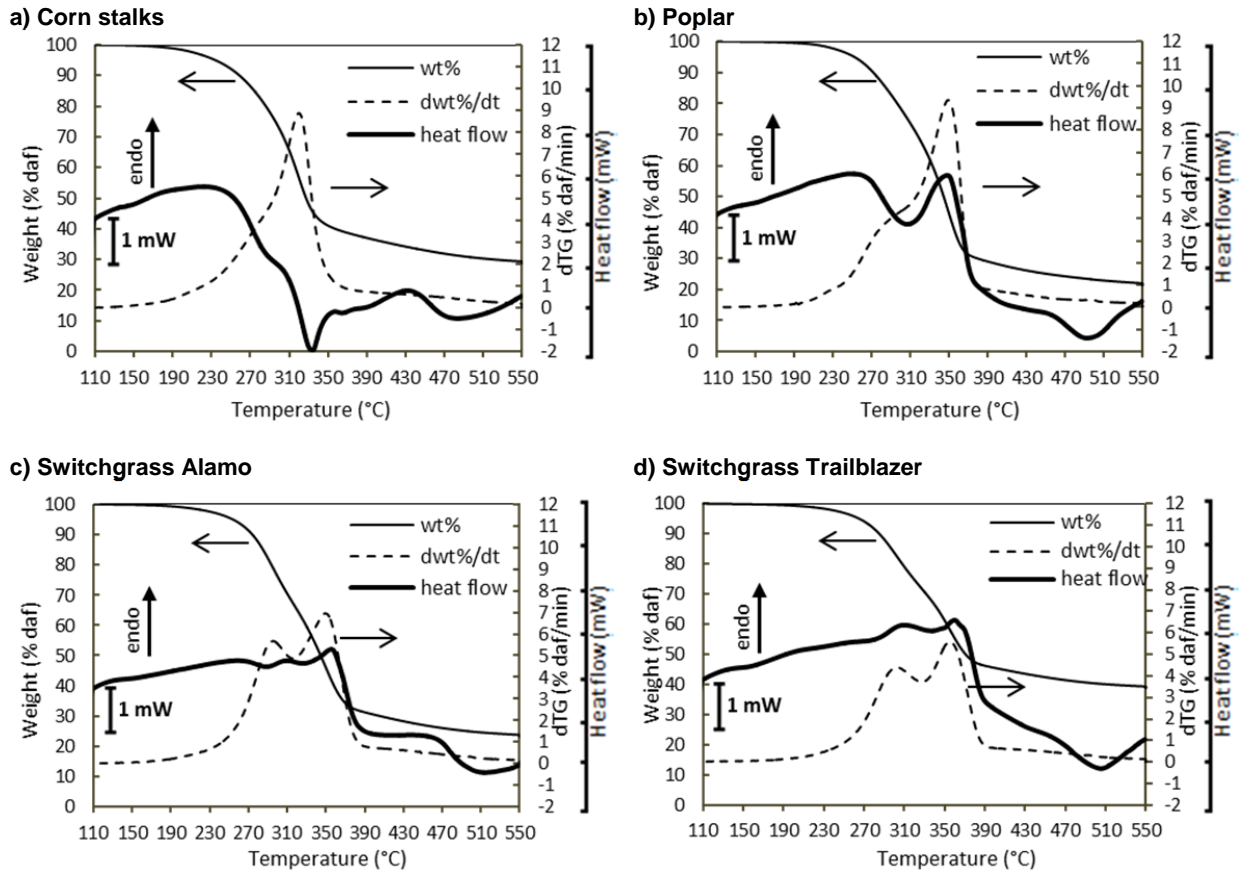


Figure 23. TG, dTG and DSC results at atmospheric pressure for corn stalks (a), poplar (b), switchgrass “Alamo” (c) and switchgrass “Trailblazer” (d). Initial sample weight of about 8mg was used in all experimental runs.

Actually it is well known that the heat of pyrolysis of different biomass samples may be endothermic or exothermic depending on the characteristics of the biomass species. Biomass species rich of extractives, hemicellulose and lignin usually show an overall exothermic pyrolysis behavior [37], [39], [60], [72]. Also the presence of ash, which catalyzes exothermic char formation, and the textural structure were reported as factors influencing the overall heat demand of the pyrolysis process [37], [56].

4.1 PRESSURE INFLUENCE

The influence of pressure on the thermal effects of the pyrolysis process has been analyzed, carrying out experimental runs at 0.5, 1, 2 and 4 MPa. Figure 24 reports an example of the raw results obtained for

poplar ($10^{\circ}\text{C}/\text{min}$ constant heating rate, pure nitrogen purge gas flow). The figure clearly evidences a modification in the DSC curve as the operating pressure is increased. In order to assess the influence of pressure on the thermal effects, it is necessary to obtain quantitative data for the heat of pyrolysis from the raw DSC curves as explained at pag. 45, separating the contribution of the pyrolysis reaction process (Q_r) from other thermal effects recorded by the DSC device.

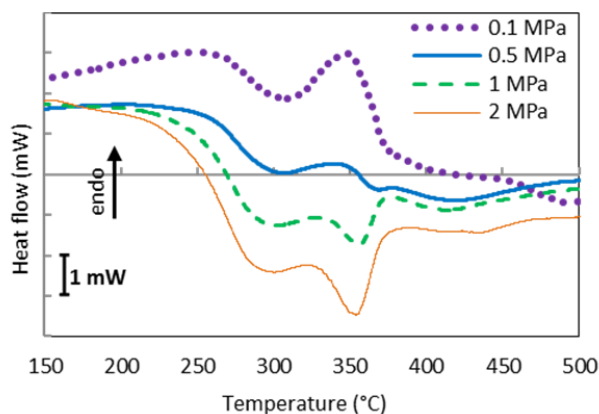


Figure 24. DSC raw data for poplar, $10^{\circ}\text{C}/\text{min}$, nitrogen purge gas, initial sample mass 8 mg.

Figure 25 compares the curves obtained for the reaction heat (Q_r) at different operating pressures. As evident from the figure, the temperature range of the pyrolysis process and the peak temperature in the heat flow during the pyrolysis process are not dependent on pressure. This result suggests that when open DSC crucibles are used, as in the present study, the pyrolysis kinetics is not enhanced as when closed crucibles are used, confirming the findings of Mok et al [69].

Nevertheless, Figure 25 confirms that pressure has a strong influence on the thermal effects of the pyrolysis process for all the four biomass samples considered. As shown in Table 27, increasing the pressure a clear decrease in the heat demand of the pyrolysis process can be observed for all the materials. When increasing the pressure from 0.1MPa to 4MPa, the total heat of pyrolysis shifts from -50 J/g to -272 J/g for corn stalks, from 29 J/g to -283 J/g for poplar, from 37 J/g to -199 J/g for switchgrass Alamo, and from 92 J/g to -210 J/g for switchgrass trailblazer (negative values are used for exothermic processes). In the case of switchgrass Trailblazer, the change is so significant that a shift from an overall endothermic to an overall exothermic process takes place. In the case of corn stalks, the pyrolysis process is exothermic even at atmospheric pressure, but the results in Figure 25 show that the heat generation in the process increases as well.

For the sake of clarity it should be remarked that the different heat demand of the pyrolysis process for different biomass species, ranging from exothermic to endothermic at atmospheric pressure, was previously reported in the literature (e.g. see the studies of Stenseng et al [64], Strezov et al [86], and Di Blasi et al. [87]). The differences were attributed to the different chemical composition of different biomass species, and in particular to the different content in extractives, hemicellulose and lignin [37], [39], [56], [60], [77], [88].

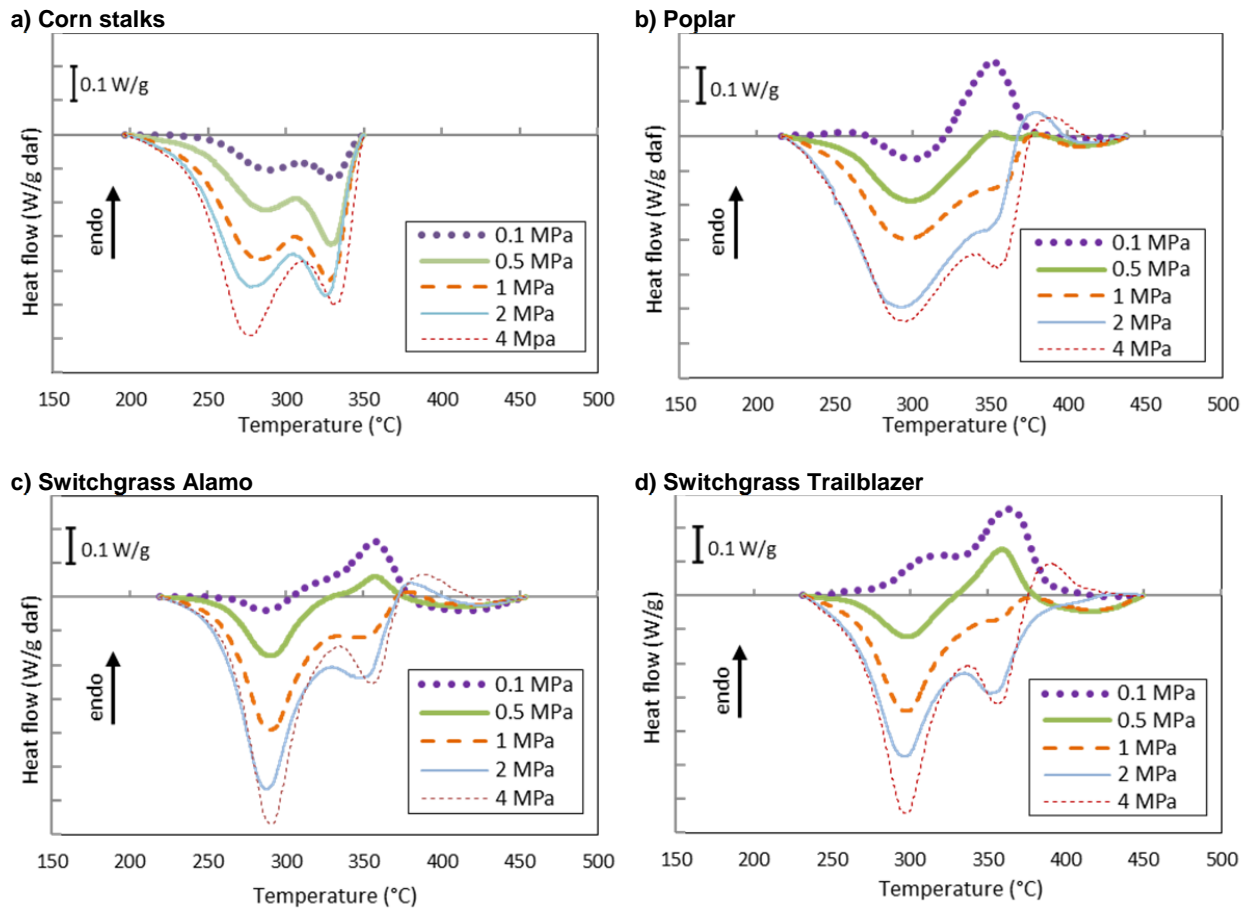


Figure 25. Heat flow at different pressure for corn stalks (a), poplar (b), switchgrass Alamo (c) and switchgrass Trailblazer (d). Conditions: Pure nitrogen, 10°C/min, crucibles without lids.

Table 27. Overall heat demand of the pyrolysis process obtained for the four biomass samples considered at different operating pressures (initial sample weight of about 8 mg). Negative values of the heat flow correspond to an exothermic behaviour.

Pressure (MPa)	Corn stalks		Poplar		Switchgrass Alamo		Switchgrass Trailblazer	
	Char yield (% daf)	Heat (J/g daf)	Char yield (% daf)	Heat (J/g daf)	Char yield (% daf)	Heat (J/g daf)	Char yield (% daf)	Heat (J/g daf)
0.1	23.8	-50	17.3	29	15.1	37	19.1	92
0.5	26.3	-118	22.1	-71	21.4	-40	21.8	-21
1	27.5	-171	26.0	-191	23.2	-134	26.3	-123
2	28.5	-229	28.2	-272	26.4	-203	29.2	-212
4	28.4	-272	30.7	-283	27.3	-199	28.5	-210

The pressure has a strong influence also on the yields of char, as evident from the data in Table 27 reporting the overall heat of reaction from the pressurized DSC tests and the residual char yield. Increasing the operating pressure an evident increase in the total yield of char can be observed. The char yield increases from 21% to 28% for corn stalks, from 17% to 29% for poplar, from 15% to 27% for switchgrass Alamo and from 19% to 29% for switchgrass trailblazer. These results confirm the findings of Mok and Antal [32], [89], that report that increasing the pressure from 0.1 to 2.5 MPa causes the pyrolysis process to shift from endothermic (heat requirement of about 230 J/g) to exothermic (heat generation of about -130 J/g), with char yield increasing from 12 to 22%.

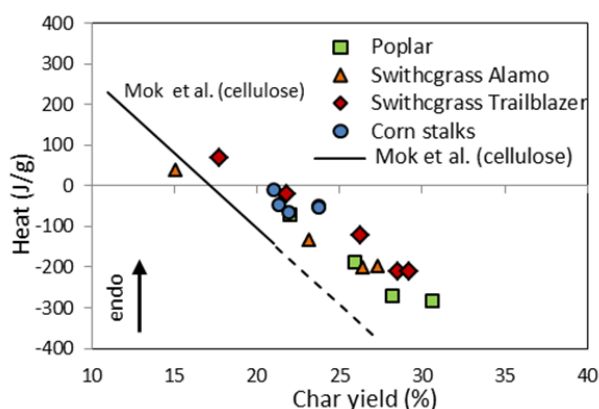


Figure 26. Comparison of the results obtained for the heat demand of the pyrolysis process of cellulose [32] with those obtained in the present study.

It is interesting to compare the results on biomass samples to those obtained by Mok et al. [32], that explored the effect of pressure on the heat demand of the pyrolysis process of cellulose samples. Figure 26 Figure 26. Comparison of the results obtained for the heat demand of the pyrolysis process of cellulose [32] with those obtained in the present study. reports a comparison of the overall heat demand with respect to char yield obtained in the present study for biomass samples and by Mok et al. [32] for cellulose. As shown in the figure, a very similar trend is found for the heat demand with respect to the char yield. However an evident offset is present, and the overall values of the heat demand at a given char yield are higher for cellulose than for the biomass samples considered in the present study. This may further confirm that the presence of lignin may decrease the heat demand of the primary pyrolysis, as reported in several previous publications [37], [39], [60], [77], [87], [88].

4.2 PHENOMENOLOGICAL MODEL

The influence of pressure on the heat requirement of the pyrolysis process can be explained by the inhibition of the evaporation processes of high molecular weight products formed in the primary pyrolysis process, and, as a consequence, by the promotion of exothermic secondary reactions of the primary pyrolysis products. Exothermic secondary reactions of tar vapors, both homogeneous and heterogeneous, include processes such as cracking, partial oxidation, re-polymerization and condensation [31], [32], [36]–[39], [56], [90]–[93].

The influence of operating conditions on the heat of pyrolysis recorded at atmospheric pressure was reported in previous studies, and was attributed to the influence of transport phenomena affecting the residence time of volatiles in the solid substrate [37], [49], [52], [56], [94], [95]. Several studies suggest that while the primary pyrolysis process is endothermic, secondary reactions of volatiles may be highly exothermic [33], [62], [64], [71], [82], [96]. Actually, higher pressures limit mass transfer, thus providing a higher residence time in the porous solid substrate of the volatile products from primary thermal degradation reactions. The highly reactive tarry vapors at high pressure have lower specific volumes. Consequently, their intra-particle residence time is prolonged. Thus, the partial pressure of the tarry vapor is higher, increasing the rate of the secondary exothermic decomposition reactions [84]. These effects can be emphasized when the flow of gas through the particle bed is small, as is the case at high pressure [32], [84], [89]. Furthermore, the formation of secondary carbon from the tarry vapor is catalyzed by the charcoal [97], [98]. Molecular diffusivities are also affected by increasing pressure and can limit the outflow of the tarry vapor from the solid particle [99].

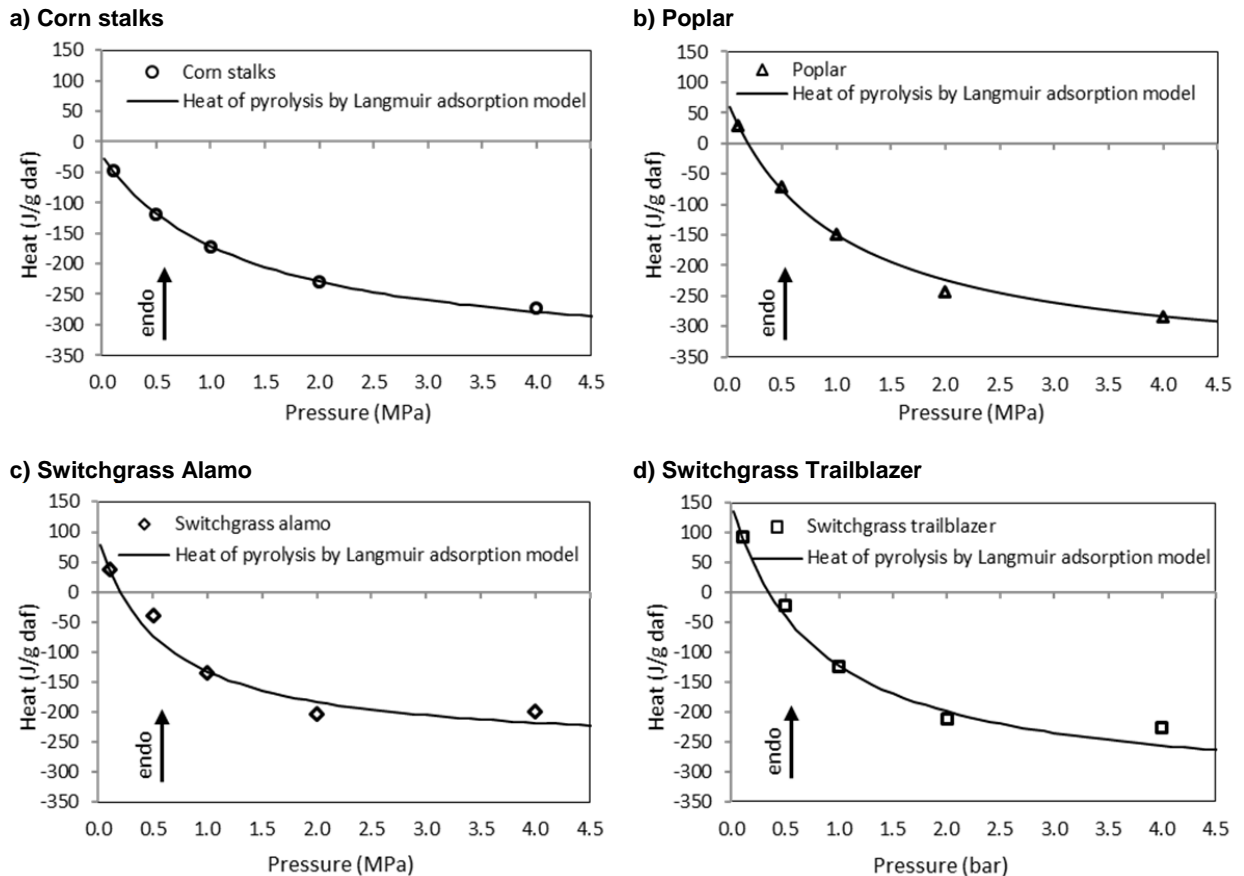


Figure 27. Dependency of heat of reaction from the pressure for corn stalks (a), poplar (b), switchgrass Alamo (c) and switchgrass Trailblazer (d). Conditions: Pure nitrogen, 10°C/min, crucibles without lids. Heat of pyrolysis curves were calculated by Langmuir adsorption model using the best-fit parameters.

In Figure 27 the values calculated for the total heat of pyrolysis were plotted as a function of the operating pressure. As shown in the figure, the heat of pyrolysis decreases as the pressure increases, with an almost linear slope between 0.1 and 1 MPa. However, a plateau appears at pressures higher than 1 MPa. Although a number of factors may justify the results obtained, it is interesting to notice that such behavior may be in accordance with a Langmuir adsorption model of the volatiles, suggesting that adsorption equilibria may play a role in the immobilization of the volatile compounds responsible of the secondary reactions.

Assuming for the sake of simplicity that volatiles generated in the primary pyrolysis process may be considered as a single pseudocomponent, a phenomenological description of the immobilization of the volatiles in the solid can be most simply obtained by a Langmuir adsorption model. The Langmuir isotherm relates the adsorption of molecules on a solid surface to the pressure of the absorbed gas at a fixed temperature:

$$\theta_v = \frac{\alpha p_v}{1 + \alpha p_v} \quad (21)$$

where θ_v is the fraction of volatile products adsorbed on the surface of the solid, p_v is the partial pressure of the adsorbate (the volatile pseudocomponent) in the gas phase and α is the Langmuir adsorption constant.

Several literature results allow assuming that the measured heat of reaction can be considered as the sum of two contribution, one due to the heat required for the primary degradation of the biomass (endothermic) and a second due to the secondary (exothermic) decomposition of volatiles [33], [62], [64], [71], [82], [96]. If volatile decomposition is assumed to be dependent on the fraction of volatile matter in the solid, the total heat of reaction can be expressed as:

$$H_p = H_1 + H_2 \bar{\theta}_v \quad (22)$$

where H_1 is the heat due to the primary degradation of biomass and H_2 is the heat due to the volatile decomposition, both assumed as independent on pressure, and $\bar{\theta}_v$ is the overall amount of pseudocomponent available for the secondary reaction. Assuming that the contribution over the entire degradation range of a dynamic adsorption-desorption equilibrium between the vapor-phase and the surface of the solid can be still described by a correlation similar to equation (21), equation (22) can be written as:

$$H_p = H_1 + H_2 \frac{\alpha y_v P}{1 + \alpha y_v P} \quad (23)$$

where y_v is the molar fraction of the volatile pseudocomponent, and P is the total pressure of the system. The values of H_1 , H_2 and the product αy_v are averaged values for the overall degradation, which were calculated by experimental data fitting. The best-fit parameters calculated from experimental runs are reported in Table 28, while Figure 27 shows the results obtained applying eq. (23) to calculate the heat of pyrolysis using the best-fit parameters of Table 28. The figure shows that eq. (23) provides a reasonable fitting of the trend recorded for the heat of pyrolysis with respect to operating pressure. Moreover, the presence of the plateau at higher operating pressures also seems to find a justification, since at higher pressures the number of molecules adsorbed increase to the point at which further adsorption is hindered by lack of space on the adsorbent surface. Clearly enough, the simplified model presented here supports

only a phenomenological interpretation of the effect of pressure on the material degradation, and is not introduced to provide a detailed description of the complex mechanism underlying secondary char formation [52], [56], [84], [94], [99]. Nevertheless, the important role of secondary gas-solid interactions on the overall heat demand of the pyrolysis process seems to be confirmed by the above findings. The total heat of reaction changes with the pressure as described by the adsorption model. This supports the hypothesis that total heat of pyrolysis is influenced by the secondary reactions occurring between the volatiles adsorbed and the primary char.

Table 28. Best-fit parameters for eq.(23) calculated from experimental runs.

Biomass	H ₁	H ₂	α_v
Corn stalks	-23	-338	0.777
Poplar	68	-442	0.976
Switchgrass Alamo	89	-352	1.70
Switchgrass Trailblazer	147	-482	1.27

Actually, the goal in the application of equation (23) is not to achieve a punctual description of the material degradation, but rather to provide an overall correlation supporting a better phenomenological interpretation of the pressure dependence for the overall heat of reaction. The model proposed is aimed at supporting a phenomenological interpretation of the experimental results exploring possible mechanisms of influence of the pressure on the overall heat of reaction. Since secondary reactions take place on a solid surface undergoing degradation, the role of adsorption of volatile compounds, rather than simple partial condensation, may be relevant. The use on a correlation based on the Langmuir adsorption model has been proposed as one of the simplest possible approached to macroscopically describe these phenomena. Clearly enough more detailed models (e.g. accounting for multi-layer adsorption, diffusion in pores, evolution kinetics) can be used if the goal is a punctual description of the interactions.

The results of the application of the Langmuir model support the hypothesis that pressure induced an inhibition of the evolution of primary pyrolysis products from the condensed phase, and that equilibrium between the evolved primary products and the adsorbed phase on the residual biomass substrate may play a role in the formation of secondary char.

4.3 INITIAL SAMPLE WEIGHT INFLUENCE

The effect of the initial sample mass on secondary reactions has been a focal point of recent studies [28], [58]. Clearly enough, the initial sample mass may affect the mass transfer process, increasing the residence time of volatiles in the solid substrate and enhancing secondary reactions.

Gomez et al. [82] observed that the pyrolysis heat demand is a strong function of the initial sample mass. Larger sample size represents a resistance to the flow of primary volatiles from the vicinity of the reacting particles towards the bulk gas.

Figure 28 compares the DSC experimental heat flow curves obtained in pyrolysis runs carried out on the biomass samples in the DSCQ2000 (atmospheric pressure) and in the DSCQ20P (2 MPa), using different initial sample weights. Increasing the sample mass, the experimental heat curves shift towards a less endothermic behavior and for some types of biomass the overall heat demand shifts from an overall endothermic to an overall exothermic. It is therefore suggested that competitive exothermic and endothermic processes are present. While primary pyrolysis reactions are endothermic, the secondary volatile-solid reactions are responsible for the exothermic behavior [56], [62], [71], [82]. Exothermic secondary reactions of tar vapors, both homogeneous and heterogeneous, include processes such as cracking, partial oxidation, re-polymerization and condensation [32], [36]–[39], [62], [90]–[93]. The extent of the secondary reactions is controlled by the residence time of volatiles in contact with the residue solid, that in turn are governed by the conditions for the outflow of the volatile products from the solid [56].

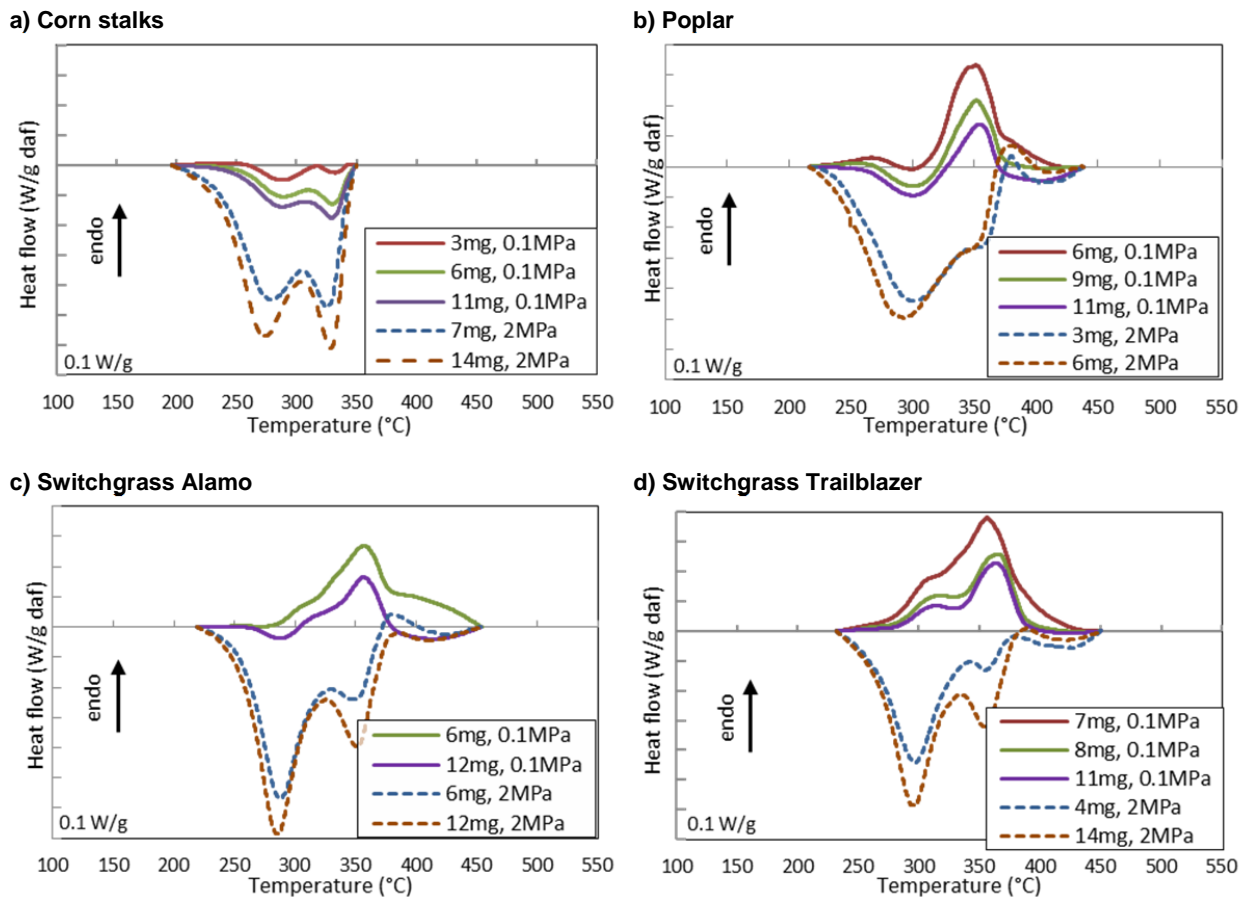


Figure 28. Heat flow at different initial sample weight for corn stalks (a), poplar (b), switchgrass Alamo (c) and switchgrass Trailblazer (d). Conditions: Pure nitrogen, 10°C/min, crucibles without lids, pressure of 0.1 and 2 MPa. Negative values of the heat flow correspond to exothermic behavior.

It can be assumed that as the sample size increases, the overall resistance to mass transfer becomes more significant and this provides a higher residence time of volatiles formed in primary reactions, favoring

gas-solid secondary exothermic reactions. An increase in sample size and weight thus results in a higher residence time and consequently in a higher extent of secondary exothermic processes [69].

Table 29. Heat demand of the pyrolysis process and char yield up to 550°C of the four biomass resulting from runs performed in DSCQ200 using pure nitrogen, 110-550 °C, 10 °C/min, 0.1 MPa. Negative values of the heat demand indicate an exothermic behavior of the process.

Biomass	Initial weight (mg)	Char yield (% daf)	Measured heat (J/g daf)
Corn stalks	3.1	21.9	-10
	6.0	22.5	-48
	9.4	25.1	-55
Poplar	5.9	14.6	93
	9.0	16.8	29
	11.3	18.1	-18
Switchgrass Alamo	6.2	14.8	113
	10.1	15.9	37
	12.2	18.6	18
Switchgrass Trailblazer	4.2	13.7	175
	7.1	21.2	162
	10.8	23.7	69

Table 30. Heat demand of the pyrolysis process and char yield up to 550°C of the four biomass resulting from runs performed in DSCQ20P using pure nitrogen, 110-550 °C, 10 °C/min, 2 MPa operating pressure. Negative values of the heat demand indicate an exothermic behavior of the process.

Biomass	Initial weight (mg)	Char yield (% daf)	Measured heat (J/g daf)
Corn stalks	7.0	29.8	-229
	14.1	30.8	-283
Poplar	3.0	25.8	-233
	7.2	26.1	-243
Switchgrass Alamo	6.1	27.2	-243
	12.6	27.5	-277
Switchgrass Trailblazer	7.1	22.7	-212
	13.6	23.2	-228

Table 29 and Table 30 summarize the char yield and the heat of reaction of the four biomass samples obtained in DSC runs as a function of the initial sample mass at two different operating pressures (respectively at 0.1 and 2 MPa). The approach of Rath et al. [71] was used to obtain quantitative data on the overall heat demand of the process from the experimental DSC curves. The values obtained for the overall heat of reaction are in sufficient agreement with values reported in the literature. Stenseng et al. [64] estimated the heat of reaction of cellulose in the range of 560-710 J/g. Van de Velden et al. [100]

reported a total heat demand of 207 J/g for the pyrolysis of poplar at a heating rate of 10°C/min, although the sample size was not specified.

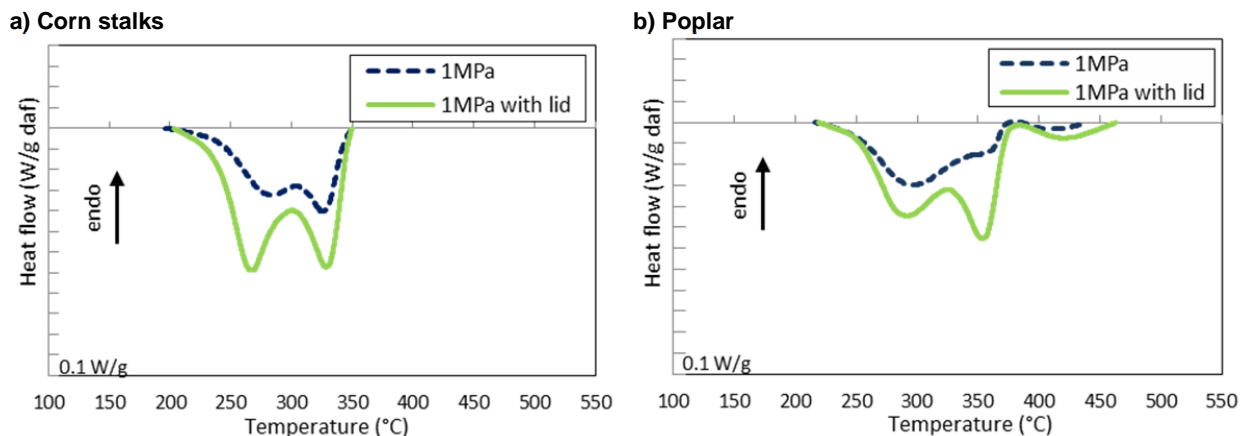
As evident from Table 29 and Table 30, an increase in the char yield and a decrease in the heat demand of the pyrolysis process were recorded increasing the sample size, both at 0.1 and 2 MPa operating pressure. Clearly enough, the initial sample mass may affect the mass transfer process, increasing the residence time of volatiles in the solid substrate and enhancing secondary reactions. These findings are in agreement with the results obtained by Antal et al. [69], [101], who observed that, under slow pyrolysis conditions, small particles of cellulose and wood show an overall endothermic pyrolysis behavior, whereas samples with larger particle size exhibit exothermic behaviors. This difference was explained in terms of the enhanced interactions of hot pyrolysis vapors with the decomposing solid, which involve exothermic processes leading to the formation of char.

4.4 MASS TRANSFER LIMITATIONS INFLUENCE

An additional set of DSC runs was carried out using pierced lids to cover the DSC crucible. Figure 29 shows a comparison between the heat flow curve obtained from the experiments without lid with those obtained with pierced lids at 1 MPa.

As evident from the figure, runs with pierced lid show a lower heat demand with respect to those without lid. The highly reactive tarry vapors have a lower specific volume at high pressure. Thus, their intra-particle residence time is prolonged, increasing the extent of secondary reactions before they leave the biomass particle. Also the concentration of the tarry vapors is higher at higher pressure, increasing the rate of the secondary reactions of volatiles [84]. These effects can be magnified when the residence time of volatiles within the particle bed is raised, as is the case when a pierced lid is used. These elements justify the lower heat demand observed in DSC pyrolysis runs when a pierced lid is used.

A set of runs has been performed varying the operating pressure between 0.1 and 4 MPa in case of sample with lids and the results have been compared to the case without lids. Figure 30 compares the curves obtained for the reaction heat (Q_r) at different operating pressures with lids.



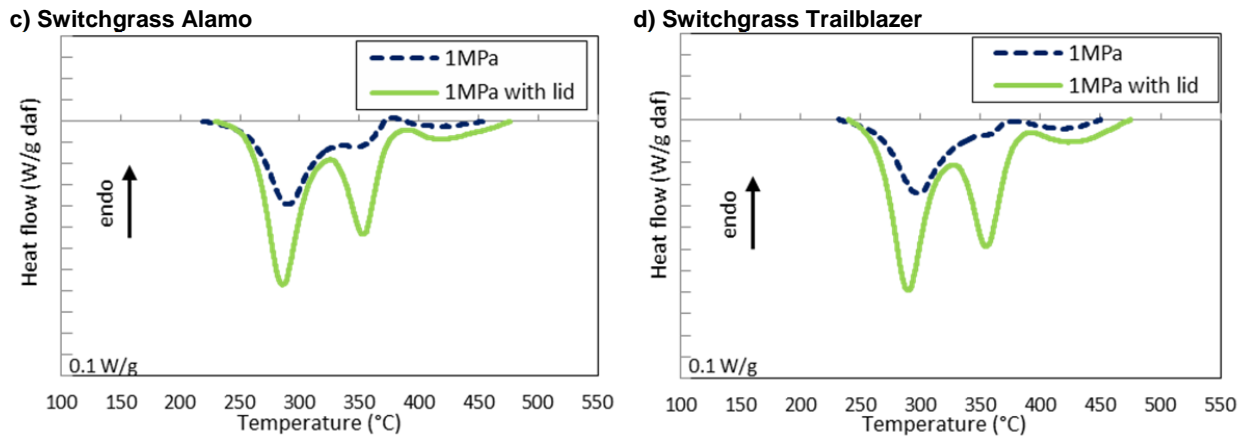


Figure 29. Heat flow for corn stalks (a), poplar (b), sw. Alamo (c) and sw. Trailblazer (d). Conditions: Pure nitrogen, 10°C/min, pressure 10bar, crucibles without lids (dashed line) and with lids (continuous line).

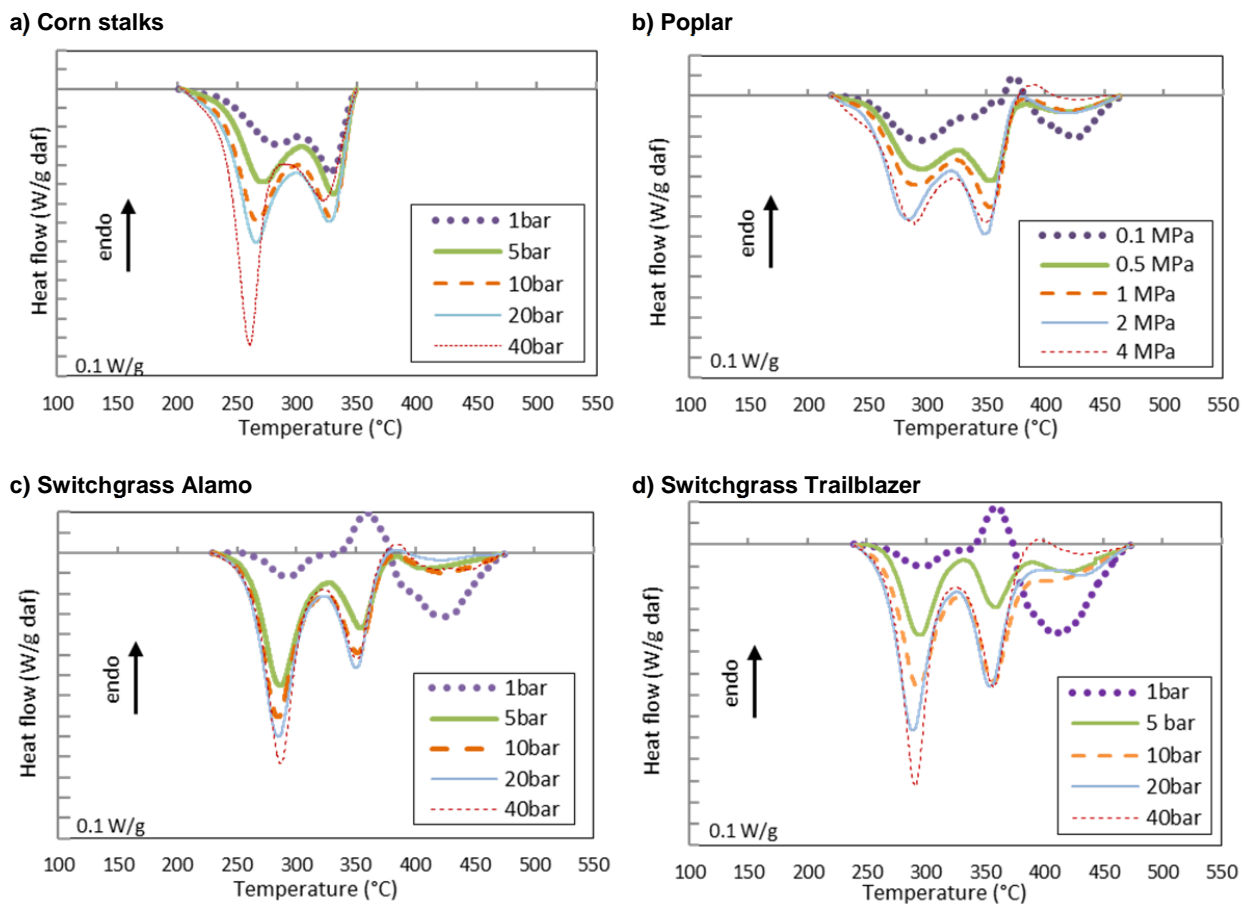


Figure 30. Heat flow at different pressure for corn stalks (a), poplar (b), switchgrass Alamo (c) and switchgrass Trailblazer (d). Conditions: Pure nitrogen, 10°C/min, crucibles with lids.

Table 31. Heat demand of the pyrolysis process obtained using an initial sample weight of about 7.5 mg, a 10°C/min heating rate, pure nitrogen and different operative pressures. Runs were carried out with and without lids on the crucibles. Negative values of the heat demand indicate an exothermic behavior of the process.

Pressure (Mpa)	Corn stalks		Poplar		Switchgrass Alamo		Switchgrass Trailblazer	
	Heat without lid (% daf)	Heat with lid (% daf)	Heat without lid (% daf)	Heat with lid (% daf)	Heat without lid (% daf)	Heat with lid (% daf)	Heat without lid (% daf)	Heat with lid (% daf)
0.1	-50	-164	29	-105	37	-31	92	-154
0.5	-118	-217	-71	-237	-40	-203	-21	-201
1	-171	-284	-191	-284	-134	-303	-123	-323
2	-229	-353	-272	-353	-203	-321	-212	-371
4	-272	-387	-283	-336	-199	-356	-210	-352

Table 31 and Table 32 reports the values of the char yield and of the overall pyrolysis heat demand at different operating pressures in runs carried out with or without a lid. As shown in the tables, both char yield and heat demand increase when a pierced lid is used in DSC runs. These findings are in agreement with the results of Mok et al. [69]. They pyrolyzed biomass in sealed reactors and they observed that the char yield from the closed experiments was higher in comparison to the experiment which left the crucible open at 0.1 MPa.

Table 32. Char yield at 550°C of the pyrolysis process obtained using an initial sample weight of about 7.5 mg, a 10°C/min heating rate, pure nitrogen and different operative pressures. Runs were carried out with and without lids on the crucibles. Negative values of the heat demand indicate an exothermic behavior of the process.

Pressure (Mpa)	Corn stalks		Poplar		Switchgrass Alamo		Switchgrass Trailblazer	
	Char yield without lid (% daf)	Char yield with lid (% daf)	Char yield without lid (% daf)	Char yield with lid (% daf)	Char yield without lid (% daf)	Char yield with lid (% daf)	Char yield without lid (% daf)	Char yield with lid (% daf)
0.1	23.8	25.5	17.3	23.4	15.1	20.2	19.1	23.2
0.5	26.3	28.9	22.1	28.6	21.4	26.6	21.8	20.7
1	27.5	29.9	26.0	28.8	23.2	28.7	26.3	25.2
2	28.5	30.0	28.2	30.5	26.4	30.8	29.2	28.5
4	28.4	31.0	30.7	32.1	27.3	32.1	28.5	33.8

The values of overall heat of pyrolysis reported in Table 5 are in line with those reported in the literature. Gomez and coworkers [82] reported that the overall heat of pyrolysis increases from an endothermic value of 20 J/g to an exothermic value of -200 J/g for char yields between 20% and 40% in the case of thistle.

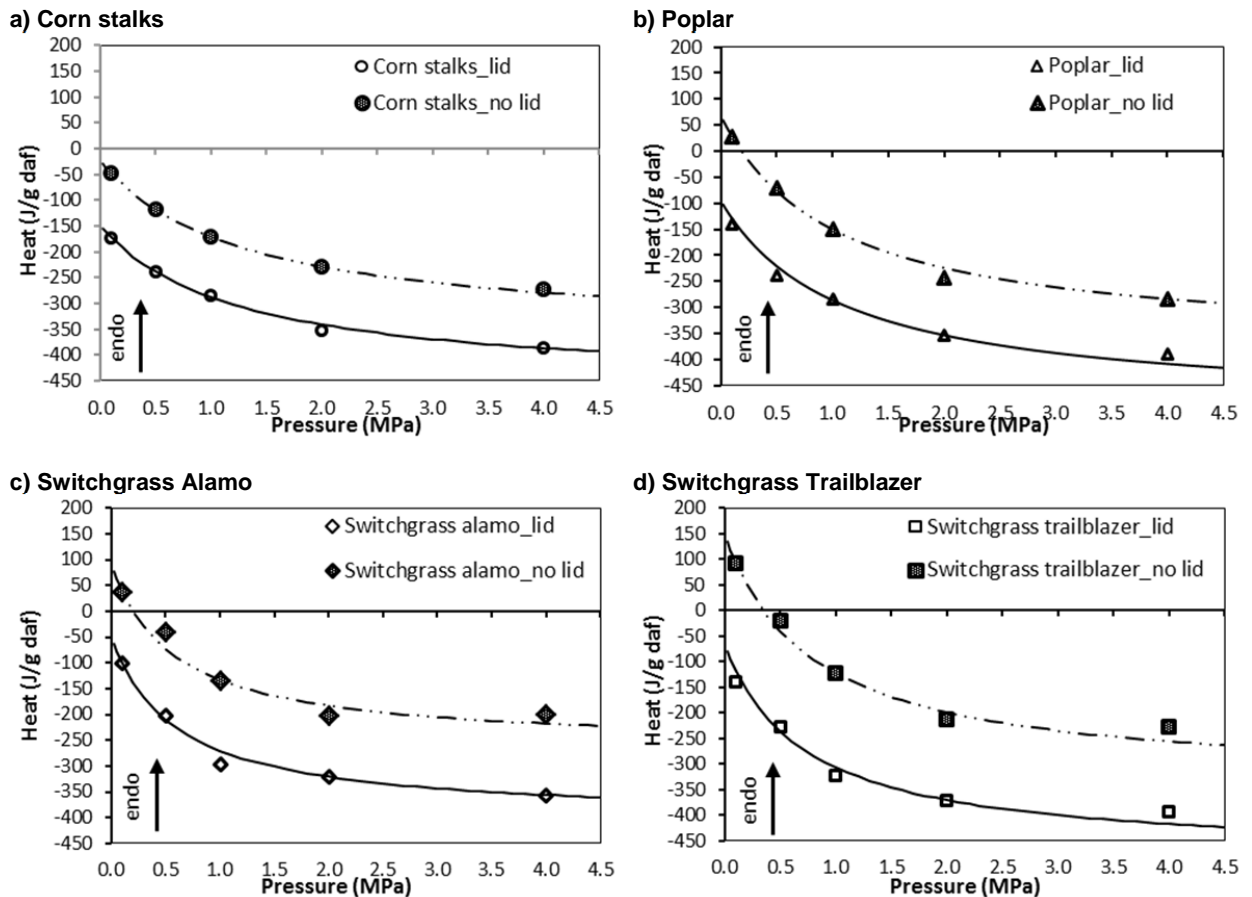


Figure 31. Dependency of heat of reaction from the pressure for corn stalks (a), poplar (b), switchgrass Alamo (c) and switchgrass Trailblazer (d). Conditions: Pure nitrogen, 10°C/min, crucibles without lids and with lids. Heat of pyrolysis curves were calculated by Langmuir adsorption model using the best-fit parameters.

Table 33. . Best-fit parameters for eq.(23) calculated from experimental runs with lids in comparison to those calculated from experiments without lids.

Biomass	H ₁		H ₂		α _v	
	Without lid	With lid	Without lid	With lid	Without lid	With lid
Corn stalks	-23	-149	-338	-312	0.777	0.802
Poplar	68	-95	-442	-398	0.976	0.923
Switchgrass Alamo	89	-52	-352	-350	1.700	1.652
Switchgrass Trailblazer	147	-68	-482	-412	1.270	1.379

In Figure 27 Figure 31 the values calculated for the total heat of pyrolysis were plotted as a function of the operating pressure, comparing with those obtained without lid and they have been interpreted with the

Langmuir adsorption model described previously. The best-fit parameters calculated from experimental runs with lids are reported in Table 28. The pressure-dependent terms H_2 and α_v are almost unchanged in the case with lid respect to the case without lid, meaning that the influence of pressure on the heat demand with or without lid has the same effect.

4.5 PURGE GAS FLOW RATE INFLUENCE

To confirm the above findings, the influence of the gas flow rate on the pyrolysis heat of reaction was assessed performing experiments using poplar wood with crucibles without lid. Although the pressure influences the volumetric flow rate, the variation has a limited effect on the gas residence time in the DSC cell, that ranges between about 0.1 and 0.9s, depending on pressure and temperature. Thus, the residence time is very low in all the experimental conditions used in the present study and is quite below the time scale of observation.

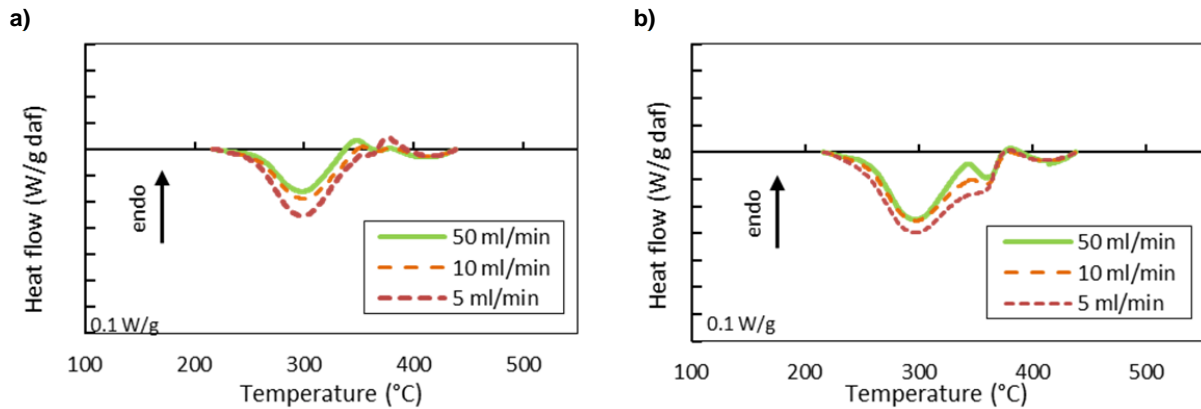


Figure 32. Heat flow at different purge gas flow rate for poplar at (a) 0.5 MPa and (b) 1 MPa. Conditions: Pure nitrogen, 10°C/min, crucibles without lids.

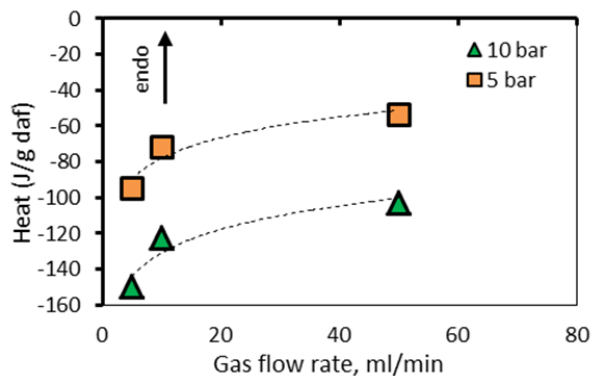


Figure 33. Dependency of heat of reaction from the gas flow rate for poplar. Conditions: Pure nitrogen, 10°C/min, crucibles without lids, pressure 0.5 and 1 MPa.

Figure 32 reports the heat flow curves varying the gas purge flow rate from 5 to 50 ml/min at 0.5 and 1 MPa. Higher gas flow rates should enhance the mass transfer of primary pyrolysis products to the gas phase, thus contributing to a limitation of secondary reactions. As expected at higher gas flow rate, the heat demand is higher (Figure 33).

5 EMPIRICAL MODEL CORRELATION FOR HEAT OF REACTION WITH CHAR YIELD

Figure 34 shows all the data obtained for the heat requirement of the pyrolysis process plotted with respect to the final char yield measured at the end of the DSC run for all the experimental conditions investigated.

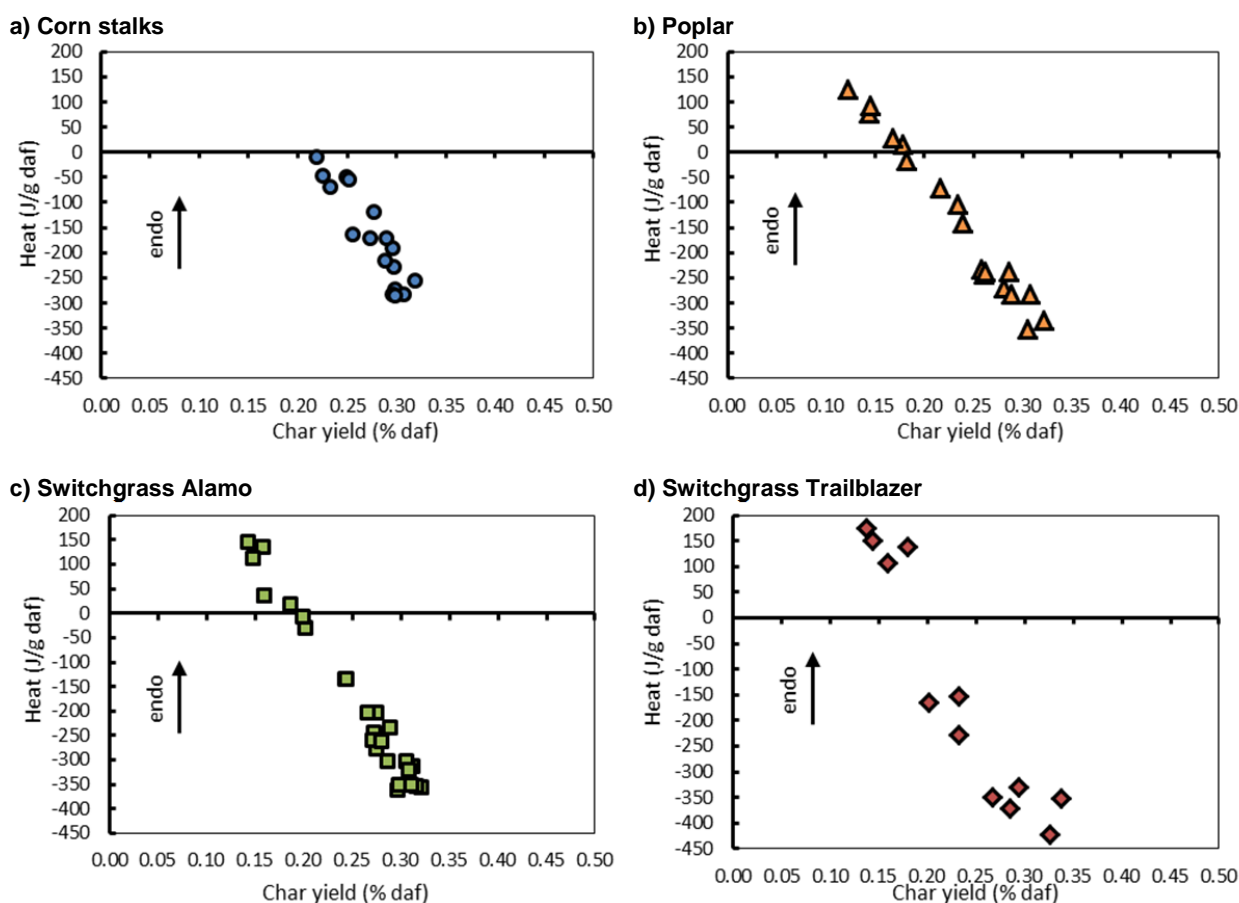


Figure 34. Heat demand of the pyrolysis process with respect to final char yield for: corn stalks (a), poplar (b), switchgrass Alamo (c) and switchgrass Trailblazer (d). Conditions: Pure nitrogen, 10°C/min. Pressure: 0.1-4 MPa. Crucibles with and without lid. Initial sample weight 3-14 mg. Purge gas flow rate 5-50 ml/min.

The trend is in agreement with previous results reported by Mok et al. [32] and by Antal and Gronli [84]. These findings further support the assumption that exothermic interactions among primary volatiles and residual solid leading to secondary char formation can strongly influence the overall thermal effects of the pyrolysis process, as observed in previous studies [32], [82].

The figure shows that a linear dependence may be assumed among the overall heat and the final char yield for all the samples analyzed. A higher char yield corresponds to a lower heat demand of the overall pyrolysis process. This confirms that the higher residence time of the primary volatiles in contact with the solid enhances exothermic secondary char formation. This trend is in agreement with previous results reported by Mok et al. [32], [69] and by Antal and Gronli [28].

Scheme 1 [37], [53], [71]	Scheme 2 [32], [38], [102]

Figure 35. Lumped schemes proposed for the interpretation of the pyrolysis process of biomass: (1) apparent parallel reaction process; (2) apparent consecutive reaction process

The data provided in Figure 34 may be used to obtain further insights on the heat required by the overall pyrolysis process. An extended discussion of models for the kinetics of the biomass pyrolysis process is provided by Ranzi [42], Di Blasi [37], [38], Ahuja [52]. In Figure 35 two lumped schemes are proposed for the interpretation of the pyrolysis process of biomass: scheme 1 is an apparent parallel reaction process, scheme 2 is an apparent consecutive reaction process. Obviously that reported in Figure 4 is an oversimplified reaction scheme, since the actual biomass pyrolysis process is by far more complex.

5.1 APPARENT PARALLEL REACTION PROCESS

Actually, several authors proposed to adopt a parallel competitive lumped reaction scheme to empirically describe the biomass pyrolysis process [37], [53], [71]. As discussed by Stenseng et al. [13], the heat of reaction measured experimentally can be considered as originated by two different categories of reactions: reactions leading to char formation (whose overall heat demand is represented by ΔH_1 in scheme 1) and endothermic cracking reactions (whose overall heat demand is represented by ΔH_2 in scheme 1). As previously underlined by Varhegyi et al. [102], when the transport of the volatile products from the sample layer is hindered, the decomposition mechanism becomes more complex and phenomena arise that cannot be explained by this oversimplified reaction scheme.

Since it proved to be useful in order to analyse kinetic data, it is interesting to apply the above model to reaction heat data. Rath et al. (2003) successfully applied this simplified scheme to approach the interpretation of the overall heat demand of the pyrolysis process [71].

The relation between the overall measured heat of reaction of the pyrolysis process and the heat demand associated to the two processes may be expressed as:

$$\Delta H = (1 - Y)\Delta H_1 + Y\Delta H_2 \quad (24)$$

where Y is the final char yield. Equation (24) can be rearranged and expressed as the sum of two contribution: one dependent from the char yield and one independent on it:

$$\Delta H = (\Delta H_2 - \Delta H_1)Y + \Delta H_1 \quad (25)$$

5.2 APPARENT CONSECUTIVE REACTION PROCESS

As suggested in the literature [32], [38], [102] an alternative scheme may be applied to the representation of the pyrolysis of biomass, based on two lumped reactions in series (Scheme 2 in Figure 35). In this scheme the first lumped reaction represents the biomass decomposition process to primary char and volatiles. The second lumped reaction represents the decomposition process of primary volatiles, catalyzed by the primary char, to form secondary volatiles and char by cracking, partial oxidation, re-polymerization and condensation processes. Actually, the experimental results evidence that secondary reactions strongly affect the overall reaction heat if a sufficient contact time between the volatiles and the primary char is allowed in the pyrolysis system. Although also Scheme 2 in Figure 35 provides an oversimplification of the process, this schematization seems more near to the actual pyrolysis process [32], [38], [102].

When Scheme 2 in Figure 35 is applied to the analysis of experimental data, a specific approach is needed to calculate the apparent heats of reaction from experimental data. A primary char yield, a secondary char yield and a maximum secondary char yield may be defined:

$$Y_1 = \frac{m_{char1}^{prod}}{m_{wood}^o} \quad Y_2 = \frac{m_{char2}^{prod}}{m_{vol1}^{prod1}} \quad Y_{2,max} = \frac{m_{char2}^{prod}}{m_{vol1}^{react2}} \quad (26)$$

The primary char yield Y_1 is the ratio between the weight of the primary char produced in reaction 1 and the initial sample weight of the biomass. The secondary char yield Y_2 is the ratio between the weight of the secondary char produced in reaction 2 and the weight of the volatiles produced in reaction 1, that are all available as reactant for reaction 2. The maximum secondary char yield $Y_{2,max}$ is the ratio between the weight of the secondary char produced in reaction 2 and the weight of the volatiles that effectively react in reaction 2. If all the volatiles produced in reaction 1 react in reaction 2, the secondary char will be equal to the maximum secondary char yield. The total weight of char may be calculated as:

$$m_{char}^{prod} = m_{char1}^{prod} + m_{char2}^{prod} \quad (27)$$

Considering valid the relation (27), the overall char yield is given by the (28):

$$Y = \frac{m_{char}^{prod}}{m_{wood}^o} \quad (28)$$

Assuming the degree of conversion of the first reaction as complete, the measured heat of reaction can be expressed as:

$$\Delta H = \Delta H_1 + x_2 \frac{m_{wood}^o}{m_{vol1}^{prod1}} \Delta H_2 \quad (29)$$

where ΔH_1 and ΔH_2 are expressed as J/g_{wood} and x_2 is the degree of conversion of the second reaction and is given by the following:

$$x_2 = \frac{m_{vol1}^{react2}}{m_{vol1}^{prod1}} = \frac{1}{Y_{2,max}} \frac{Y - Y_1}{1 - Y_1} \quad (30)$$

Substituting the equation (30) in the (29), the measured heat of reaction is given by a linear relation respect to the char yield:

$$\Delta H = \Delta H_1 + \frac{Y - Y_1}{Y_{2,max}} \Delta H_2 \quad (31)$$

Even the proposed lumped reaction scheme in series gives an equation for the heat of reaction linear in the parameter Y. In this equation, Y_1 is the primary pyrolysis yield and it can be interpreted as the yield that would occur if the experimental conditions didn't favor the secondary volatiles-solid interactions. Since the gas-solid primary reaction occurs at completion, the limiting step of the primary reaction is the diffusion of the volatiles within the residual char. The characteristic time of diffusion is given by:

$$t = \frac{L^2}{D} \quad (32)$$

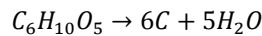
where L is the characteristic dimension and D the diffusion coefficient; with the hypothesis of plane geometry the characteristic time of diffusion is proportional to the squared sample weight.

In Figure 36 it has been reported the char yield as a function of the squared initial sample weight. Extrapolating the straight line to the ideal condition of zero mass (zero diffusion), it is possible to evaluate the primary char yield Y_1 .

The maximum secondary char yield $Y_{2,max}$ is the maximum yield of the secondary reaction, that is one that would occur if all volatiles producing in the first reaction reacted to form secondary char. This is not experimentally determined, but it can be obtained by subtracting the primary char yield to the maximum theoretical yield:

$$Y_{2,max} = Y_{max} - Y_1 \quad (33)$$

where Y_{max} is the maximum theoretical char yield, that is one leading to the formation of pure carbon [69], [84], [103]. According to the stoichiometric equation corresponding to the decomposition of cellulose:



the theoretical yield of carbon which can be realized from cellulose is 44% on a mass fraction basis [69]. Because biomass charcoal contains some hydrogen and oxygen, and because biomass contains lignin (which is rich in carbon relative to cellulose) and other components, it is not possible to calculate an exact value for the theoretical yield of charcoal from biomass. Table 34 summarizes representative compositions of the biomass present in this thesis [104].

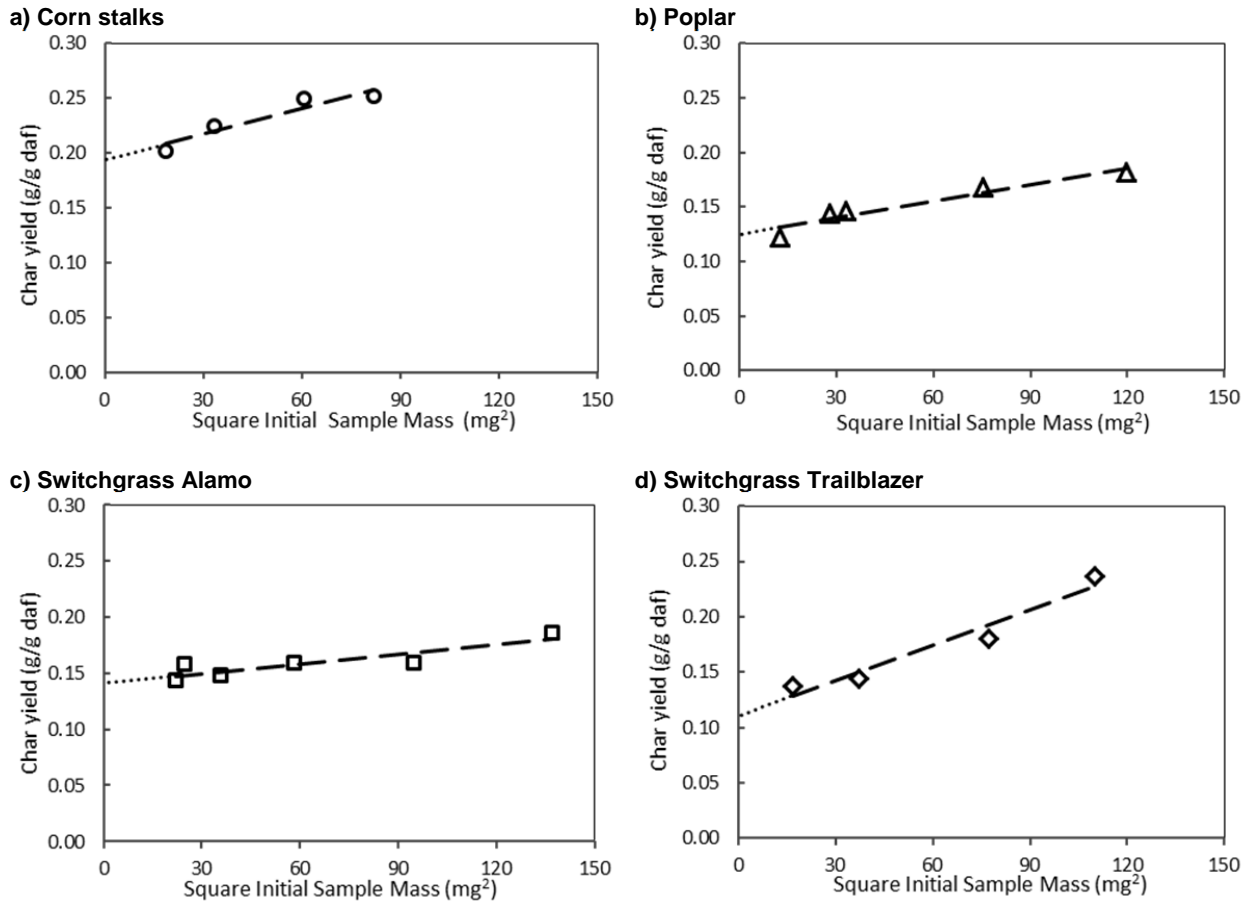


Figure 36. Dependency of char yield from squared initial sample weight for corn stalks (a), poplar (b), switchgrass Alamo (c) and switchgrass Trailblazer (d). Conditions: Pure nitrogen, 10°C/min, crucibles without lids. Pressure: 1 bar.

Considering value in Table 34, it has been estimated the maximum theoretical yield in char. The values are reported in Table a1, and they are in well accordance with those reported in literature. Antal [60] estimated the theoretical yield of a high-quality charcoal from biomass to be between 44 and 55%.

Table 34. Representative compositions of the studied biomass [104]

Biomass	Cellulose % daf	Hemicellulose % daf	Lignin % daf
Corn stalks	41	29	30
Poplar	48	30	22
Switchgrass Alamo	41	31	28
Switchgrass Trailblazer	45	29	26

Table 35. Theoretical primary and secondary char yield for the studied biomass according to the apparent consecutive reaction process

Biomass	Y_1 % daf	Y_{max} % daf	$Y_{2,max}$ % daf
Corn stalks	20	50	30
Poplar	12	49	37
Switchgrass Alamo	14	49	35
Switchgrass Trailblazer	13	49	36

5.3 VALIDATION OF THE MODEL WITH EXPERIMENTAL DATA

From the experimental data in Figure 34 it was possible to calculate the apparent heats of the two reaction processes, ΔH_1 and ΔH_2 , for both the lumped reaction schemes considered in Figure 35. A linear least square approach was applied to obtain the values of the apparent heats for Scheme 1 [105]. The results obtained were reported in Table 36 for all the biomass species considered. Figure 37 shows the predictions obtained applying both models to available experimental data. As shown in the figure, both the empirical lumped reaction schemes provide a good fitting of the experimental data.

As shown in Table 36, limited variations of the apparent reaction heats are obtained when different types of biomass are considered, confirming that possibly common classes of reactions are active in biomass pyrolysis. The estimated values of the exothermic reaction heat of char formation in Scheme 1 (reaction 1, Scheme 1 in Figure 35) are in the range between -2000 and -2500 J/g, while the values of the endothermic reaction heat of thermal cracking range between 440 and 610 J/g. In Scheme 2, an endothermic process is associated to solid decomposition yielding char and volatiles, with apparent reaction heat comprised between 65 and 170 J/g. A strong exothermicity results associated to the decomposition of primary volatiles, with a reaction heat ranging between -950 and -1090 J/g. The strong exothermicity associated to secondary char formation well explains the sensitivity of the overall heat to the final char yield. Moreover, both the lumped reaction schemes considered suggest that only an exothermic char formation process, either during primary solid decomposition or due to volatile further reactions, may justify the experimental results obtained.

Both models were derived from the same experimental data set, thus provide similar values of the overall heat of the pyrolysis process. Estimated values of the overall reaction heats are in well accordance with previous values reported in the literature.

Milosavljevic et al. [33] studied the thermo-chemistry of cellulose pyrolysis by a combination of DSC and thermogravimetric analysis. They found that the main thermal degradation pathway was endothermic in the absence of mass transfer limitations that promoted char formation. They concluded that the endothermicity, which was estimated to be about 538 J/g of volatiles evolved, was mainly due to latent heat requirement for vaporizing the primary tar decomposition products. It was also reported that the pyrolysis could be driven in the exothermic direction by char forming processes that would compete with tar forming processes. The formation of char, which was favored at low heating rates, was estimated to be exothermic to the extent of 2000 J/g of char formed. Table 36 shows that such values are in sufficient

accordance with those obtained by the present approach when Scheme 1 in Figure 35 is applied to the interpretation of experimental data.

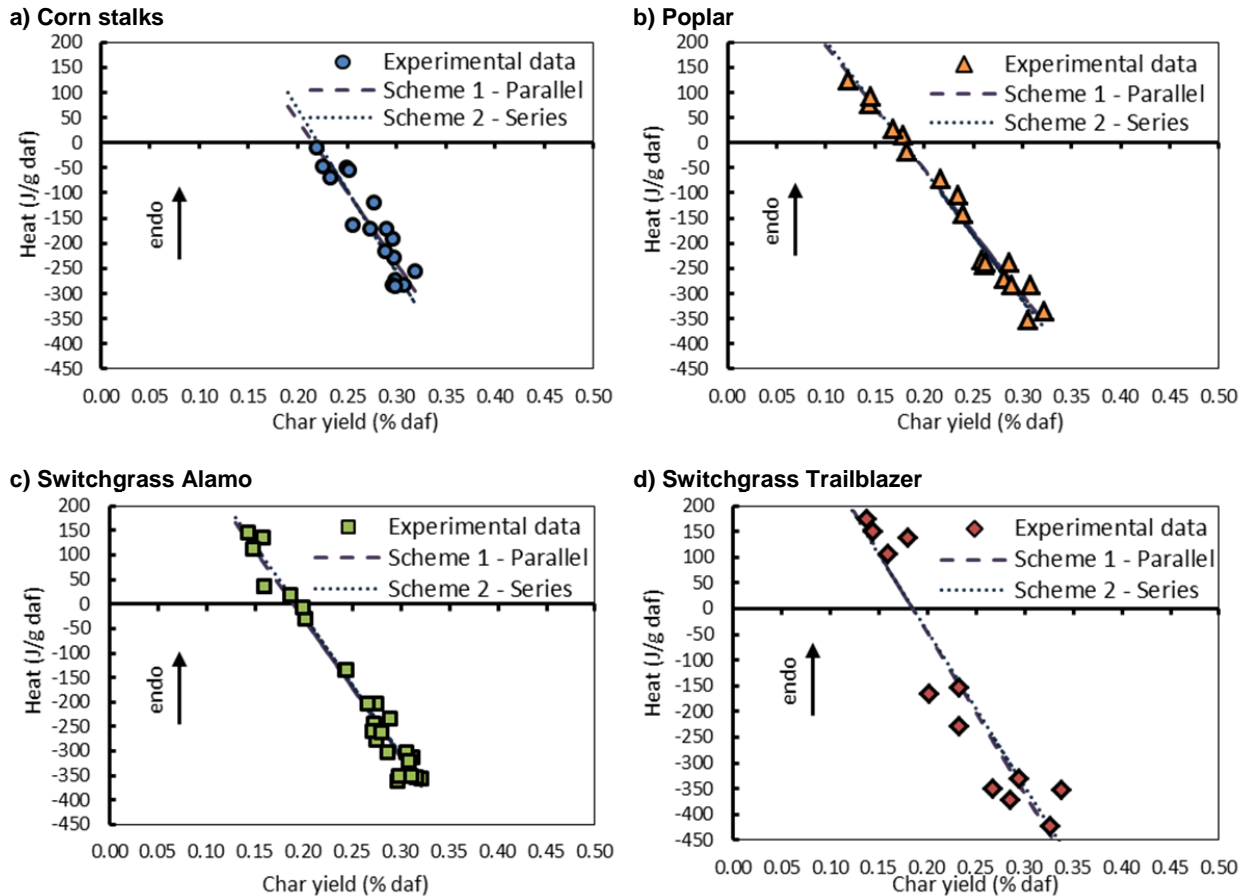


Figure 37. Experimental data and predictions for: corn stalks (a), poplar (b), switchgrass Alamo (c) and switchgrass Trailblazer (d). Conditions: Pure nitrogen, 10°C/min. Pressure: 0.1-4 MPa. Crucibles with and without lid.

Table 36. Heat of reaction calculated for the lumped reactions in Schemes 1 and 2 in Figure 35.

Biomass	Scheme 1 in Figure 35 (Parallel Reactions)			Scheme 2 in Figure 35 (Consecutive Reactions)		
	ΔH_1 (J/g daf)	ΔH_2 (J/g daf)	Av. Std. Deviation	ΔH_1 (J/g daf)	ΔH_2 (J/g daf)	Av. Std. Deviation
Corn stalks	-2232	614	22.5	67	-972	23.7
Poplar	-2045	443	15.1	152	-956	15.1
Switchgrass Alamo	-2275	530	17.5	149	-999	17.1
Switchgrass Trailblazer	-2545	578	41.6	167	-1086	41.6

Varhegyi et al. [102] applied the alternative reaction scheme to describe cellulose pyrolysis, assuming that one reaction determines the rate of solid phase reaction and the other describes the secondary reactions of the volatiles. The value they found for the heat of reaction of cellulose at solid state was in the range 170,190 J/g, while the heat of secondary reaction was in the range -450,-500 J/g. Such values are in sufficient accordance with those obtained by the present approach when Scheme 2 in Figure 35 is applied.

CHAPTER V

MACRO-COMPONENTS SUMMATIVE APPROACH FOR THE OVERALL HEAT DEMAND

1 BIOMASS COMPOSITION: MACROCOMPONENTS

Cellulosic biomass pyrolysis can be assumed as a simultaneous pyrolysis of its three main constituents namely cellulose, lignin and hemicellulose. To establish a large scale, reliable, and economic lignocellulosic industry, biomass recalcitrance must be well understood and overcome. Therefore, to clarify the origin of the wood thermal behavior is interesting to study the major wood constituents thermal behavior [106].

Cellulose and hemicellulose make up 60–90 wt% of terrestrial biomass. Lignin is the other major component of cellulosic biomass. Differences exist between hardwoods and softwoods in the chemical composition deriving from variable contents of the main components (cellulose is around 40–50%, hemicellulose around 28% in softwoods and 35% in hardwoods, and lignin between 23 and 33% for softwoods and 16–25% for hardwoods) and mainly between wood and agricultural residues which present much wider ranges of variation in their chemical composition, not to mention the much higher contents of extractives and ashes [6], [87]. Cellulose consists of a long linear chain polysaccharide formed by d-glucose units, linked by β -1,4 glycosidic bonds and is a crystalline material with an extended, flat, helical conformation. Hemicellulose is a complex, branched and heterogeneous polymeric network, based on pentoses such as xylose and arabinose, hexoses such as glucose, mannose and galactose, and sugar acids; in this amorphous polymer, the major component is a xylose monomer unit. Lignin is a large polyaromatic compound: racemic, heteropolymer consisting of three hydroxycinnamyl alcohol monomers differing in their degree of methoxylation: p-coumaryl, coniferyl and sinapyl alcohols [74], [75].

Comparisons of the thermal decomposition and devolatilisation of wood with its major constituents has been a subject of earlier works. So far, numerous studies on the pyrolytic decomposition of the main components have been carried out [107]. Amongst the individual components of biomass, cellulose has received the most attention because of its abundance and well defined structure [64], [89]. At relatively low temperature cellulose degrades to rather stable anhydro-cellulose resulting in the production of high char but at high temperature the cellulose decomposes to produce volatile products. Cellulose contributes mainly to the production of tar which eventually is a mixture of discrete ketones, aldehydes, organic liquids

and char. Although the pyrolysis products of hemicellulose are assumed to be similar to those obtained from other carbohydrates such as cellulose, very little data is available in the literature regarding hemicellulose pyrolysis. Lignin primarily produces char and small amount of water on pyrolysis. A typical product distribution from lignin pyrolysis has been reported as: gaseous species (12 wt.%), water soluble fraction of bio-oil (consists mainly of water, acetic acid and other low molecular weight compounds, 20 wt.%), water insoluble fraction of bio-oil (15 wt%) and char (40 wt%) [35].

Studies over the biomass structure revealed that cellulose, hemicellulose and lignin are the main ingredients of biomass which influence the product yield of pyrolysis. Cellulose and hemicellulose component in biomass are liable to the volatile products and lignin for the char yield [108]. The yield of gaseous content was reported to grow on as the cellulose increases but the char and tar decrease. It has also been found that the structural difference in the biomass also produces compositional change in the pyrolysis product. Generation of the char from lignin is the outcome of fracturing of relatively weak bonds and the consequent formation of more condensed solid structure [109]. Both cellulose and lignin present in the biomass enhance the formation of biochar but the biochar production is higher in the biomass which has more lignin as compared to cellulose [110]. Demirbas [111] by the pyrolysis of olive husk, corn cob and tea waste showed that olive husk having the most lignin content produced the highest amount of char and corncob with least lignin content lend up with least biochar yield. Similar findings were reported by Lv et al. [112]: rice husk containing most lignin as compared to other biomass has the highest char yield and sugarcane bagasse with the lowest lignin content produced lowest biochar.

The thermal behavior of different types of real biomass has rarely been investigated with the aim of correlating it to the thermal characteristics of its main constituents. Such an approach may be used to better explore pyrolysis mechanism. Since they are the three key building blocks of cellulosic biomass, their thermal behavior is the key-step to analyze the outcomes of the thermal conversion of a biomass feedstock in pyrolysis processes. In order to predict the decomposition behavior of any biomass, first the characteristics of the single components need to be identified [113]. The pyrolysis characteristics of the three main components were investigated using, respectively, a thermogravimetric analyzer (TGA) with differential scanning calorimetry (DSC). A further goal of this study has been to establish the reaction enthalpy effects accompanying cellulose, hemicellulose and lignin pyrolysis, in particular concerning about the factors that influence char formation during pyrolysis, and how these, in turn, influence the thermodynamics of decomposition.

2 WEIGHT LOSS ANALYSIS

Cellulose, hemicellulose, and lignin all have a different thermal decomposition behavior. Figure 38 presents the thermogravimetric and differential thermogravimetric curves of the three basic components. Xylan and lignin are less stable than cellulose and starts their decomposition, respectively, at 200°C and 250°C, while cellulose degradation begins at about 270°C. Xylan and cellulose degradation is qualitatively similar as it happens in a narrow range of temperature, though mass loss rate of cellulose appears sharper than the one observed in the case of xylan. On the contrary, lignin pyrolysis is spread over a wider temperature range.

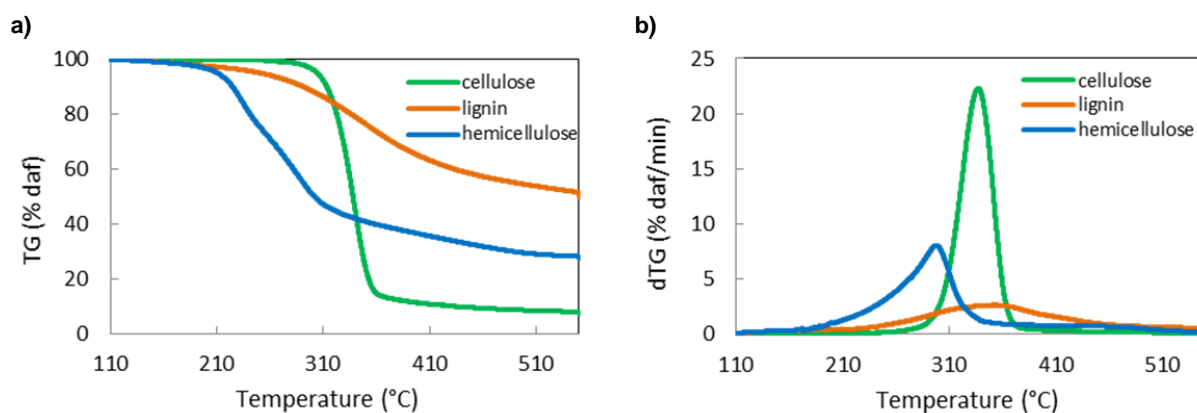


Figure 38. TG (a) and DTG (b) profiles for biomass macrocomponents; the curves are calculated for the ash-free mass of the samples. Reference initial sample mass at 105°C 7mg. Heating rate 10°C/min.

The pyrolysis data are presented in Table 37. Cellulose decomposition rate is the highest and char yield the lowest; lignin on the other hand decomposes over a wider temperature range with the highest char yield. Xylan starts its decomposition easily, with the weight loss mainly happened at 200-330°C. It has the maximum mass loss rate (0.08 wt./min) at 298°C, and there is still 17.6% wt. solid residue left at 550 °C. Cellulose pyrolysis is focused at a higher temperature range (270-390°C) with the maximum weight loss rate (0.22 % wt./min) attained at 337°C and with a very low solid residue left at 550°C (5.7% wt.). Among the three components, lignin is the most difficult one to decompose. Its decomposition happens slowly under a wider temperature range (from 260 to 450 °C), but at a very low mass loss rate (<0.02 % wt./min). The solid residue left from lignin pyrolysis (48.7 % wt.) is the highest.

Table 37. Pyrolysis parameters of the biomass macrocomponents as for TGA results. Reference Initial sample mass at 105°C 7mg. Heating rate 10°C/min.

	Char yield at 550°C (% wt. daf)	Max decomposition rate (10 ² min ⁻¹)	Temperature at max decomposition rate (°C)
Cellulose	5.7	22.30	337
Xylan	17.6	8.02	298
Lignin Alkali	48.7	2.60	351

The differences in the inherent structures and chemical nature of the three components possibly account for the different behaviors observed [10], [114]. Hemicellulose consists of various saccharides (xylose, mannose, glucose, galactose, etc.), it appears a random, amorphous structure, rich of branches, which are very easy to remove from the main stem and to degrade to volatiles evolving out (CO, CO₂, and some hydrocarbon, etc.) at low temperatures [6]. Different to hemicellulose, cellulose is consisted of a long polymer of glucose without branches, its structure is in a good order and very strong, and the thermal stability of cellulose is high. Lignin is full of aromatic rings with various branches, the activity of the

chemical bonds in lignin covered an extremely wide range, which led to the degradation of lignin occurring in a wide temperature range [77].

As it is known from the literature [6], [107], [115], [116], cellulose degradation produce anhydrocellulose and levoglucosan. Hemicellulose decomposes giving rise to more volatiles, less tars, and less chars than cellulose. Lignin pyrolysis yields phenols via the cleavage of ether and carbon-carbon linkages. Lignin is more difficult to dehydrate than cellulose or hemicelluloses and it produces more residual char than does the pyrolysis of cellulose [45].

3 HEAT DEMAND ANALYSIS

All DSC runs were started at 105°C. A constant heating rate of 10°C/min, was used up to the final temperature, set at 550°C. At the end of each run, the furnace was cooled down to 30°C under nitrogen purge gas flow and a second run was performed on the char sample using the same temperature-time program. At the end of the DSC runs the char residue was weighed, and the yields in char and volatile products were estimated.

Figure 39 compares the curves obtained for the reaction heat (Q_r) of the three building blocks. It has to be remarked that the initial and final temperature of the heat flow curve are the initial and final temperatures of the decomposition process. The values of these temperatures depend on the specific component and have been evaluated from the dTG curve as the endpoints of the temperature interval for which the dTG value equals -0.5%/min. As evident from the figure, cellulose behaves differently from xylan and lignin; the pyrolysis of the former is endothermic while that of the latter is exothermic [5]. With temperature increasing (>200 °C), the first DSC profile to appear is the xylan. Cellulose showed a big endothermic peak at 337°C, different from those of xylan and lignin. Xylan and lignin show their peaks at 298 and 351°C respectively, indicating that their pyrolysis reactions are exothermic. It might be attributed to the different reactions or mechanisms involved in pyrolyzing the three components.

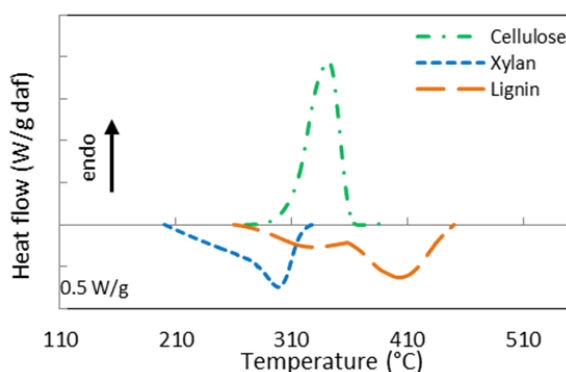


Figure 39. Heat flow for cellulose, xylan and lignin. Conditions: Pure nitrogen, 10°C/min, 7 mg initial sample weight, pressure 1 bar, crucibles without lids.

Ball et al. [117] pointed out that the charring process was highly exothermic whereas volatilization was endothermic. With the much higher solid residues generated from hemicellulose and lignin pyrolysis, the exothermic peaks observed in hemicellulose and lignin pyrolysis could be attributed to the charring, while the full decomposition of cellulose might be attributed to the quick devolatilization reactions, leading to very few solid residues left. Similarly, Mok and Antal [32] in their differential scanning calorimeter (DSC) analysis of cellulose and levoglucosan pyrolysis established some important points in relation to process energetics. Formation of char and gas is an exothermic process, whereas levoglucosan (tar) formation and evaporation are endothermic processes. It is quite plausible that the measured heat of pyrolysis is actually a composite of several different contributions. The role of exothermic char formation is counterbalanced by an endothermic heat of the volatiles release process [33].

As for biomass, even for biomass components it has been investigated the effect of parameters limiting the mass transfer of the volatiles from the decomposing solid to the gas phase. The initial sample weight has been varied between 3 and 18 mg and both open crucibles and crucibles with a pierced lid were used. The effect of the operating pressure will be discussed in the following section. Attention is first directed to the effect of loading (sample mass contained in the DSC crucible), which determines the vapor-phase concentrations of the volatile products. Table 38 summarized the results in terms of heat demand and char yield during the pyrolysis of cellulose, xylan and lignin varying the sample weight with open crucibles.

Table 38. Heat demand and char yield of the pyrolysis process and char yield up to 550°C of the biomass macrocomponents resulting from runs performed in DSCQ2000 using pure nitrogen, 110-550 °C, 10 °C/min, 0.1 MPa operating pressure, crucibles without lids, initial sample weight 3-17mg. Negative values of the heat demand indicate an exothermic behavior of the process.

Biomass	Initial weight (mg)	Char yield (% daf)	Measured heat (J/g daf)
Cellulose	3.5	4.4	595
	8.0	5.7	444
	10.0	6.8	375
	17.0	9.5	345
Xylan	3.5	14.0	-240
	9.5	17.6	-240
	14.0	19.1	-250
	16.5	17.6	-265
Lignin	3.8	43.7	-489
	8.0	48.3	-355
	10.0	48.5	-282
	17.5	49.3	-221

Milosavljevic et al. [33] studied the thermo-chemistry of cellulose pyrolysis by a combination of DSC and thermogravimetric analysis. They found that the main thermal degradation pathway was endothermic in the absence of mass transfer limitations that promoted char formation. They concluded that the endothermicity, which was estimated to be about 538 kJ/kg of volatiles evolved, was mainly due to latent

heat requirement for vaporizing the primary tar decomposition products. In this study it has been found that at atmospheric pressure the heat of cellulose pyrolysis ranges between 345-595 J/g. This value is in accordance with the value reported by Milosavljevic et al. [33]. Stenseng et al. [64] measured the heat of pyrolysis for Sigma cellulose to be 450 J/g, the same value has been found from Fisher et al. [118]. As reported in Table 38, the heat of pyrolysis for xylan varies from -240 to -265 J/g and for lignin from -221 to -489 J/g. Bilbao et al. [60] found an exothermic heat of lignin pyrolysis of -353 J/g. The exothermic character of the lignin relies on liberation of hydrocarbons, phenolic and neutral oils [119].

The influence of the sample weight is different on the three components (Figure 40). For cellulose the heat of reaction decreases and the char yield increases as sample weight increases. Stenseng et al. [64] found that small samples of Avicell cellulose (2 and 5 mg) show the largest heat of reaction, between 630 and 710 J/g daf, while larger samples (20 mg) showed a lower heat of reaction of approximately 560 J/g daf. For xylan there is no clear trend neither in the heat of reaction nor in the char yield. For lignin a slight trend of increasing char yield with loading can be seen and on the contrary to cellulose a trend of increasing heat of reaction with increasing sample weight.

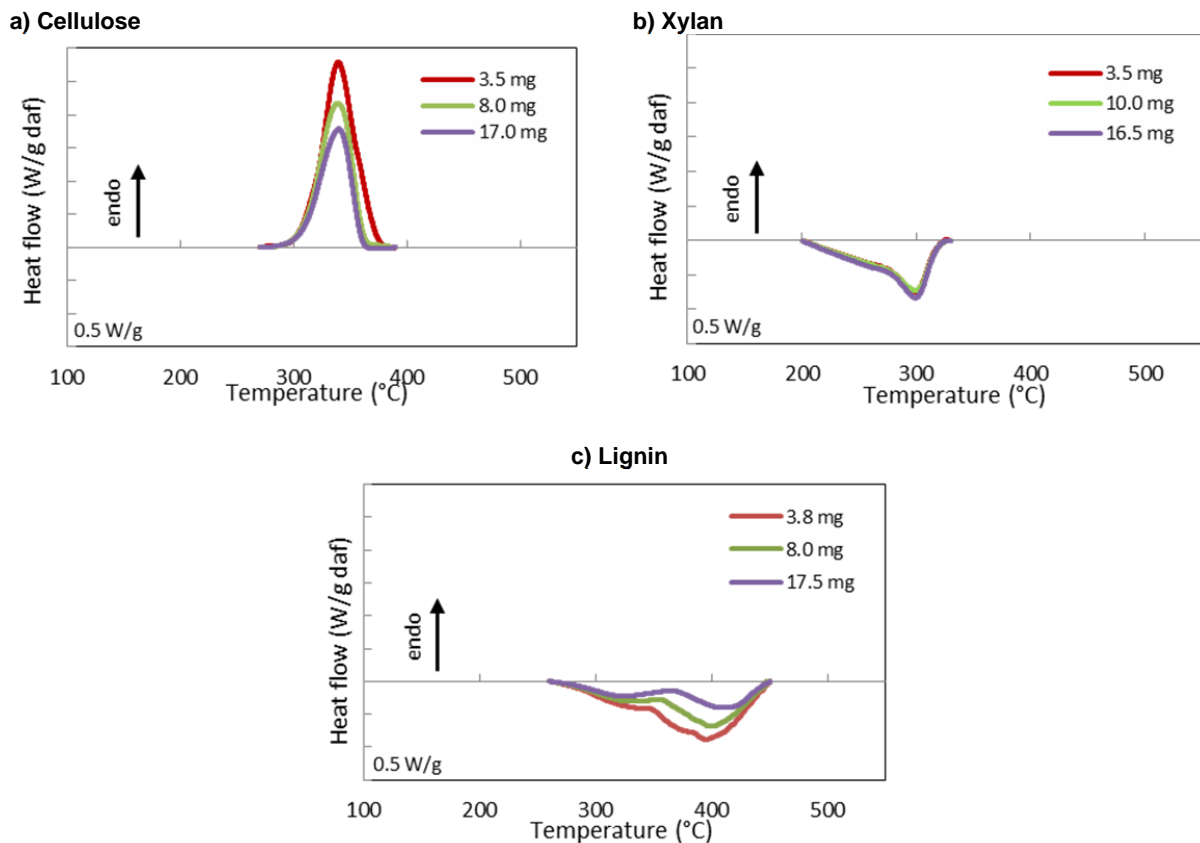


Figure 40. Heat flow at different initial sample weight for cellulose (a), xylan (b), lignin (c). Conditions: Pure nitrogen, 10°C/min, crucibles without lids, pressure of 0.1 MPa. Negative values of the heat flow correspond to exothermic behavior.

As indicated in Table 39, the char yield from cellulose pyrolysis with the closed crucible experiment is 18.9%. In comparison, the char yield from an experiment with the same amount of sample which leaves the crucible open to nitrogen at 1 atm pressure is 5.7%. This is in good accordance with the findings of Mok and Antal [69] confirming that char formation from cellulose can be increased remarkably by pyrolysis within a sealed reactor. At the same time, when the lid is used the heat of pyrolysis decreases from 444 J/g to 152 J/g using a closed crucible. This result suggests that when closed DSC crucibles are used the pyrolysis kinetics is enhanced, confirming the findings of Mok et al [69].

Table 39. Heat demand and char yield of the pyrolysis process and char yield up to 550°C of the biomass macrocomponents resulting from DSC runs using pure nitrogen, 110-550 °C, 10 °C/min, 0.1 MPa operating pressure, crucibles with and without lids, initial sample weight 8 mg approx. Negative values of the heat demand indicate an exothermic behavior.process.

Biomass	Char yield (% daf)		Measured heat (J/g daf)	
	without lid	with lid	without lid	with lid
Cellulose	5.7	18.9	444	152
Xylan	17.6	27.3	-240	-319
Lignin	48.3	52.4	-348	-248

The use of the open crucible reduces the residence time of the volatiles in the pores reducing tar cracking that would otherwise be promoted by the presence of the lid. In the small sample the gases that are generated simply leave the particle. In a lid-covered crucible, the volatiles produced from biomass pyrolysis take longer time to diffuse out of the crucible than in an open crucible, which leads to more secondary reactions of these vapour products with solid residue. In the tests without lids, secondary reactions are less severe since the released volatiles diffuse more quickly out of the crucible.

For xylan the trend is the same: when the lid is used the char yield increases from 17.6 to 27.3% daf and the heat of pyrolysis becomes more exothermic varying from -240 to -319 J/g. For lignin the char yield increases from 48.3 to 52.4 but the heat of pyrolysis becomes more endothermic, increasing from -348 to -248 J/g in the presence of a lid on the sample, with the same trend observed increasing the sample weight. This is also clear from Figure 41. Heat flow curves are highly influenced by the lids on the crucibles. In the case without lids for cellulose and xylan the peak temperature of decomposition increases. When biomass pyrolysis takes place in a crucible with a lid, the primary volatiles would first be trapped in the crucible and thus enhance secondary char formation reactions. In an open crucible, however, the released volatile matter could readily diffuse into the purge gas stream. The partial pressure of the volatiles around the primary char surface remains low and more refractory components could decompose, leading to higher termination temperature and lower char yields in the tests without lids. [120]

It has to be remarked that in general the DSC curve without lid differ significantly from that of the case with lids as the baseline bended to endothermic side due to the radiative heat effects [70]. However in this study the heat flow of radiation has been considered for a correct interpretation of the DSC data, as described at pag. 45.

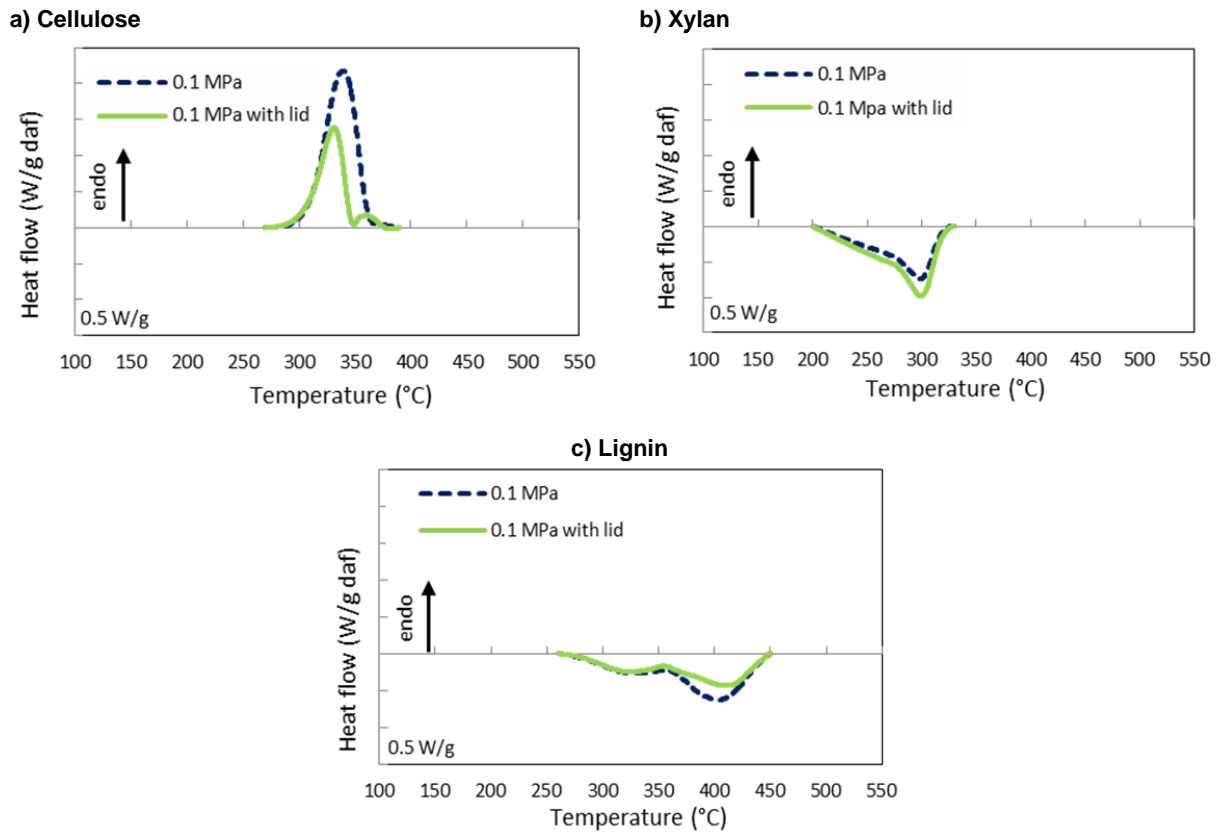


Figure 41. Heat flow for cellulose (a), xylan (b) and lignin (c). Conditions: Pure nitrogen, 10°C/min, 7.5 mg initial sample weight, pressure 1 bar, crucibles without lids (dashed line) and with lids (continuous line).

4 INFLUENCE OF PRESSURE ON THE HEAT OF PYROLYSIS OF BIOMASS MACROCOMPONENTS

DSC runs were carried out to study the heat demand of pyrolysis at the following operating pressures: 0.1, 0.5, 1, 2, and 4 MPa. The inlet nitrogen flow rate was fixed at 5 ml/min. Samples with initial weight of 7.5 mg in open crucible were used. Figure 42a reports the heat flow of cellulose pyrolysis between 0.1 and 4 MPa. Results of this series of experiments show that with increasing pressure the heat of pyrolysis decreases, shifting towards exothermic. Considering the dimensionless sample conversion $X(T)$ previously defined as:

$$X(T) = \frac{m_0 - m_T}{m_0 - m_{char}} \quad (34)$$

it has been plotted as a function of the heat flow at different pressure in Figure 42b. It can be seen that as the pressure increases the heat flow becomes less endothermic.

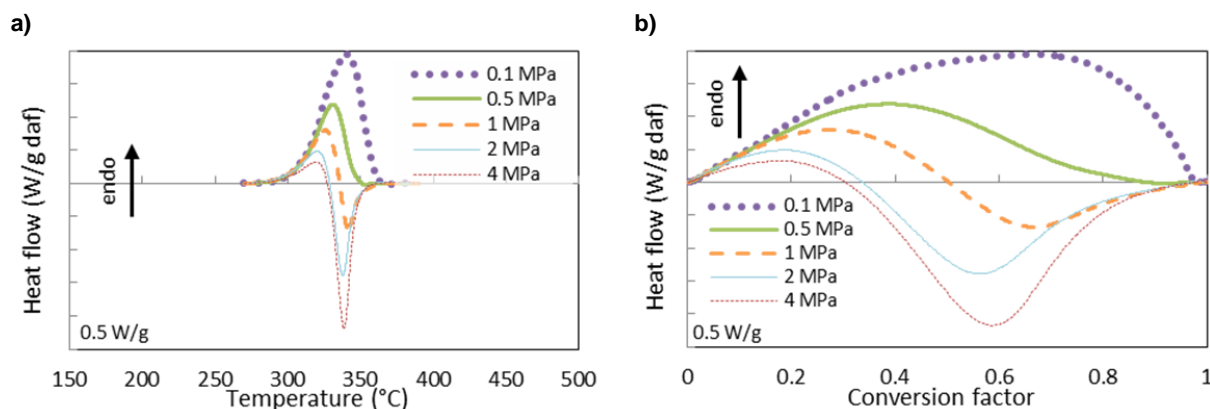


Figure 42. Heat flow at different pressure (a) and conversion factor (b) for cellulose. Pure nitrogen, 10°C/min, crucibles without lids. Initial sample weight 7.5 mg.

In Table 40 the conversion factor and the shifting temperature of the heat flow from endo- to exothermic are summarized as a function of pressure. At atmospheric pressure cellulose pyrolysis is completely endothermic, but at 0.5 MPa it has a shift at 351°C, indicating the change from endothermic to exothermic behavior of the pyrolysis phenomenon. At 4 MPa the shift occurs in the early stage of the pyrolysis process, at 327°C, resulting in a small endothermic peak followed by a major exothermic interval. The shifting temperature results dependent on the operating pressure, showing the presence of two separate reaction steps: the first endothermic corresponding to the main decomposition of cellulose into volatiles, while the second one due exothermic char formation reactions [32].

Table 40. Conversion factor and shifting temperature of the cellulose pyrolysis process analyzed at different operating pressures (initial sample weight of about 7.5 mg).

Pressure (MPa)	Conversion factor (-)	T shift endo-exo (°C)
0.1	-	-
0.5	0.88	351
1	0.50	336
2	0.34	329
4	0.30	327

As already known from the literature [32], [89], [121], [122], the operating pressure of the pyrolysis process influences also the yield in char. In 1983 Mok and Antal [89], using a tubular flow reactor embedded in a

differential scanning calorimeter, report an increase in the yield of char from cellulose from 12 to 22% when the operating pressure is increased from 0.1 to 2.5 MPa. Richard and Antal [122] report an increase in the char yield from cellulose from 19 to 41% when pressure is increased from 0.1 to 2.0 MPa. Fundamental studies of the influence of pressure on biomass pyrolysis have shown that very high yields of charcoal are obtained when pyrolysis is conducted at elevated pressure in a closed vessel, wherein the vapors are held captive and in contact with solid products of pyrolysis [69], [103]. It is well-known that the volatiles are not stable at elevated temperatures in the presence of charcoal or decomposing solid biomass. The volatiles adsorb onto the surface of the solid and quickly carbonize, releasing water, carbon dioxide, and methane as byproducts. High pressure increases the yield of char from pure cellulose, because it favors one of the competing, solid-phase pyrolysis reactions that preferentially forms char. Under pressure, the highly reactive, tarry vapors have a smaller specific volume; consequently, their intraparticle residence time is prolonged, increasing the extent of their decomposition as they escape the biomass particle. Also the concentration (partial pressure) of the tarry vapor is higher, increasing the rate of the decomposition reaction. Molecular diffusivities are also affected by increasing pressure and can influence the escape of the tarry vapor from the solid particle. In Figure 43 the char yield and the heat of pyrolysis have been plotted as a function of the pressure. The figure clarifies the pressure influence on both the decrease in the heat of pyrolysis and the increase in the formation of char.

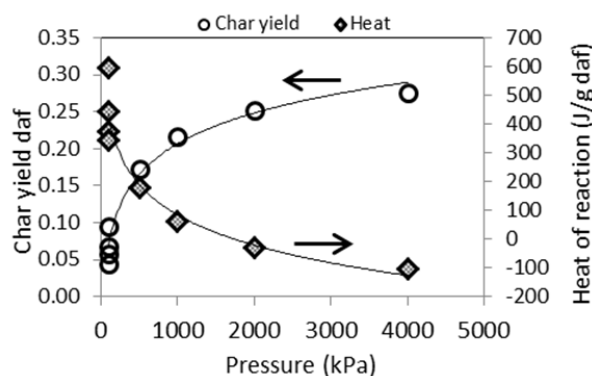


Figure 43. Dependency heat demand and final char yield with pressure for cellulose. Pure nitrogen, 10°C/min, crucibles without lids. Initial sample weight 7.5 mg.

Figure 44 shows values of the enthalpy of pyrolysis obtained under various pyrolysis conditions, leading to various char yields in comparison with values obtained from Mok and Antal (1983) [32]. There is good agreement between us and Mok and Antal on the conclusion that there is a linear decrease in the endothermic heat of pyrolysis as char yield increases [32].

Figure 44, again, illustrates that the yield of char is the main factor determining whether the overall pyrolysis process is endo- or exothermic. This is an important global feature to build into any model of pyrolysis. The role of exothermic char formation is counterbalanced by an endothermic heat of volatiles release. Several other studies evidence a relation among secondary reactions of volatiles and the overall heat demand of the pyrolysis process even at atmospheric pressure [33], [52], [56], [71], [82], [100].

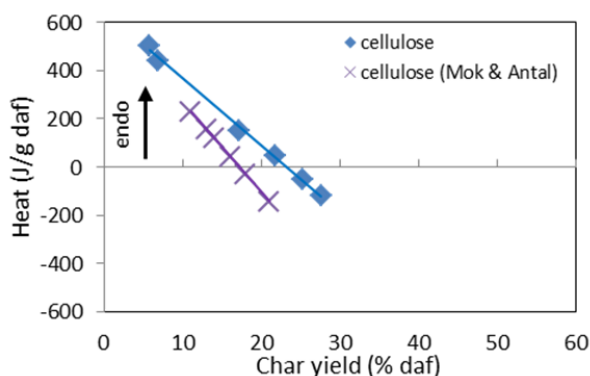


Figure 44. Comparison of the results obtained for the heat demand of the pyrolysis process of cellulose by Mok and Antal [32] with those obtained in the present study.

Similar experimental runs were performed on xylan and lignin, in order to analyze the effect of pressure on the other two biomass components. Figure 45 shows the heat flow for xylan and lignin from 0.1 to 4 MPa. The operating pressure has on xylan the same effect observed on cellulose but at lower extent. Lignin exhibits a different behavior: pressure has not a significant effect on the heat flow.

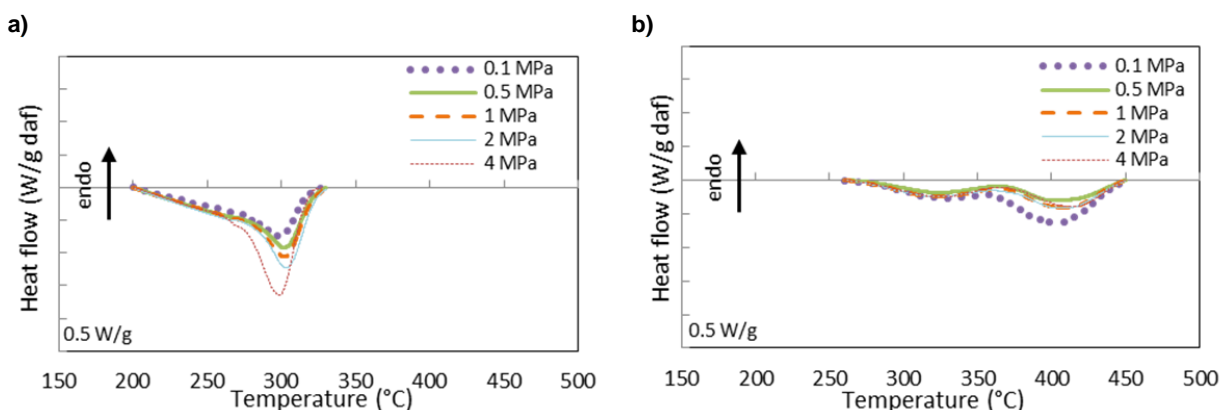


Figure 45. Heat flow at different pressure for xylan (a) and lignin (b). Pure nitrogen, 10°C/min, crucibles without lids. Initial sample weight 7.5 mg.

In Table 41 the values for overall heat demand and char yield have been summarized for all the three biomass components. As shown in the table, increasing the pressure a clear decrease in the heat demand of the pyrolysis process can be observed for cellulose and slightly for xylan. When increasing the pressure from 0.1 MPa to 4 MPa, the total heat of pyrolysis shifts from 504 J/g to -120 J/g for cellulose and from -240 J/g to -403 J/g for xylan. Lignin total heat of pyrolysis ranges between -343 and -471 J/g, without any clear trend respect to the pressure. Mok showed that increasing pressure causes the total heat of cellulose pyrolysis to shift from values near 230 J/g at 0.1 MPa to values near -130 J/g at 2.5 MPa [103]. An increase in pressure also affects the pyrolysis of hemicellulose: Mok observed one broad exotherm within

a temperature range of 195-235 °C during the pyrolysis of a xylan extract in a flowing inert gas at 0.1 MPa [32]. This exotherm shifted to lower temperatures at higher pressures. Increasing pressure at low flow rates also caused lignin to undergo exothermic pyrolysis with a small increase in yield [32].

The pressure has a strong influence also on the yields of char, as evident from the data in Table 41. Increasing the operating pressure an evident increase in the total yield of char can be observed for all the components. The char yield increases from 5.7% to 27.6% for cellulose, from 17.6% to 29.8% for xylan, from 48.7% to 56.0% for lignin. It can be argued that cellulose exhibits the greatest effect, since it contains the higher content in volatiles; volatiles evolving during pyrolysis react with char and influence the thermal behavior at great extent.

On the other hand, lignin undergoes pyrolysis to form much higher yields of char than either pure cellulose or isolated hemicellulose. The high yield of char from lignin is, in part, a result of its enrichment in carbon relative to the carbohydrate components. In addition, the presence of water vapor at elevated pressure not only lowers the temperature needed for decomposition of lignin, but also promotes the formation of polyhydric non-volatile phenols by saponification of ether bonds between the lignin fragments [103].

Table 41. Overall heat demand and char yield of the pyrolysis process obtained for the three biomass components analyzed at different operating pressures (initial sample weight of about 7.5 mg). Negative values of the heat flow correspond to an exothermic behaviour.

Pressure (Mpa)	Cellulose		Xylan		Lignin	
	Heat (J/ g daf)	Char yield (% daf)	Heat (J/ g daf)	Char yield (% daf)	Heat (J/ g daf)	Char yield (% daf)
0.1	504	5.7	-240	17.6	-449	48.7
0.5	153	17.2	-288	27.5	-343	51.6
1	47	21.7	-321	28.3	-401	54.2
2	-50	25.3	-364	28.4	-471	55.3
4	-120	27.6	-403	29.8	-354	56.0

Figure 46 displays the relationship that exists between the pyrolytic heat of reaction and the observed char yield for biomass components and lignocellulosic biomass studied in the previous chapter. The relation is linear for cellulose and biomass [33], [39], [69], [123]. For them, the heat evolved by pyrolysis is proportional to the amount of charcoal produced by the primary and secondary carbonization reactions. When the yield of charcoal is high, the pyrolysis chemistry is strongly exothermic. For xylan the relation is linear, but the change in char yield is very limited. Whereas the values obtained for lignin do not show any definite trend. Lignin exhibits in general the most exothermic behavior and the highest char yield compared to the other biomass components. The linear correlation between char yield and heat of pyrolysis in the biomass has the same shape of the cellulose, but translated towards lower values of heat due to the content of xylan and lignin in it.

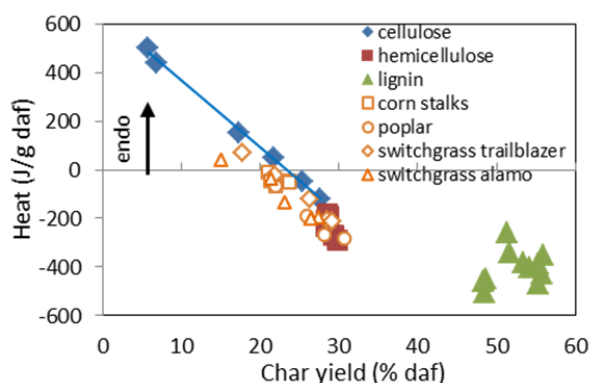


Figure 46. Heat demand of the pyrolysis process with respect to final char yield for corn stalks, poplar, switchgrass Alamo and switchgrass Trailblazer, cellulose, xylan and lignin. Conditions: Pure nitrogen, 10°C/min. Pressure: 0.1-4 MPa. Crucibles with and without lid. Initial sample weight 3-14 mg. Purge gas flow rate 5-50 ml/min.

5 COMPARISON BETWEEN BIOMASS AND BIOMASS MACROCOMPONENTS

Thermogravimetric studies show that each kind of biomass has unique pyrolysis characteristics, by virtue of the specific proportions of the components present in it. In Figure 47 derivative thermogravimetric curves of lignocellulosic biomass are presented by superimposing them to derivative thermogravimetric curves of biomass components. As can be seen, the thermal decomposition of the biomass samples starts at about 220°C, followed by a major loss of weight zone between 280 and 400°C, and a flat tailing zone up to about 550°C, after which the devolatilization is essentially completed. The major weight loss zone takes the form of a shoulder and peak curve, with the shoulder corresponding to the decomposition of hemicelluloses and the peak to the cellulose. Both the cultivars of switchgrass present a more accentuated peak corresponding to hemicellulose. The exception is corn stalks, where the two devolatilization ranges of the two components overlap and the shoulder is much less pronounced. The tailing zone corresponds to the decomposition of lignin, which is the least reactant component.

Taking into account [64], [77], [87], [113] that hemicellulose degrades exothermally in the range 220-320°C, cellulose degrades endothermally in the temperature range 270-390°C, and the large part of the exothermic degradation of lignin takes place between 260-450°C, the thermal behavior of lignocellulosic biomass is influenced by the proportions of the components present in it. In Figure 48 heat flow curves of lignocellulosic biomass are presented by superimposing them to heat flow curves of biomass components. Corn stalks presents two exothermic peaks corresponding to hemicellulose and lignin degradation and as a result it has an overall exothermic behavior. It is well known in literature that biomass species rich of extractives, hemicellulose and lignin usually show an overall exothermic pyrolysis behavior [37], [39], [60], [77]. Also the presence of ash, which catalyzes exothermic char formation, and the textural structure were reported as factors influencing the overall heat demand of the pyrolysis process [37], [56]. It is well

distinguishable in the heat flow curves of poplar the sequence of exothermic, endothermic and exothermic effects in the order due to degradation of hemicellulose, cellulose and lignin. In the literature [60], [88] the exothermic lignin decomposition is presumed to be responsible for the exothermic thermal behavior in the final stage of wood pyrolysis. For both the cultivars of switchgrass the first reaction corresponding to hemicelluloses (approximately 220-340°C) partially overlaps with the second reaction, corresponding to cellulose, (290-400°C).

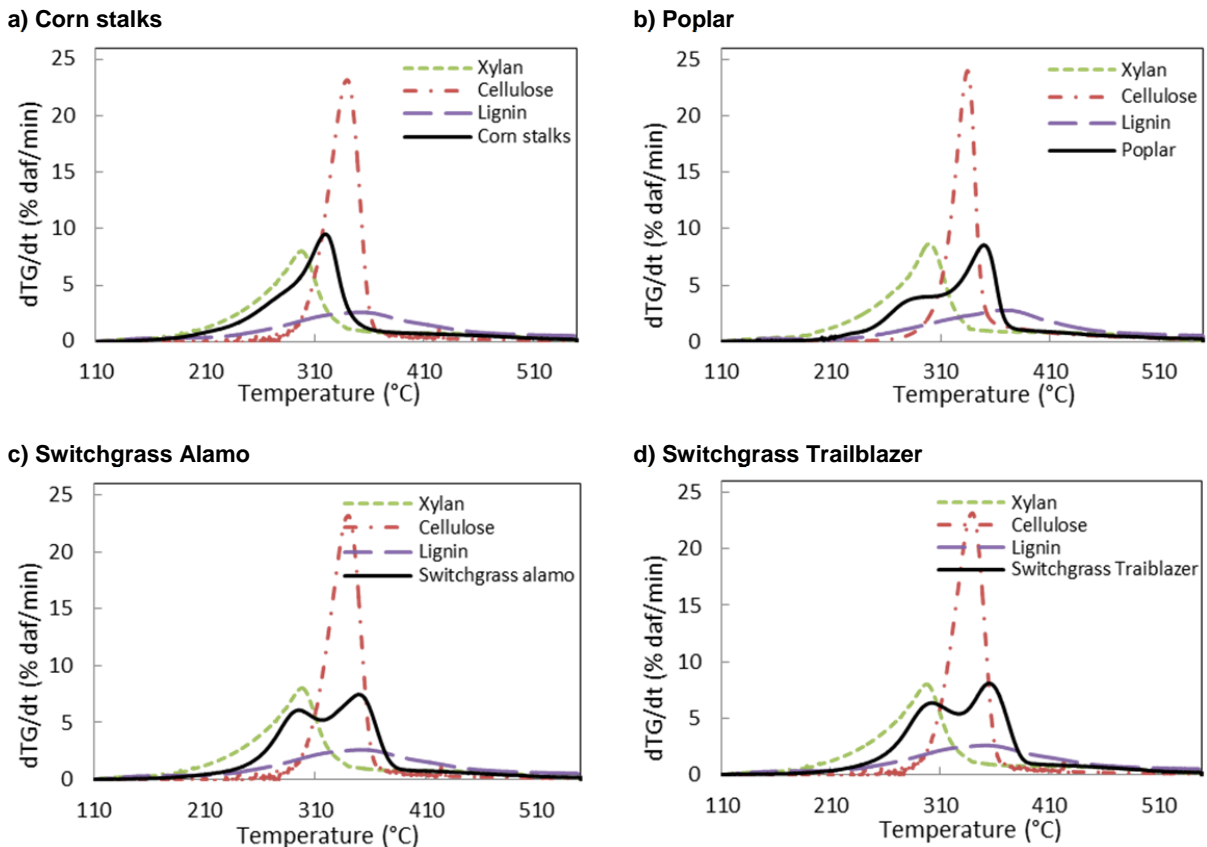
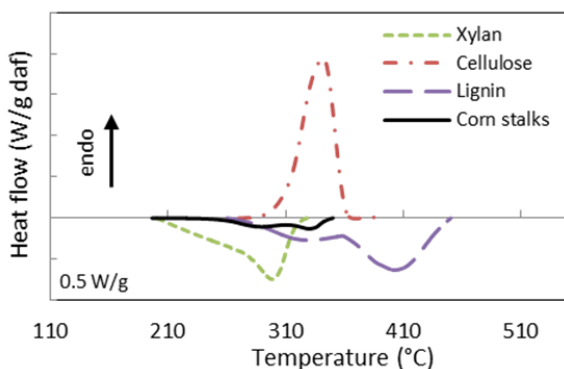


Figure 47. DTG curves for corn stalks (a), poplar (b), switchgrass Alamo (c) and switchgrass Trailblazer (d) correlated to DTG curves for biomass components. Conditions: Pure nitrogen, 10°C/min, 7.5 mg initial sample weight, pressure 1 bar, crucibles without lids.

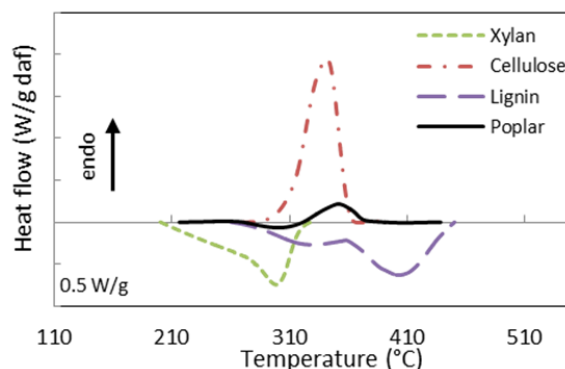
In literature it is common to attribute the thermal behavior of a biomass to the thermal behavior of its components. Bilbao et al. [60] measured an enthalpy of reaction for *Pinus Pinaster* using DSC (differential scanning calorimeter) in order to use it as input data for their wet wood pyrolysis model. They expressed their results as: for the first endothermic reaction stage (up to 60% conversion) a value of 274 kJ/kg and for the second exothermic reaction stage (remaining 40% conversion) a value of -353 kJ/kg. They presumed that the first endothermic reaction corresponds to cellulose and hemicellulose decomposition and lignin decomposition accounts for the second exothermic reaction.

Di Blasi et al. [88] reported that the inner core of the wood cylinder decomposition showed endo/exothermic reactions. They observed that the two reactions are more distinguishable at lower heating rates. At higher heating rates, the endothermic and exothermic reactions overlap producing a smaller temperature peak at the center. They also explained this thermal behavior by presuming endothermic decompositions of holocellulose and extractives and exothermic lignin decomposition.

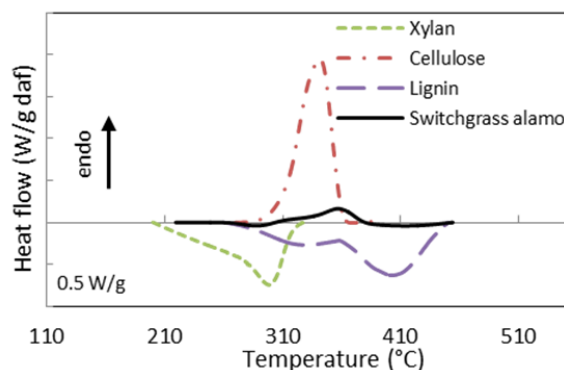
a) Corn stalks



b) Poplar



c) Switchgrass Alamo



d) Switchgrass Trailblazer

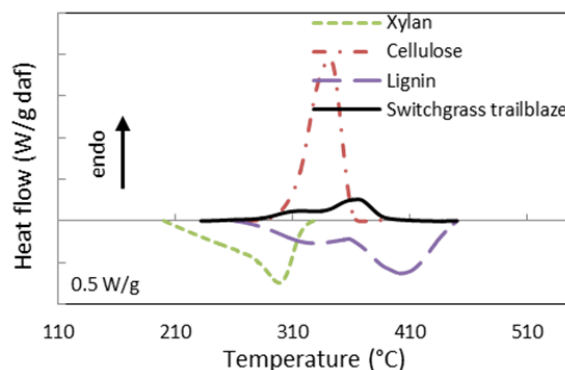


Figure 48. Heat flow curves for corn stalks (a), poplar (b), switchgrass Alamo (c) and switchgrass Trailblazer (d) correlated to heat flow curves for biomass components. Conditions: Pure nitrogen, 10°C/min, 7.5 mg initial sample weight, pressure 1 bar, crucibles without lids.

Koufopoulos et al. [36] also measured the center temperature of dry wood cylinders during pyrolysis and obtained results similar to Di Blasi et al. [88]. However, they attributed the center temperature peak to the exothermic secondary reaction between volatiles and char. Strezov et al. [119] measured the heat of pyrolysis of cellulose, hemicellulose, lignin and four different sawdust biomass samples in an infrared furnace. They reported that all of the samples showed both endothermic and exothermic reactions during pyrolysis. They attributed the exothermic behavior to the exothermic tar cracking [124] and the decomposition of dehydrocellulose [33], [34].

6 MIXTURES OF BIOMASS MACROCOMPONENTS

As previously discussed, thermal analysis curves for wood often exhibit three peaks and it has led researchers to believe that the mechanism of wood pyrolysis is a superposition of the mechanisms of its components. Inorganic substances are known to affect wood polysaccharide pyrolysis significantly, and these are reported to enhance the formation of glycolaldehyde, hydroxyacetone and carbonized products with reduced formation of anhydrosugars [35], [125], [126]. On the other hand, cellulose, hemicellulose and lignin are believed to be pyrolyzed independently in wood without interactions [102], [107]. Some authors have attempted to predict thermal and kinetic behavior of biomass from its composition by the superposition of the decomposition of the single components.

The influence of biomass composition and ash content on pyrolysis characteristics has been studied by Raveendran et al. [107]. With simultaneous studies on isolated biomass components as well as synthetic biomass, they showed that the interactions among the components are not of as much significance as the composition of the biomass and proposed a direct summative correlations based on biomass component pyrolysis to explain both the pyrolysis characteristics and product distribution of biomass. An attempt was made to represent mathematically the correlation between the pyrolysis characteristics of biomass and those of its components. This simple additive correlation assumes that the overall pyrolysis behavior of a biomass is the weighted sum of the partial contributions of its components, the relative proportions in the total composition defining the respective weight losses of the components.

Roberts [62] showed that the structural properties of the components influence the pyrolysis characteristics, so he did not attempt to correlate the pyrolysis behavior of biomass with that of its components. Antal [127] proposed that a mathematical superposition of the components' TGA curves should explain their interaction adequately. According to Ranzi et al. [42], since the components differ significantly in their decomposition behavior [76], it is possible to determine clear trends in decomposition time, reaction enthalpy, gas yield and composition of any biomass according to its composition of lignin, cellulose and hemicellulose.

Table 42. Composition of biomass available in literature [78], [104], [107], [120], [128] or estimated by TG experiments.

	Cellulose (% wt. daf)	Hemicellulose (% wt. daf)	Lignin (% wt. daf)
Corn stalks	41	29	30
Poplar	48	30	22
Switchgrass Alamo	41	31	28
Switchgrass Trailblazer	45	29	26

Predictions from these models correctly reproduce the experimental thermogravimetric (TG) curves during the pyrolysis of several biomasses [117], [129], [118]. However several recent works assume the non-interaction hypothesis in the thermal decomposition of these three constituents. Hosoya et al. [126] recently contradicted these assumption by demonstrating the existence of cellulose-hemicellulose and cellulose-lignin interactions in wood pyrolysis at gasification temperature. The study indicates that some

interactions between wood constituents other than inorganic substance exist in wood pyrolysis. They studied cellulose-hemicellulose and cellulose-lignin interactions during pyrolysis at gasification temperature (800°C) with various cellulose samples mixed with hemicellulose (glucomannan or xylan) or milled wood lignin. Significant interactions were observed in cellulose-lignin pyrolysis; lignin inhibited the thermal polymerization of levoglucosan formed from cellulose and enhanced the formation of the low molecular weight products from cellulose with changes in the secondary degradations mechanisms of volatiles species and reduced yield of char; cellulose reduced the secondary char formation from lignin and enhanced the formation of some lignin-derived products including guaiacol, 4-methyl-guaiacol and 4-vinyl-guaiacol. The interaction between cellulose and lignin significantly influence char and liquid yields decreasing the char yield and increasing the liquid yield [126]. Comparatively weak interactions were also observed in cellulose-hemicellulose pyrolysis [126], [130]. Their interaction affects weakly liquid and gas yields that are higher than the one expected, while char yield is lower [77], [126]. While gas yield and composition is only weakly affected [115]. Finally, the extent of primary pyrolysis of xylan was found not to be altered by the presence of lignin.

In order to analyze the interactions among the components, synthetic biomass samples were prepared by mixing each of the individual biomass constituents (cellulose, xylan, lignin) proportionately. In Table 42 there are reported the composition of lignocellulosic biomass analyzed in this thesis; the compositions have been recovered in literature if available or estimated by empirical correlation from the thermogravimetric curves. To investigate whether the effects of the individual components of a biomass are simply additive, a mixture of cellulose, hemicellulose and lignin has been prepared with the same composition of poplar and named synthetic poplar. Its thermal behavior has been compared to those of the poplar. Figure 49 presents the derivative weight loss curve for synthetic poplar in comparison to the curve for fresh poplar.

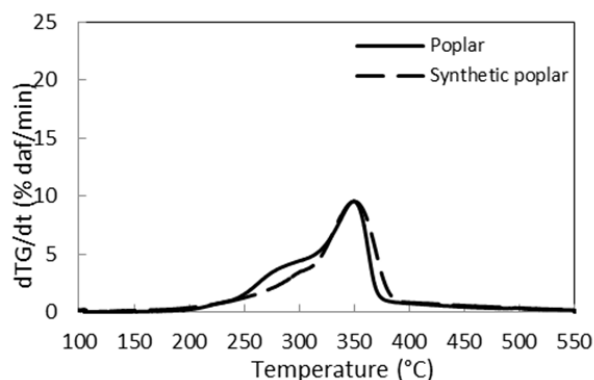


Figure 49. DTG curves for poplar and synthetic poplar. Conditions: Pure nitrogen, 10°C/min, 7.5 mg initial sample weight, pressure 1 bar, crucibles without lids.

The synthetic poplar curve matches quite well the fresh poplar curve. Thermogravimetric results show correspondence between the real biomass and the mixture of components, suggesting that the interactions among components are not of so much significance. Thermogravimetric studies show that each kind of biomass has unique pyrolysis characteristics, by virtue of the specific proportions of the

components present in it. However there is no detectable interactions in TG curves among the components during pyrolysis. These results are supported by synthetic biomass analysis.

7 ADDITIVE CORRELATION FOR BIOMASS HEAT DEMAND

It is easily understandable that the differences in the chemical composition affect the primary degradation reactions and the nature of the vapor-phase products which exhibit a different reactivity. Moreover changes in the chemical composition are expected to influence the intra-particle residence times of tar vapors and thus the activity of secondary reactions. In this way the primary and secondary reaction heat effects are also affected and hence vary with the biomass composition. In fact thermogravimetric analysis shows that the different percentages and structure of chemical components influence significantly the rates of biomass weight loss [36], but the reaction heat effects have not yet been given extensive consideration [87].

Similar to the correlation proposed by Raveendran et al. [107] for TGA data and discussed above, an additive model is suggested in this study for predicting the heat demand during the pyrolysis process obtained in the DSC. The following macrocomponent summative approach to the interpretation of overall biomass pyrolysis heat demand has been proposed.

$$\Delta H_{wood}(T) = \Delta H_{cell.}(T)\%wt_{.cell.} + \Delta H_{xylan}(T)\%wt_{.xylan} + \Delta H_{lignin}(T)\%wt_{.lignin} \quad (35)$$

where $\%wt_{.cell.}$, $\%wt_{.xylan}$, $\%wt_{.lignin}$, are the content of respectively cellulose, xylan and lignin in poplar. In Figure 50 there are reported the heat flow measured for poplar and synthetic poplar at 0.1 and 0.5 MPa, compared with the heat flow calculated by correlation (35).

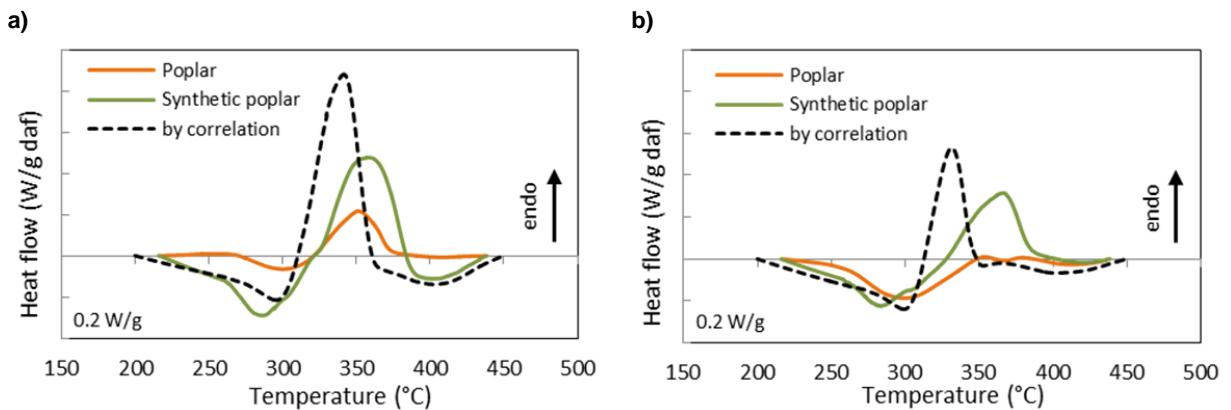


Figure 50. Heat flow for poplar, synthetic poplar and calculated by correlation (35) (b) at 0.1 MPa (a) and 0.5 MPa (b). Pure nitrogen, 10°C/min, crucibles without lids. Initial sample weight 7.5 mg.

First of all, it can be seen that the heat flow of poplar and synthetic poplar are not correspondent neither at 0.1 MPa nor at 0.5 MPa; from a chemical point of view, the difference between poplar and synthetic poplar is the presence of ash and extractives in the real biomass. It shows that ash present in biomass has a

strong influence on the thermal behavior. Moreover the comparison between the heat flow measured and heat flow calculated shows that the interactions among components are significant. The summative correlation between three major biomass constituents and the selected lignocellulosic biomass samples was found to be inadequate to describe the heat of pyrolysis.

The specificity of biomass is seen in the heat of pyrolysis, which cannot be predicted by a summative approach: a simple additive correlation is not thorough to describe the thermal behavior. These results supported by DSC runs on mixtures of components emphasize the fact that the feedstock composition and properties play a significant role in determining pyrolysis and thermal characteristics, and these are generically specific for each kind of biomass, under given operating conditions. Table 43 presents the theoretical heat calculated by Equation (35) and the experimental values. To explain the deviation between the experimental and calculated heat of pyrolysis, the possible influence of two factors can be accounted: interaction among the components and influence of ash elements. It can be noticed that the overall heat demand calculated is overestimated respect the measured heat of poplar, since it is more endothermic than the latter both at 0.1 and 0.5 MPa. In contrast the char yield is higher. Whereas the measured heat of synthetic poplar is lower respect the real poplar at 0.1 MPa and higher at 0.5 MPa but the char yield is almost the same. The comparison between heat flow of biomass and biomass components mixture has shown that ash present in biomass has a strong influence on the thermal behavior.

Table 43. Overall heat demand and char yield of the pyrolysis process measured for poplar and synthetic poplar and calculated by correlation (35) at 0.1 and 0.5 MPa (initial sample weight of about 7.5 mg). Negative values of the heat flow correspond to an exothermic behavior.

	Heat flow (J/g daf)		Char yield (% wt. daf)	
	0.1 MPa	0.5 MPa	0.1 MPa	0.5 MPa
Poplar	28.9	-71.4	0.16	0.20
Synthetic poplar	-0.2	-8.1	0.16	0.21
By correlation	38.2	-39.9	0.20	0.28

The main factors affecting the heat of biomass pyrolysis could be its main constituents (hemicellulose, cellulose, and lignin) and inorganic mineral matter. It was demonstrated that the weight loss during biomass pyrolysis and product distribution could roughly be expressed by linearly summative correlations of those obtained from the pyrolysis of three main constituents [77], [107]. As far as the heat of pyrolysis is concerned, however, this kind of linearly summative relationship seems no longer valid between the composite biomass samples and individual constituents.

CHAPTER VI

LIQUEFACTION OF LIGNIN IN ITS PRODUCED OIL: PROCESS PARAMETERS SCREENING

1 LIGNIN LIQUEFACTION: STATE OF ART

Lignin is the second most abundant biomass component and the only renewable aromatic resource in nature [131]. The pulp and paper sector and lignocellulosic biorefineries produce large lignin-containing side streams resulting from the fractionation of lignocellulosic biomass [27]. Most of the biorefinery are focused on utilizing easily convertible fractions while lignin remains relatively underutilized to its potentials [25]. The lignocellulosics-to-ethanol process makes use of the cellulose and hemicelluloses, leaving lignin as waste. In addition, pulp and paper refineries also generate huge amounts of lignin. Presently, lignin is being utilized as a low-grade boiler fuel to provide heat and power to the process [132]. Lignin valorization is a key-issue for enhanced profitability of sustainable bio-based industries. Degradation and conversion of lignin can be achieved by thermal treatment in the presence or absence of some solvents, chemicals, additives and catalysts. Among the various conversion technologies, pyrolysis has been reported as one of the most economic [27], [133]. The main products of lignin pyrolysis are char and gas [131]. From the 1980s to the early 2000s, many lignin pyrolysis researches focused on the gas products [134]–[136]. Carbon monoxide and carbon dioxides are the top two most abundant components in the gas phase of pyrolysis of lignin [133]. In literature it has been reported that char from pyrolysis of lignin has a condensed aromatic structure and reserve up to 50% of energy from starting biomass [133]. Studies on lignin pyrolysis for the production of biofuels and high-value-added chemical products have also been conducted and to produce a better quality product from pyrolysis, heterogeneous catalysts are employed [137].

The challenge, however, is that lignin is very difficult to decompose and generates very high amounts of solid residue as compared to other components of lignocelluloses [132]. Moreover, the pyrolysis of lignin is difficult because of the challenging processing of the recalcitrant nature and thermoplastic behavior of lignin, resulting in relatively low yields of valuable products [27]. From a recent study, it was concluded that typical state-of-the-art reactors for biomass fast pyrolysis cannot effectively pyrolyze pure lignins [131].

A variation of the pyrolysis process for the production of bio-oil is the liquefaction using a solvent [23], [138]. Limited experimental study are available concerning the direct liquefaction processes on lignin. Comprehensive overviews have been given by Behrendt et al. [139], and Elliott et al. [140]. Van Rossum et al. [141] showed the possibility to liquefy wood with high carbon yields (>90 C%) using a phenolic solvent. In their work, it was found that guaiacol performs better than water and other organic solvents, as hexanoic acid and n-undecane. They also proposed to use the produced bio-oil from biomass as liquefaction medium by recycling it to the liquefaction reactor. The option of recycling the produced bio-oil as a liquefaction solvent was also investigated by Kumar et al. [142]. They found that despite good initial performance, the liquefaction is rapidly hindered by the formation of heavy components (molecular weight higher than 1000 Da).

Data concerning the direct liquefaction processes on lignin are even more limited than on biomass. Toshitaka et al. studied liquefaction of lignin sulphonate with subcritical and supercritical water in a batch tube-type bomb reactor and found that liquefaction at 400°C in supercritical water gives much higher oil yields respect to pyrolysis at the same temperature [143]. Hydrolytic eucalyptus lignin was liquefied with formate in water under pressure in a batch reactor and in a continuous flow reactor by Schuchardt et al. [144] and it was found that using the continuous-flow at 300°C and 12 MPa, the oil yield is 61% and is mostly composed of substituted phenols, 42% of which is distillable as guaiacol.

The present study is intended to explore lignin liquefaction as an option to convert lignin in a flowable bio-oil product with improved properties like lower oxygen content and molecular weight. Guaiacol has been chosen as starting solvent, because of its aromatic chemical structure similar to lignin and its pyrolysis/solvolytic products. Liquefaction experiments of lignin in guaiacol have been performed in a batch fixed-bed reactor in isothermal condition at 5 bar of nitrogen. Several operative parameters have been investigated: the temperature has been varied between 300 and 450°C, the residence time between 1 and 25 min, the lignin loading between 20 and 60 % wt. In further experiments, the effect of a recycling feed has been investigated, using the lignin liquefaction oil as liquefaction medium to simulate a continuous recycle. Recycle experiments have been carried out by subsequent refill of fresh lignin into the liquid product. The quality of the produced bio-oil and of the gas has been analyzed.

The study aims to show that during lignin liquefaction experiments in guaiacol or in recycled liquefaction oil, lignin can be converted in a flowable bio-oil product with lower oxygen content and molecular weight compared to the lignin feedstock which might be used as a source of aromatics in further upgrading process by the use of a cracking catalyst. In addition, knowledge will be obtained on the thermal stability of lignin.

2 LIGNIN LIQUEFACTION EXPERIMENTS AND VALIDATION

Liquefaction experiments of lignin in guaiacol has been tested up to 60 % wt. of lignin in the feed. Several operative parameters have been investigated: the temperature has been varied between 300 and 450°C, the residence time between 1 and 25 min, the lignin loading between 20 and 60 % wt. The effectiveness of lignin solvolysis in a continuous recycle (4 refill runs) of the lignin liquefaction product has been proven reaching a nominal lignin liquefaction product of up to 60wt%.

The overall mass balance has been typically above 95 % wt. Gas yield is calculated using composition analyzed by the off-line GC, and available gas volume and reactor pressure. The bio-oil yield is determined by the weight of the liquid product recovered after experiment and the liquid recovered after acetone evaporation.

The liquid product has been further divided into two fractions, based on apparent molecular weight (as determined by GPC), namely solvent/guaiacol with molecular weight < 210 Da and bio-oil with molecular weight > 210 Da. In the bio-oil, the light fraction is considered the molecules with a molecular weight < 1000 Da (light fraction), and the vacuum residue > 1000 Da. Then the vacuum residue and light fraction have been defined as the fraction of the bio-oil (excluding guaiacol, 210 Da) that is found in the liquid product based on the equation (36) and (37) respectively.

$$\text{Vacuum fraction} = \frac{\text{Area GPC with MW} > 1000}{\text{Area GPC with MW} > 210} \quad (36)$$

$$\text{Light fraction} = \frac{150 < \text{Area GPC with MW} < 1000}{\text{Area GPC with MW} > 210} \quad (37)$$

In Figure 51 it's possible to analyze the effect of the liquefaction on the guaiacol, comparing the apparent molecular weight distribution of the liquid product coming from blank experiments on guaiacol at 350°C and 25 min and 400°C and 1 min respect to the apparent molecular weight distribution of the guaiacol feedstock. It can be seen that after liquefaction experiments guaiacol is for a small part degraded in lighter components: in particular there's one peak around 70 g/mol before the main of the guaiacol and some very small peaks in the range of molecular weight between 150-400 g/mol in the case of refractive index signal. For the ultraviolet index, peaks can be observed in the range between 140-2500 g/mol. This peaks are rather large. Carefulness should be taken when interpreting the liquefaction experimental data.

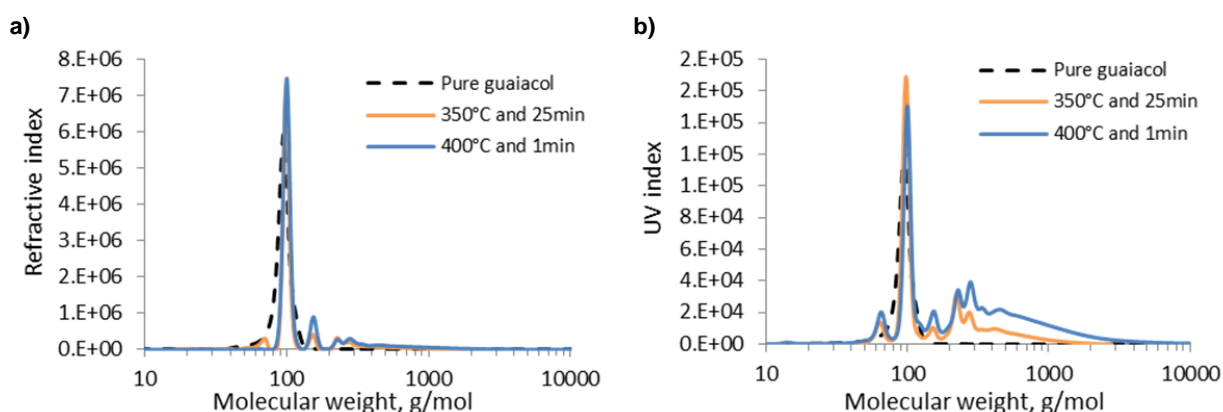


Figure 51. Apparent molecular weight distribution of guaiacol feedstock and of liquid product after liquefaction experiment at 400°C and 1 min, and 350°C and 25 min of pure guaiacol. a) refractive index signal; b) ultraviolet index signal.

Guaiacol content in the liquid product has been measured by GC-MS. In Figure 52 has been reported the theoretical value calculated considering that guaiacol present in the feed does not react. The experimental content measured by GC-MS is very close to the theoretical value both at a reactor temperature of 300 and 350°C. It means that guaiacol is only slightly consumed during the process and it can be eventually distilled and recovered from the product. Schuchardt et al. [144] performed liquefaction of lignin in water and sodium formate in a batch reactor at 13 MPa and 270°C; they distilled the oils obtained after liquefaction at 1.33 Pa between 30°C and 280°C and obtained 42% of colorless oil, 11% of which was guaiacol.

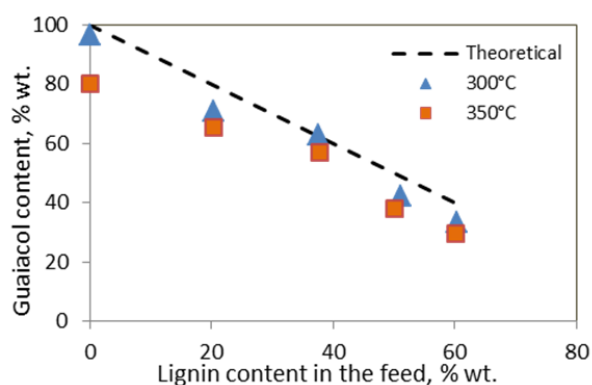


Figure 52. Guaiacol content measured by GC-MS of the liquid product after liquefaction experiments at a residence time of 25 min and a temperature of 300°C and 350°C of lignin mixed in guaiacol before the run at different loading (0-60% wt).

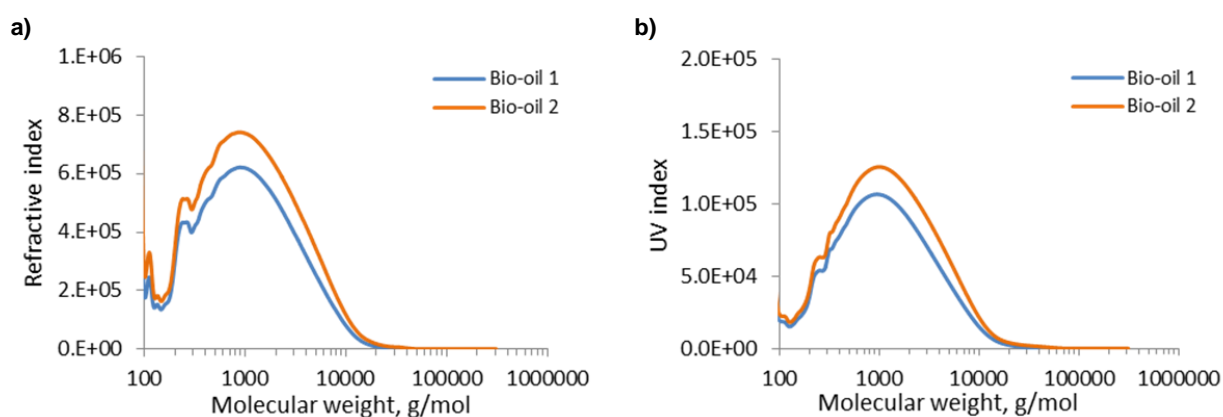


Figure 53. Apparent molecular weight distribution of guaiacol feedstock and of liquid product after liquefaction experiment at 400°C and 1 min, and 350°C and 25 min of pure guaiacol. a) refractive index signal; b) ultraviolet index signal.

In this study guaiacol is not only a product of lignin degradation but even the solvent of the process, its concentration in the liquid product is much higher. Furthermore guaiacol is an expensive solvent; for these reasons it's important to show that it is slightly consuming and it could be eventually distilled and recovered. Note, feeding lignin at room temperature resulted in the formation of sticky lumps especially at higher concentrations (>37 wt%). Figure 53 shows the apparent molecular weight distribution of bio-oil1 and bio-oil2 after liquefaction experiments at 300°C and 25 min of 37 % wt. lignin mixed in recycled oil. The spectra of bio-oil2 is comparable with bio-oil1; for this reason, analysis of bio-oil1 is considered representative for the total liquid product.

2.1 INFLUENCE OF TEMPERATURE AND RESIDENCE TIME

The influence of the reaction temperature on the oil and gas yield has been studied in experiments performed at 300, 350, 400, 450°C. The residence time was 1 or 25 min. Temperature has the strongest effect on liquefaction. The highest yield of oil has been achieved at a temperature of 300°C; as the temperature increases, the bio-oil yield decreases and the gas yield increases due to cracking reactions (Figure 54). The gas production resulted in an increases in the reactor pressure (Table 44). The gas phase mainly consists of CO, CO₂ and CH₄, see Table 45. The methane content (expressed on lignin basis) increases as the temperature increases as a product of guaiacol and lignin decomposition from 16.4 % wt. at 300°C up to 81.4 % wt. at 400°C, as can be seen from (Table 45). At 450°C, the main product is char and there was almost no liquid product formed.

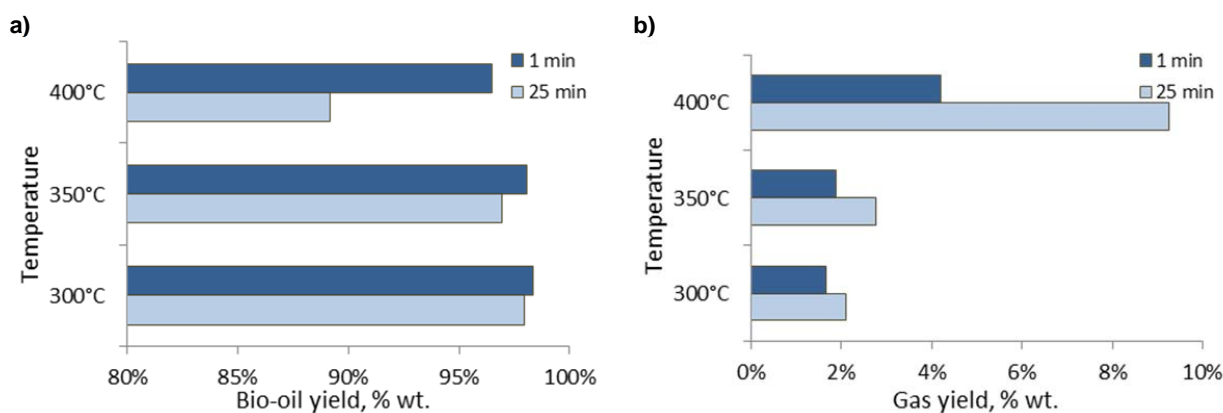


Figure 54. Bio-oil (a) and gas (b) yields after liquefaction experiments at a residence time of 1-25 min and a temperature of 300, 350, 400°C of 50% lignin mixed in guaiacol before the run.

Table 44. Reactor pressure and vacuum fractions after liquefaction experiments at a residence time of 1-25 min and a temperature of 300-400°C of 50% lignin mixed in guaiacol before the run.

	300°C		350°C		400°C	
	1 min	25 min	1 min	25 min	1 min	25 min
Max reactor pressure, bara	36	557	52	97	98	244
Vacuum fraction, % wt.	78.2	56.3	72.0	58.9	63.9	-

As the residence time increases, the reactor pressure increases and the gas yield increases slightly due to a higher extent of cracking reaction. At 400°C the effect is much more significant: reactor pressure is 98 bara at 1 min and even 244 bara at 25 min. Funazukuri et al. [143] found that during lignin sulphonate liquefaction in supercritical water at 400°C and reaction time of 5-120 min low molecular weight components increase considerably with increasing reaction time. It has been also found in the current study that increasing the reaction time the vacuum fraction decreases (Table 44). Thus as the time proceed the amount of very heavy products decreases. It suggests that vacuum residue is a primary reaction product that undergoes further depolymerization with time. The same finding has been underlined by Kumar et al. [142] during biomass liquefaction in guaiacol at 320°C and with a residence time between 100 s and 3 h. The effect of the temperature on the vacuum fraction is not so appreciable between 300 and 350°C: at 1 and 25 min there are respectively 6 and 3 % of difference; whereas between 350 and 400°C the difference is more pronounced, showing that at 400°C and 1 min the effect of the cracking reactions is more significant.

Table 45. Gas composition after liquefaction experiments at a residence time of 25 min. of 50% lignin mixed in guaiacol before the run.

Gas components	300°C	350°C	400°C
CH ₄ , % wt.	16.4	62.2	81.4
CO, % wt.	23.2	12.9	5.6
CO ₂ , % wt.	59.6	24.0	11.9
C ₂ H ₄ , % wt.	0.2	0.1	-
C ₂ H ₆ , % wt.	0.4	0.6	0.9
C ₃ H ₆ , % wt.	0.1	0.1	0.1
C ₃ H ₈ , % wt.	0.1	0.1	0.1

2.2 INFLUENCE OF LIGNIN LOADING

Lignin loading in the feed has been varied between 20% and 60 % wt. As the lignin content in the feed increases, the bio-oil yield decreases and the gas yield increases slightly (Figure 55) and the reactor pressure increases as well (Figure 56). It means that with less solvent circulating in the reactor, cracking to gasses is occurring at higher extent. Analyzing the gas phase composition (Figure 57), it can be seen that increasing the lignin content in the feed the CO e CO₂ content in the gas phase increases, coming from lignin degradation. The major difference in the composition at 350°C respect to the composition at 300°C is a higher content of CH₄, coming from guaiacol decomposition.

In Figure 58a the water content in liquid product measured by Karl Fisher can be seen. The water production can be seen in Figure 58b. For comparison the theoretical moisture content, coming from the moisture in the liquid feedstock, is included in the both graphs. It can be seen that water is produced during the process, due to some dehydration reactions. Furthermore water content in the experiments at 400°C is higher respect to that one at 300°C, confirming that these dehydration reactions are more favored at higher temperature. The production of water results in less oxygen content in the liquefaction product.

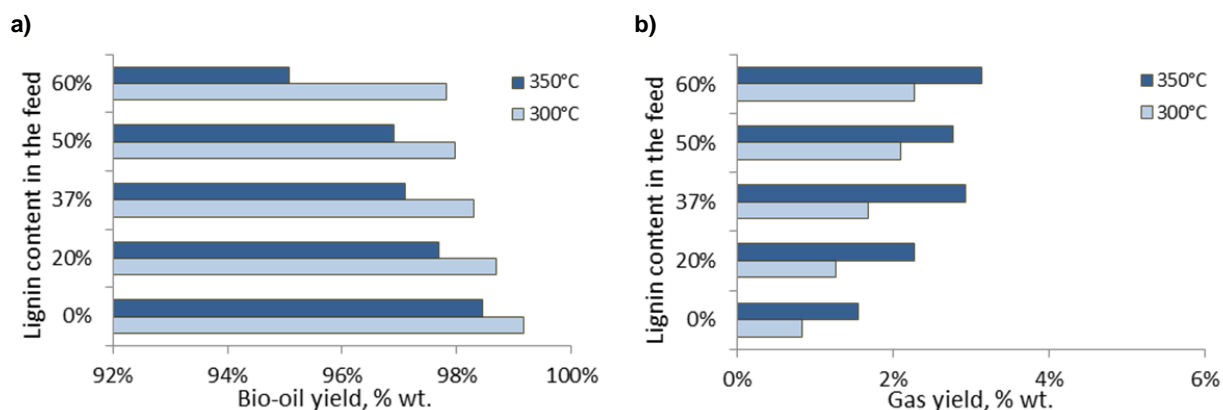


Figure 55. Bio-oil (a) and gas yields (b) during liquefaction experiments at a residence time of 25 min and a temperature of 300°C and 350°C of lignin mixed in guaiacol before the run at different loading (0-60 % wt.).

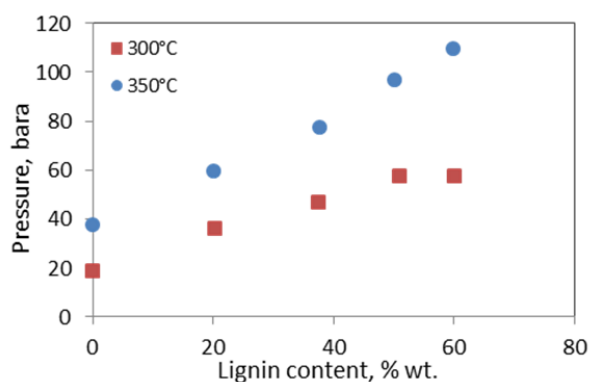


Figure 56. Final reactor pressure of liquefaction experiments at a residence time of 25 min and a temperature 300 and 350°C of lignin mixed in guaiacol before the run at different loading (20-60 % wt.).

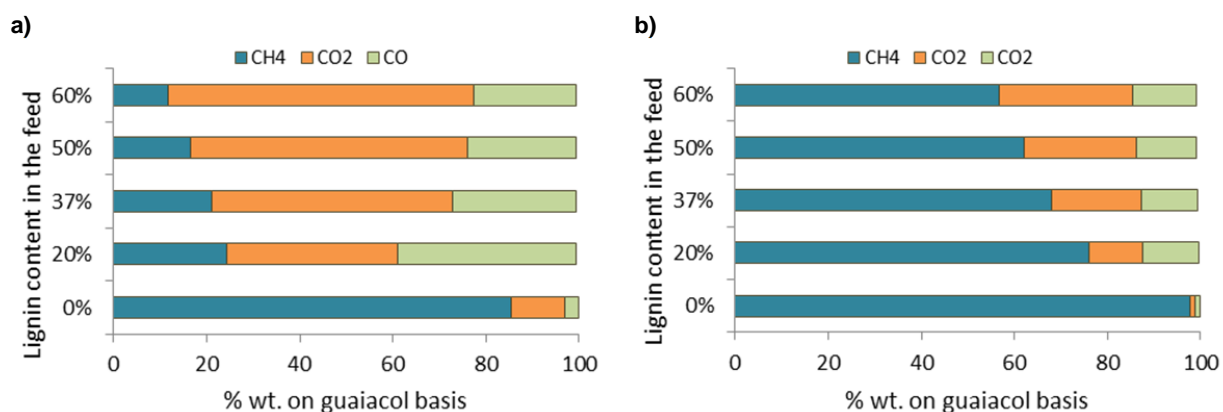


Figure 57. Bio-oil (a) and gas (b) yields after liquefaction experiments at a residence time of 1-25 min and a temperature of 300, 350, 400°C of 50% lignin mixed in guaiacol before the run.

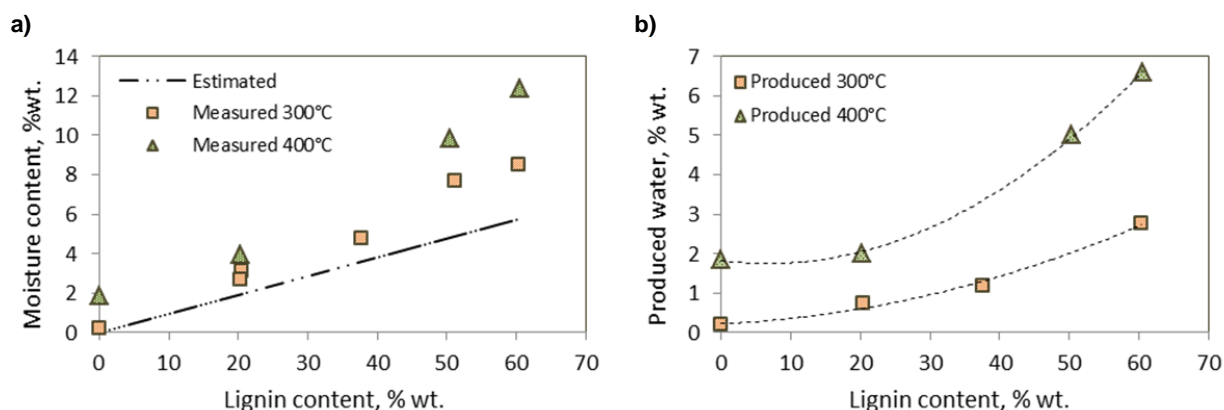


Figure 58. Moisture content in the bio-oil (a) and water produced (b) after liquefaction experiments at a residence time of 25 min and a temperature 300°C and at a residence time of 1 min and a temperature of 400°C of lignin mixed in guaiacol before the run at different loading (0-60 % wt.).

Figure 59a shows the molecular weight distribution of the liquefaction oils as function of the load. Figure 59b shows the aromatic compounds in the oil. In these graphs it's visible the effect of the liquefaction comparing the apparent molecular weight distribution of the liquid product respect to the apparent molecular weight distribution of the pure lignin. First of all it has to be underlined that lignin is not completely dissolving in THF used for the GPC analysis; it has been estimated that 26.8 wt% of the lignin is not dissolved in THF. The lignin spectra has been rescaled considering that. The liquid product spectra's have been rescaled respect to the lignin content in the feed. Comparing them, it's possible to state that the effect of the liquefaction is on one hand forming lighter components in the weight range 200-400 g/mol coming from cracking reactions and on the other hand forming heavier components in the range 1000-100000 g/mol coming from re-condensation and re-polymerization reactions as can be seen from the heavier tail.

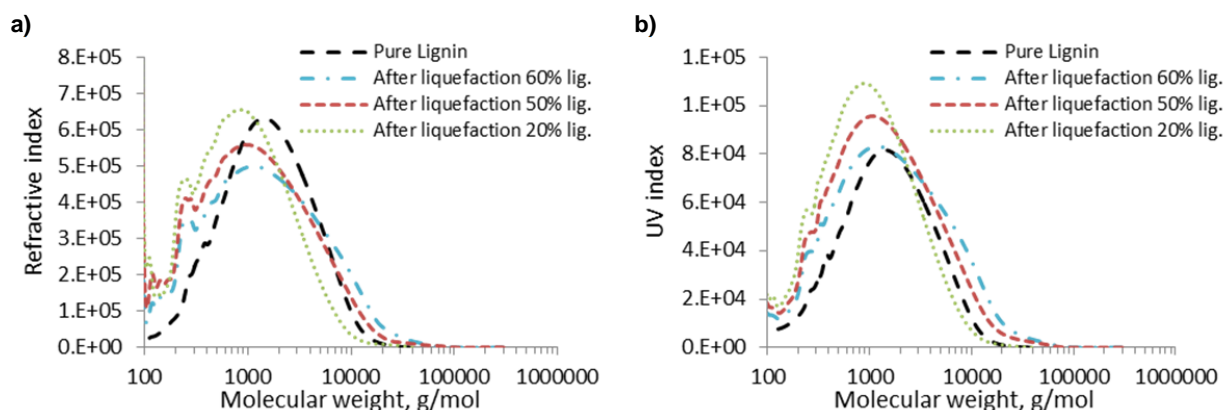


Figure 59. Apparent molecular weight distribution of pure lignin, and liquid obtained after liquefaction experiment at 25 min and 300°C of 20, 50, 60 % wt. lignin mixed in guaiacol before the run. a) refractive index signal; b) ultraviolet index signal.

Comparing the two graphs the trends are similar. It basically means that that almost the complete oil is aromatic. Firstly, at 20 wt% lignin loading in guaiacol, the molecular weight decreases compared to the lignin feedstock. Increasing the lignin content in the feed, the liquid product becomes more heavy. In all cases there were also severe depolymerization reactions as proven by the production of light molecules. These compounds might be interesting for chemicals production. Another interesting option is that this light fraction is recovered from the produced oil and used as solvent in liquefaction of lignin [142], [145].

3 LIGNIN LIQUEFACTION IN RECYCLED OIL

Recycle experiments were carried out by subsequent refill of fresh lignin feedstock into the reaction product. In the previous experiments, the feed was prepared by cold mixing of fresh lignin and pure guaiacol; whereas in the recycle experiments, the feed was prepared by cold mixing of 20 % wt. fresh lignin and produced oil from a previous experiment of 20 % wt. lignin mixed in guaiacol. In the following experiment, the recycling feed was prepared mixing 20 % wt. lignin with the produced oil from the first recycle experiment. This procedure was reiterated 4 times, reaching a nominal lignin content of 60 % wt.

These experiments were indented to mimic the continuous operation with complete recycle of produced liquefaction bio-oil. The oil yield in case of recycling is higher compared to the experiments without recycle for the same total lignin amount added (Figure 60); this suggests that liquefaction intermediates/products stimulate further liquefaction of lignin [141]. The recycled oil appears to be very effective to liquefy the lignin and even surpasses the start-up solvent guaiacol, but become increasingly heavy and more viscous after each refill.

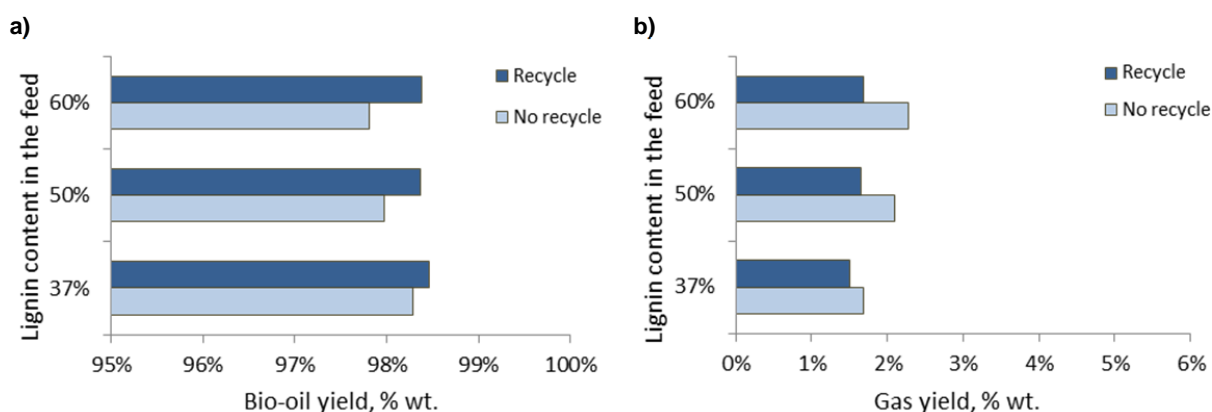


Figure 60. Effect of recycling option on bio-oil (a) and gas (b) yields after liquefaction experiments at 300°C and 25min of lignin mixed in recycled oil at different loading (37-60 % wt.).

As can be seen from Figure 61, the vacuum fraction of the liquid product obtained after recycle is lower respect to the liquid obtained after direct liquefaction in guaiacol for the same amount of lignin in the feed. A possible explanation for the lower vacuum residue might be that most of the lignin in the recycle

experiments experience an overall longer residence time at the liquefaction temperature. From Table 44 it became clear that longer residence time results in an overall lower vacuum residue.

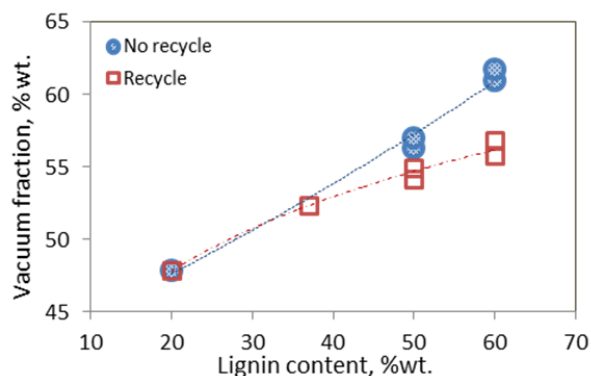


Figure 61. Vacuum fraction of the liquid products after liquefaction experiments at 25 min and 300°C of lignin mixed in recycled oil and in guaiacol at different loading (20-60 % wt.)

In Table 46, there are results of elemental analysis of the liquid product after recycle with a nominal lignin content of 0, 20, 37, 50, 60 % wt. The measured oxygen content decreases as the nominal lignin content increases. It means that deoxygenation has taken place and the oxygen content decreased from approximately 38.5% to approximately 24.4% after the fifth run. This finding is confirmed by the production of water, see Figure 58 and the production of CO and CO₂ see Figure 57.

Table 46. Elemental analysis dry and ash free of the liquid products after liquefaction at 25 min and 350°C of lignin mixed in recycled oil at different loading

Lignin content	Elemental composition (%wt.)			
	Carbon	Hydrogen	Nitrogen	Oxygen (by diff.)
20%	60.4	5.8	0.3	33.5
37%	60.7	5.6	0.8	32.9
50%	62.9	5.5	0.5	31.1
60%	70.5	5.1	0.0	24.4

The viscosity at 80°C of the liquid product can be seen in Figure 62. The liquid product obtained after liquefaction experiments of 60 % wt. lignin mixed in guaiacol at a residence time of 25 min and a temperature of 300°C and 350°C is still flowable and has a viscosity at 80°C still acceptable. It can be concluded that as the lignin content in the feed increases, the product becomes heavier but it is still flowable and thus pumpable at increasing temperature.

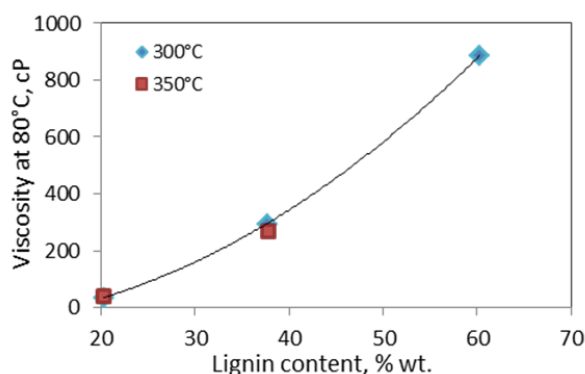


Figure 62. Viscosity at 80°C of the bio-oil after liquefaction experiments at a residence time of 25 min and a temperature of 300°C and 350°C of lignin mixed in guaiacol before the run at different loading (20-60 % wt.)

4 UPGRADING OF LIGNIN LIQUEFACTION OIL: HYDROTREATMENT

A hydrotreatment experiment was performed with the 60wt% lignin content, recycle oil. The temperature was 300°C, the initial hydrogen pressure was 120 bara and the reaction time was 2 hours. Ru/C (5wt% of the oil mass) was used as catalyst. Clearly, hydrotreating a liquefaction oil containing 40wt% of “expensive” guaiacol solvent is economically not viable. Therefore, this experiment should be interpreted as indicative. It turned out that the liquefaction oil could be very well hydrotreated without any experimental problems even not at the relatively high heating rate of 60°C/min. The oil was nicely flowable and no significant production of char was observed. The oil has an oxygen content of 17 wt% and the vacuum residue is reduced with 42.5%. To conclude, the stable liquefaction oil could be further processed in high temperature (upgrading units) in the presence of an catalyst producing a fuel like liquid.

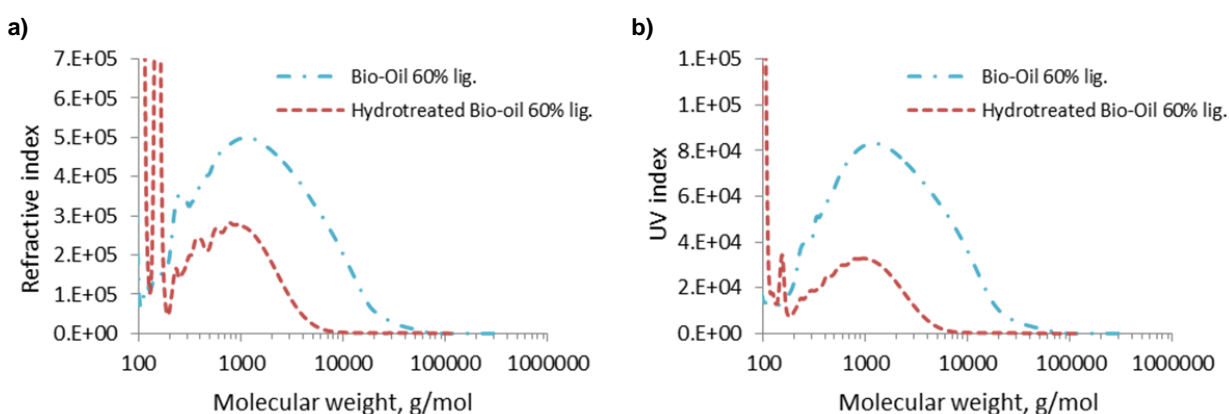


Figure 63. Apparent molecular weight distribution of liquid obtained after liquefaction experiment at 25 min and 300°C and of liquid obtained after hydrotreating experiment at 120 bara and 300°C. a) refractive index signal; b) ultraviolet index signal.

CHAPTER VII

CONCLUSIONS

The aim of this study has been to clarify the pyrolysis mechanism and to better understand the outcomes of the biomass pyrolysis process, in order to assist the design and operation of new thermal conversion processes of biomass feedstock. In the first part of this thesis (Chapter IV and V), the study has been focused on understanding how process conditions and feedstock selection influence the overall heat demand during the biomass pyrolysis. Thermoanalytic techniques were used to estimate the heat demand during the pyrolysis process using different operating conditions. Four different lignocellulosic biomass and their respective components (cellulose, xylan and lignin) were considered in the experimental investigation carried out. The second part of this thesis (Chapter VI) has been focused on the screening of experimental parameters during lignin pyrolysis in a fixed bed reactor using a solvent (liquefaction). The focus on lignin was motivated since it is the only renewable aromatic resource in nature at the moment, obtained as a waste in several industrial application and relatively underutilized to its potentials. The study aims to show that during lignin liquefaction experiments, lignin can be converted in a flowable bio-oil product with better characteristics compared to the lignin feedstock which might be used as a source of aromatics in further upgrading process by the use of a cracking catalyst. In addition, knowledge has been obtained on the thermal stability of lignin.

Depending on the process conditions and on the type of feedstock, the yield distribution among the three product fractions (solid, liquid and gas) and their composition may present significant differences. Temperature, pressure, and particle size are the main operative factors which affect the heat and mass transfer phenomena during biomass pyrolysis, therefore having an important influence on the outcomes of the thermal decomposition process. This thesis shows that the thermal effects of the pyrolysis process have a great variation as the process conditions change. The results evidence that an increase in the operating pressure reduces the heat requirements of the pyrolysis process, and the heat of pyrolysis reactions may shift from endothermic to exothermic. The heat of reaction as a function of pressure has shown to fit a Langmuir adsorption curve. The results suggest that the role of exothermic secondary reactions and the inhibition of the evaporation of high molecular weight compounds formed in the primary pyrolysis process may be among the main factors affecting the heat demand of the overall pyrolysis process. Further experiments evidence that increasing the vapour residence time by an increasing initial sample weight or an increasing operative pressure, as well as by the use of a lid, results in an increasing char yield and in a decreasing heat demand. To confirm this assumption, a strong correlation has been found between the final char yield and the overall reaction heat. The results obtained represent a further

element towards the thorough understanding of biomass pyrolysis processes, that are a key-step in the thermal conversion of biomass substrates. Lumped reaction schemes were used for data interpretation. Both experimental and model results pinpoint the crucial role of exothermic char-forming reactions on the overall heat demand of the pyrolysis process. Influence of pressure, residence time and initial sample mass on biomass heat demand could be correlated considering the influence on the final char yield. Thus, the char yield resulted the main parameter to which the overall heat demand of the biomass pyrolysis process could be correlated. It has been found that the char yield is the main factor determining whether the overall pyrolysis process is endo- or exothermic. This is an important global feature to build into any model of pyrolysis.

The thermal effects associated to biomass macrocomponents pyrolysis (cellulose, hemicellulose and lignin) have also been investigated. An increase of the operating pressure resulted in an effect both in the heat demand and in the final char yield. The results obtained suggest the presence of a competitive mechanism between primary decomposition process, leading to the formation of volatiles, and vapour-solid interactions, leading to secondary char formation. These effects on the macrocomponents heat demand can be combined to obtain a model for a summative approach to describe the overall biomass pyrolysis heat demand depending on the biomass composition. Thermogravimetric and calorimetric studies on isolated biomass components as well as on lignocellulosic biomass and on mixture of biomass components have shown that the interactions among components are significant to determine the biomass thermal behavior. It has been verified that a summative approach is not possible to describe the heat of pyrolysis of the overall biomass.

Liquefaction experiments of lignin in guaiacol and in its own liquefaction product have been carried out. Several operative parameters have been investigated: the temperature has been varied between 300 and 450°C, the residence time between 1 and 25 min, the lignin loading in the feed between 20 and 60 % wt. Recycle experiments have been carried out by subsequent refill of fresh lignin into the liquid liquefaction product. The dissolution of lignin in guaiacol at room temperature turned out to be troublesome especially at higher concentrations (>37 wt%). Under all conditions studied the oil yield was always above approximately 90 % wt. At higher temperature and longer residence time, cracking reactions are favored as shown by an increase in gas formation and decreased vacuum residue. The heavy residue seems to be a primary reaction product that undergoes further reactions with time. As the lignin content in the feed increases, the liquid product becomes heavier; however it is still flowable at a temperature higher than 80°C. Nevertheless, also significant amounts of "light" aromatic molecules are formed (MW between 100-300 g/mol). Liquefaction experiments in guaiacol are shown to be feasible up to 60 % wt. of lignin in the feed and guaiacol is slightly consumed during the process. It was found that guaiacol could be recovered by distillation and re-used if required.

In further experiments, the effect of recycling the liquefaction product has been investigated using the lignin liquefaction oil as liquefaction medium to simulate a continuous recycle. Recycle experiments have been carried out by subsequent refill of fresh lignin into the liquid product. Results show that it's possible to recycle for at least four times reaching a nominal lignin content in the feed of 60 % wt. The recycled oil appears to be very effective to liquefy the lignin, even more compared to the guaiacol. Unfortunately, the liquefaction product becomes increasingly heavy and more viscous after each refill meaning that the cracking to smaller molecules is not sufficient enough under our studied conditions. The oxygen content decreases during liquefaction from 33.5 till 24.4 % wt. at 350°C and a residence time of 25 minutes. The

decrease in oxygen content is accompanied water, CO and CO₂ production. The liquefaction oil containing 60 % wt. lignin (processed at 300°C and 25 minutes residence time) was further upgraded by Hydrotreatment using Ru/C catalyst. It was found that the liquefaction oil could be upgraded without experimental problems even at the high heating rate (60°C/min.) applied. The nicely flowing oil was had an oxygen content of 17 wt% and the vacuum residue was reduced to 42.5%. No char was formed. The liquefaction of lignin in guaiacol or in recycled liquefaction oil is a good method to convert lignin in a flowable and pumpable bio-oil product that has the potential to be used as a source of fuel or aromatic chemicals in further upgrading process.

Overall, the results obtained represent a step forward in the understanding of the pyrolysis process of biomass and of biomass macrocomponents, that may become a key element in supporting the routes in the valorization of biomass for the production of energy and chemicals.

REFERENCES

- [1] [Http://www.iea.org/](http://www.iea.org/), "2014 Key world energy statistics, International Energy Agency." [Online]. Available: www.iea.org. [Accessed: 01-Nov-2015].
- [2] [Https://www.worldenergy.org/](https://www.worldenergy.org/), "World energy council, 2013 survey of energy resources." [Online]. Available: www.worldenergy.org. [Accessed: 01-Nov-2015].
- [3] [Http://www.shell.com/](http://www.shell.com/), "Shell energy scenarios 2050." [Online]. Available: www-static.shell.com. [Accessed: 01-Nov-2015].
- [4] G. Boyle, *Renewable Energy: Power for a sustainable Future*, 3rd ed. 2002.
- [5] K. Jacobson, K. C. Maheria, and A. Kumar Dalai, "Bio-oil valorization: A review," *Renew. Sustain. Energy Rev.*, vol. 23, pp. 91–106, 2013.
- [6] D. Mohan, C. U. Pittman, and P. H. Steele, "Pyrolysis of Wood/Biomass for Bio-oil: A Critical Review," *Energy & Fuels*, vol. 20, no. 3, pp. 848–889, 2006.
- [7] [Http://europa.eu/](http://europa.eu/), "Communication from the Commission. Energy for the future: renewable sources of energy. White Paper for a Community Strategy and Action Plan." [Online]. Available: europa.eu. [Accessed: 01-Nov-2015].
- [8] [Http://www.iea.org/](http://www.iea.org/), "World Energy Outlook 2011." [Online]. Available: www.iea.org. [Accessed: 01-Nov-2015].
- [9] [Http://www.iea.org/](http://www.iea.org/), "Greenhouse Gas Balances of Biomass and Bioenergy Systems." [Online]. Available: www.biomassenergycentre.org.uk. [Accessed: 01-Nov-2015].
- [10] P. McKendry, "Energy production from biomass (part 1): Overview of biomass," *Bioresour. Technol.*, vol. 83, no. 1, pp. 37–46, 2002.
- [11] W. E. Hillis, *Wood and biomass ultra structure. In Fundamentals of thermochemical biomass conversion*. .
- [12] B. . Jenkins, L. . Baxter, and T. . Miles, "Combustion properties of biomass," *Fuel Process. Technol.*, vol. 54, no. 1–3, pp. 17–46, Mar. 1998.
- [13] S. V. Vassilev, C. G. Vassileva, and V. S. Vassilev, "Advantages and disadvantages of composition and properties of biomass in comparison with coal: An overview," *Fuel*, vol. 158, pp. 330–350, 2015.

- [14] T. Faravelli, a. Frassoldati, G. Migliavacca, and E. Ranzi, "Detailed kinetic modeling of the thermal degradation of lignins," *Biomass and Bioenergy*, vol. 34, no. 3, pp. 290–301, 2010.
- [15] B. Joffres, D. Laurenti, N. Charon, a. Daudin, a. Quignard, and C. Geantet, "Thermochemical Conversion of Lignin for Fuels and Chemicals: A Review," *Oil Gas Sci. Technol. – Rev. d'IFP Energies Nouv.*, vol. 68, no. 4, pp. 753–763, 2013.
- [16] Q. Bu, H. Lei, A. H. Zacher, L. Wang, S. Ren, J. Liang, Y. Wei, Y. Liu, J. Tang, Q. Zhang, and R. Ruan, "A review of catalytic hydrodeoxygenation of lignin-derived phenols from biomass pyrolysis," *Bioresour. Technol.*, vol. 124, pp. 470–477, 2012.
- [17] A. V. Bridgwater, "Review of fast pyrolysis of biomass and product upgrading," *Biomass and Bioenergy*, vol. 38, pp. 68–94, 2012.
- [18] A. V. Bridgwater, "Renewable fuels and chemicals by thermal processing of biomass," *Chem. Eng. J.*, vol. 91, no. 2–3, pp. 87–102, 2003.
- [19] P. Mckendry, "Energy production from biomass (part 2): conversion technologies," vol. 83, no. July 2001, pp. 47–54, 2002.
- [20] C. Higman and M. Van der Burgt, *Gasification*. 2003.
- [21] J. Coombs and K. Hall, "Chemicals and polymers from biomass," *Renew. Energy*, vol. 15, no. 98, pp. 54–59, 1998.
- [22] C. N. Hamelinck and a. P. C. Faaij, "Outlook for advanced biofuels," *Energy Policy*, vol. 34, no. 17, pp. 3268–3283, 2006.
- [23] J.-P. Lange, "Lignocellulose conversion: an introduction to chemistry, process and economics," *biofuels Bioprod. biorefining*, vol. 1, no. 1, pp. 39–48, 2007.
- [24] D. C. Elliott, "Catalytic hydrothermal gasification of biomass," *Biofuels, Bioprod. Biorefining*, vol. 2, no. 3, pp. 254–265, 2008.
- [25] M. Kleinert and T. Barth, "Towards a lignocellulosic biorefinery: Direct one-step conversion of lignin to hydrogen-enriched biofuel," *Energy and Fuels*, vol. 22, no. 2, pp. 1371–1379, 2008.
- [26] [Http://www.biosynergy.eu/](http://www.biosynergy.eu/), "BIOmass for the market competitive and environmentally friendly SYNthesis of bio-products together with the production of secondary enERGY carriers through the biorefinery approach.," 2007. .
- [27] P. de Wild and H. W. J. J., "Lignin pyrolysis for profitable lignocellulosic biorefineries," *Biofuels, Bioprod. Biorefining*, 2014.
- [28] L. Wang, Ø. Skreiberg, M. Gronli, G. P. Specht, and M. J. Antal Jr, "Is Elevated Pressure Required to Achieve a High Fixed-Carbon Yield of Charcoal from Biomass? Part 2: The Importance of Particle Size," *Energy & Fuels*, vol. 27, no. 4, pp. 2146–2156, 2013.
- [29] D. Vamvuka, "Bio-oil, solid and gaseous biofuels from biomass pyrolysis processes - An overview," *Int. J. energy Res.*, vol. 35, pp. 835–862, 2011.

- [30] A. Broido and M. A. Nelson, "Char yield on pyrolysis of cellulose," *Combust. Flame*, vol. 24, pp. 263–268, Feb. 1975.
- [31] A. G. W. Bradbury, Y. Sakai, and F. Shafizadeh, "A kinetic model for pyrolysis of cellulose," *J. Appl. Polym. Sci.*, vol. 23, no. 11, pp. 3271–3280, Jun. 1979.
- [32] W. S.-L. Mok and M. J. Antal, "Effects of pressure on biomass pyrolysis. II. Heats of reaction of cellulose pyrolysis," *Thermochimica Acta*, vol. 68, no. 2–3, pp. 165–186, 1983.
- [33] I. Milosavljevic, V. Oja, and E. M. Suuberg, "Thermal Effects in Cellulose Pyrolysis: Relationship to Char Formation Processes," *Ind. Eng. Chem. Res.*, vol. 35, no. 3, pp. 653–662, 1996.
- [34] I. Milosavljevic and E. M. Suuberg, "Cellulose thermal decomposition kinetics: Global mass loss kinetics," *Ind. Eng. Chem. Res.*, vol. 34, no. 4, pp. 1081–1091, 1995.
- [35] F. Shafizadeh, R. H. Furneaux, T. G. Cochran, J. P. Scholl, and Y. Sakai, "Production of levoglucosan and glucose from pyrolysis of cellulosic materials," *J. Appl. Polym. Sci.*, vol. 23, no. 12, pp. 3525–3539, Jun. 1979.
- [36] C. a Koufopoulos, N. Papayannakos, G. Maschio, and a Lucchesi, "Modelling of the Pyrolysis of Biomass Particles. Studies on Kineticcs, Thermal and Heat Transfer Effects," *The Canadian Journal of Chemical Engineering*, vol. 69, pp. 907–915, 1991.
- [37] C. Di Blasi, "Modeling chemical and physical processes of wood and biomass pyrolysis," *Prog. Energy Combust. Sci.*, vol. 34, no. 1, pp. 47–90, 2008.
- [38] C. Di Blasi, "Modeling intra- and extra-particle processes of wood fast pyrolysis," *Aiche J.*, vol. 48, no. 10, pp. 2386–2397, 2002.
- [39] C. Di Blasi, C. Branca, F. Masotta, and E. De Biase, "Experimental Analysis of Reaction Heat Effects during Beech Wood Pyrolysis," *Energy & Fuels*, vol. 27, no. 5, pp. 2665–2674, 2013.
- [40] B. . Babu and a. . Chaurasia, "Modeling for pyrolysis of solid particle: kinetics and heat transfer effects," *Energy Convers. Manag.*, vol. 44, no. 14, pp. 2251–2275, 2003.
- [41] B. V. Babu and a. S. Chaurasia, "Heat transfer and kinetics in the pyrolysis of shrinking biomass particle," *Chem. Eng. Sci.*, vol. 59, no. 10, pp. 1999–2012, 2004.
- [42] E. Ranzi, a Cuoci, T. Faravelli, a Frassoldati, G. Migliavacca, S. Pierucci, and S. Sommariva, "Chemical kinetics of biomass pyrolysis," *Energy and Fuels*, vol. 22, no. 6, pp. 4292–4300, 2008.
- [43] C. Dupont, L. Chen, J. Cances, J.-M. Commandre, A. Cuoci, S. Pierucci, and E. Ranzi, "Biomass pyrolysis: Kinetic modelling and experimental validation under high temperature and flash heating rate conditions," *J. Anal. Appl. Pyrolysis*, vol. 85, no. 1–2, pp. 260–267, 2009.
- [44] a.V. Bridgwater, D. Meier, and D. Radlein, "An overview of fast pyrolysis of biomass," *Org. Geochem.*, vol. 30, no. 12, pp. 1479–1493, 1999.
- [45] R. H. Venderbosch and W. Prins, "Fast pyrolysis technology development," *Biofuels, Bioprod. Biorefining*, vol. 4, pp. 178–208, 2010.

- [46] A. V. Bridgwater, "A survey of thermochemical biomass processing activities," *Biomass*, vol. 22, no. 1–4, pp. 279–292, Jan. 1990.
- [47] M. Tripathi, J. N. Sahu, and P. Ganesan, "Effect of process parameters on production of biochar from biomass waste through pyrolysis: A review," *Renew. Sustain. Energy Rev.*, vol. 55, pp. 467–481, Mar. 2016.
- [48] B. V. Babu and a. S. Chaurasia, "Parametric study of thermal and thermodynamic properties on pyrolysis of biomass in thermally thick regime," *Energy Convers. Manag.*, vol. 45, no. 1, pp. 53–72, 2004.
- [49] L. J. Curtis and D. J. Miller, "Transport model with radiative heat transfer for rapid cellulose pyrolysis," *Ind. Eng. Chem. Res.*, vol. 27, pp. 1775–1783, 1988.
- [50] T. Nunn and J. Howard, "Product compositions and kinetics in the rapid pyrolysis of sweet gum hardwood," ... *Process Des. ...*, pp. 836–844, 1985.
- [51] K. L. Lam, A. O. Oyedun, and C. W. Hui, "Experimental and modelling studies of biomass pyrolysis," *Chinese J. Chem. Eng.*, vol. 20, no. 3, pp. 543–550, 2012.
- [52] P. Ahuja, S. Kumar, and P. C. Singh, "A model for primary and heterogeneous secondary reactions of wood pyrolysis," *Chem. Eng. Technol.*, vol. 19, no. 3, pp. 272–282, 1996.
- [53] W. C. Park, A. Atreya, and H. R. Baum, "Experimental and theoretical investigation of heat and mass transfer processes during wood pyrolysis," *Combust. Flame*, vol. 157, no. 3, pp. 481–494, 2010.
- [54] R. K. Jalan and V. K. Srivastava, "Studies on pyrolysis of a single biomass cylindrical pellet—kinetic and heat transfer effects," *Energy Convers. Manag.*, vol. 40, no. 5, pp. 467–494, 1999.
- [55] A. K. Sadhukhan, P. Gupta, and R. K. Saha, "Modelling and experimental studies on pyrolysis of biomass particles," *J. Anal. Appl. Pyrolysis*, vol. 81, no. 2, pp. 183–192, 2008.
- [56] A. F. Roberts, "The Heat of Reaction During the Pyrolysis of Wood," *Combust. Flame*, vol. 17, pp. 79–86, 1971.
- [57] W.-C. R. Chan, M. Kelbon, and B. B. Krieger, "Modelling and experimental verification of physical and chemical processes during pyrolysis of a large biomass particle," *Fuel*, vol. 64, no. 11, pp. 1505–1513, Nov. 1985.
- [58] L. Wang, M. Trninic, Ø. Skreiberg, M. Gronli, R. Considine, and M. J. Antal, "Is Elevated Pressure Required To Achieve a High Fixed-Carbon Yield of Charcoal from Biomass? Part 1: Round-Robin Results for Three Different Corncob Materials," *Energy & Fuels*, vol. 25, no. 7, pp. 3251–3265, Jul. 2011.
- [59] J. A. HAVENS, H. T. HASHEMI, L. E. BROWN, and J. R. WELKER, "A Mathematical Model of the Thermal Decomposition of Wood," *Combust. Sci. Technol.*, vol. 5, no. 1, pp. 91–98, Mar. 1972.
- [60] R. Bilbao, J. F. Mastral, J. Ceamanos, and M. E. Aldea, "Modelling of the pyrolysis of wet wood," *J. Anal. Appl. Pyrolysis*, vol. 36, no. 1, pp. 81–97, 1996.

- [61] C. A. Koufopoulos, N. Papayannakos, G. Maschio, and A. Lucchesi, "Modelling of the pyrolysis of biomass particles. Studies on kinetics, thermal and heat transfer effects," *Can. J. Chem. Eng.*, vol. 69, no. 4, pp. 907–915, 1991.
- [62] A. F. Roberts, "Problems associated with the theoretical analysis of the burning of wood," *Symp. Combust.*, vol. 13, no. 1, pp. 893–903, 1971.
- [63] M. Sibulkin, "CALCULATIONS OF THE HEAT OF GASIFICATION OF CELLULOSE.," in *Chemical and Physical Processes in Combustion, Fall Technical Meeting, The Eastern States Section*, 1984.
- [64] M. Stenseng, a Jensen, and K. Dam-Johansen, "Investigation of biomass pyrolysis by thermogravimetric analysis and differential scanning calorimetry," *J. Anal. Appl. Pyrolysis*, vol. 58, pp. 765–780, 2001.
- [65] P. Borjesson, "Energy analysis of biomass production and transportation," *Biomass and Bioenergy*, vol. 11, no. 4, pp. 305–318, 1996.
- [66] S. Sokhansanj, A. Kumar, and A. F. Turhollow, "Development and implementation of integrated biomass supply analysis and logistics model (IBSAL)," *Biomass and Bioenergy*, vol. 30, no. 10, pp. 838–847, 2006.
- [67] a. V. Bridgwater, "Principles and practice of biomass fast pyrolysis processes for liquids," *J. Anal. Appl. Pyrolysis*, vol. 51, no. 1–2, pp. 3–22, 1999.
- [68] D. E. Dugaard and R. C. Brown, "Enthalpy for pyrolysis for several types of biomass," *Energy and Fuels*, vol. 17, no. 4, pp. 934–939, 2003.
- [69] W. S. L. Mok, M. J. Antal, P. Szabo, G. Varhegyi, and B. Zelei, "Formation of charcoal from biomass in a sealed reactor," *Ind. Eng. Chem. Res.*, vol. 31, no. 4, pp. 1162–1166, 1992.
- [70] M. G. Wolfinger, J. Rath, G. Krammer, F. Barontini, and V. Cozzani, "Influence of the emissivity of the sample on differential scanning calorimetry measurements," *Thermochim. Acta*, vol. 372, no. 1–2, pp. 11–18, 2001.
- [71] J. Rath, M. G. Wolfinger, G. Steiner, G. Krammer, F. Barontini, and V. Cozzani, "Heat of wood pyrolysis," *Fuel*, vol. 82, no. 1, pp. 81–91, 2003.
- [72] M. Gupta, J. Yang, and C. Roy, "Specific heat and thermal conductivity of softwood bark and softwood char particles," *Fuel*, vol. 82, no. 8, pp. 919–927, 2003.
- [73] G. Kaletunç, "Prediction of specific heat of cereal flours: A quantitative empirical correlation," *J. Food Eng.*, vol. 82, no. 4, pp. 589–594, 2007.
- [74] J. Raes, A. Rohde, J. H. Christensen, Y. Van De Peer, and W. Boerjan, "Genome-Wide Characterization of the Lignification Toolbox in Arabidopsis 1 [w]," vol. 133, no. November, pp. 1051–1071, 2014.
- [75] A. Ebringerová and T. Heinze, "Xylan and xylan derivatives - Biopolymers with valuable properties, 1: Naturally occurring xylylans structures, isolation procedures and properties," *Macromol. Rapid Commun.*, vol. 21, no. 9, pp. 542–556, 2000.

- [76] J. J. M. Orfão, F. J. a. Antunes, and J. L. Figueiredo, "Pyrolysis kinetics of lignocellulosic materials—three independent reactions model," *Fuel*, vol. 78, no. 3, pp. 349–358, 1999.
- [77] H. Yang, R. Yan, H. Chen, D. H. Lee, and C. Zheng, "Characteristics of hemicellulose, cellulose and lignin pyrolysis," *Fuel*, vol. 86, no. 12–13, pp. 1781–1788, 2007.
- [78] E. Karampinis, D. Vamvuka, S. Sfakiotakis, P. Grammelis, G. Itskos, and E. Kakaras, "Comparative Study of Combustion Properties of Five Energy Crops and Greek Lignite," *Energy & Fuels*, vol. 26, no. 2, pp. 869–878, 2012.
- [79] O. Senneca, R. Chirone, and P. Salatino, "A thermogravimetric study of nonfossil solid fuels. 2. Oxidative pyrolysis and char combustion," *Energy and Fuels*, vol. 16, no. 3, pp. 661–668, 2002.
- [80] L. Gašparovič, Z. Koreňová, and L. Jelemenský, "Kinetic study of wood chips decomposition by TGA," *Chem. Pap.*, vol. 64, no. 2, pp. 174–181, 2010.
- [81] H. P. Anthony, D.B., Howard, J.B., Hottel, H.C., Meissner, "Rapid devolatilization and hydrogasification of bituminous coal," *Fuel*, vol. 5, no. 2, pp. 121–128, 1976.
- [82] C. Gomez, E. Velo, F. Barontini, and V. Cozzani, "Influence of Secondary Reactions on the Heat of Pyrolysis of Biomass," *Ind. Eng. Chem. Res.*, vol. 48, no. 23, pp. 10222–10233, 2009.
- [83] K. Papadikis, S. Gu, and a. V. Bridgwater, "Computational modelling of the impact of particle size to the heat transfer coefficient between biomass particles and a fluidised bed," *Fuel Process. Technol.*, vol. 91, no. 1, pp. 68–79, 2010.
- [84] M. J. Antal and M. Grønli, "The Art, Science, and Technology of Charcoal Production," *Ind. Eng. Chem. Res.*, vol. 42, no. 8, pp. 1619–1640, 2003.
- [85] C. Di Blasi, C. Branca, A. Galgano, and P. D'Agostino, "Thermal Behavior of Beech Wood during Sulfuric Acid Catalyzed Pyrolysis," *Energy & Fuels*, vol. 29, no. 10, pp. 6476–6484, 2015.
- [86] V. Strezov, B. Moghtaderi, and J. a. Lucas, "Computational calorimetric investigation of the reactions during thermal conversion of wood biomass," *Biomass and Bioenergy*, vol. 27, no. 5, pp. 459–465, 2004.
- [87] C. Di Blasi, C. Branca, F. E. Sarnataro, and A. Gallo, "Thermal runaway in the pyrolysis of some lignocellulosic biomasses," *Energy and Fuels*, vol. 28, no. 4, pp. 2684–2696, 2014.
- [88] C. Di Blasi, C. Branca, A. Santoro, and E. Gonzalez Hernandez, "Pyrolytic behavior and products of some wood varieties," *Combust. Flame*, vol. 124, no. 1–2, pp. 165–177, 2001.
- [89] W. S.-L. Mok and M. J. Antal Jr, "Effects of pressure on biomass pyrolysis. I. Cellulose pyrolysis products," *Thermochim. Acta*, vol. 68, pp. 155–164, 1983.
- [90] C. Branca, C. Di Blasi, and R. Elefante, "Devolatilization and heterogeneous combustion of wood fast pyrolysis oils," *Ind. Eng. Chem. Res.*, vol. 44, no. 4, pp. 799–810, 2005.
- [91] H. Bennadji, K. Smith, S. Shabangu, and E. M. Fisher, "Low-Temperature Pyrolysis of Woody Biomass in the Thermally Thick Regime," *Energy & Fuels*, vol. 27, no. 3, pp. 1453–1459, 2013.

- [92] M. Pérez, M. Granda, R. Santamaría, T. Morgan, and R. Menéndez, "A thermoanalytical study of the co-pyrolysis of coal-tar pitch and petroleum pitch," *Fuel*, vol. 83, no. 9, pp. 1257–1265, 2004.
- [93] P. Morf, P. Hasler, and T. Nussbaumer, "Mechanisms and kinetics of homogeneous secondary reactions of tar from continuous pyrolysis of wood chips," *Fuel*, vol. 81, no. 7, pp. 843–853, 2002.
- [94] V. Seebauer, J. Petek, and G. Staudinger, "Effects of particle size, heating rate and pressure on measurement of pyrolysis kinetics by thermogravimetric analysis," *Fuel*, vol. 76, no. 13, pp. 1277–1282, 1997.
- [95] P. T. Williams and S. Besler, "The influence of temperature and heating rate on the slow pyrolysis of biomass," *Renew. Energy*, vol. 7, no. 3, pp. 233–250, 1996.
- [96] Y. Haseli, J. a. van Oijen, and L. P. H. de Goey, "Modeling biomass particle pyrolysis with temperature-dependent heat of reactions," *J. Anal. Appl. Pyrolysis*, vol. 90, no. 2, pp. 140–154, 2011.
- [97] X. Xu, Y. Matsumura, J. Stenberg, and J. M. Antal, "Carbon-catalyzed gasification of organic feedstock in supercritical water.," *Ind. Eng. Chem. Res.*, vol. 35, pp. 2522–2530, 1996.
- [98] P. Brandt, E. Larsen, and U. Henriksen, "High tar reduction in a two-stage gasifier," *Energy and Fuels*, vol. 14, no. 4, pp. 816–819, 2000.
- [99] M. HAJALIGOL, J. HOWARD, and W. PETERS, "An experimental and modeling study of pressure effects on tar release by rapid pyrolysis of cellulose sheets in a screen heater☆," *Combust. Flame*, vol. 95, no. 1–2, pp. 47–60, Oct. 1993.
- [100] M. Van de Velden, J. Baeyens, A. Brems, B. Janssens, and R. Dewil, "Fundamentals, kinetics and endothermicity of the biomass pyrolysis reaction," *Renew. Energy*, vol. 35, no. 1, pp. 232–242, 2010.
- [101] M. J. Antal, "Cellulose Pyrolysis Kinetics : The Current State of Knowledge," *Ind. Eng. Chem. Res.*, vol. 34, no. 3, pp. 703–717, 1995.
- [102] G. Várhegyi, P. Szabó, W. S.-L. Mok, and M. J. Antal, "Kinetics of the thermal decomposition of cellulose in sealed vessels at elevated pressures. Effects of the presence of water on the reaction mechanism," *Journal of Analytical and Applied Pyrolysis*, vol. 26, no. 3, pp. 159–174, 1993.
- [103] M. J. Antal Jr, S. G. Allen, X. Dai, B. Shimizu, M. S. Tam, and M. Grønli, "Attainment of the Theoretical Yield of Carbon from Biomass," *Ind. Eng. Chem. Res.*, vol. 39, no. 11, pp. 4024–4031, 2000.
- [104] <https://www.ecn.nl/phyllis2/>, "Database for biomass and waste." .
- [105] S. Bergamini, "Analysis of the heat of reaction of biomass pyrolysis.," University of Bologna, 2013.
- [106] L. Burhenne, J. Messmer, T. Aicher, and M.-P. Laborie, "The effect of the biomass components lignin, cellulose and hemicellulose on TGA and fixed bed pyrolysis," *J. Anal. Appl. Pyrolysis*, vol. 101, pp. 177–184, 2013.

- [107] K. Raveendran, "Pyrolysis characteristics of biomass and biomass components," *Fuel*, vol. 75, no. 8, pp. 987–998, 1996.
- [108] H. Yang, R. Yan, H. Chen, C. Zheng, D. H. Lee, and D. T. Liang, "In-Depth Investigation of biomass pyrolysis based on three major components: Hemicellulose, cellulose, and lignin," *Energy & Fuels*, vol. 20, no. 1, pp. 388–393, 2006.
- [109] R. B. Santos, P. W. Hart, H. Jameel, and H. M. Chang, "Wood Based Lignin Reactions Important to the Biorefinery and Pulp and Paper Industries," *BioResources*, vol. 8, no. 1, pp. 1456–1477, 2013.
- [110] V. I. Sharypov, N. Marin, N. G. Beregovtsova, S. V. Baryshnikov, B. N. Kuznetsov, V. L. Cebolla, and J. V. Weber, "Co-pyrolysis of wood biomass and synthetic polymer mixtures. Part I: influence of experimental conditions on the evolution of solids, liquids and gases," *J. Anal. Appl. Pyrolysis*, vol. 64, no. 1, pp. 15–28, Jul. 2002.
- [111] A. Demirbas, "Effects of temperature and particle size on bio-char yield from pyrolysis of agricultural residues," *J. Anal. Appl. Pyrolysis*, vol. 72, no. 2, pp. 243–248, 2004.
- [112] D. Lv, M. Xu, X. Liu, Z. Zhan, Z. Li, and H. Yao, "Effect of cellulose, lignin, alkali and alkaline earth metallic species on biomass pyrolysis and gasification," *Fuel Process. Technol.*, vol. 91, no. 8, pp. 903–909, 2010.
- [113] M. G. Grønli, G. Várhegyi, and C. Di Blasi, "Thermogravimetric Analysis and Devolatilization Kinetics of Wood," *Ind. Eng. Chem. Res.*, vol. 41, no. 17, pp. 4201–4208, 2002.
- [114] T. R. Rao and A. Sharma, "Pyrolysis rates of biomass materials," *Energy*, vol. 23, no. 11, pp. 973–978, 1998.
- [115] P. Giudicianni, G. Cardone, and R. Ragucci, "Cellulose, hemicellulose and lignin slow steam pyrolysis: Thermal decomposition of biomass components mixtures," *J. Anal. Appl. Pyrolysis*, vol. 100, pp. 213–222, 2013.
- [116] Ramiah Mv, "Thermogravimetric and Differential Thermal Analysis of Cellulose, Hemicellulose, and Lignin," *Journal of Applied Polymer Science*, vol. 14, no. 5, pp. 1323–1337, 1970.
- [117] R. Ball, A. C. McIntosh, and J. Brindley, "Feedback processes in cellulose thermal decomposition: implications for fire-retarding strategies and treatments," *Combust. Theory Model.*, vol. 8, no. 2, pp. 281–291, Jun. 2004.
- [118] T. Fisher, M. Hajaligol, B. Waymack, and D. Kellogg, "Pyrolysis behavior and kinetics of biomass derived materials," *J. Anal. Appl. Pyrolysis*, vol. 62, pp. 331–349, 2002.
- [119] V. Strezov, B. Moghtaderi, and J. a Lucas, "Thermal study of decomposition of selected biomass samples.," *J. Therm. Anal. Calorim.*, vol. 72, no. 3, pp. 1041–1048, 2003.
- [120] Q. Chen, R. Yang, B. Zhao, Y. Li, S. Wang, H. Wu, Y. Zhuo, and C. Chen, "Investigation of heat of biomass pyrolysis and secondary reactions by simultaneous thermogravimetry and differential scanning calorimetry," *Fuel*, vol. 134, pp. 467–476, 2014.

- [121] W. Blackadder and E. Rensfelt, "Pressurized thermo balance for pyrolysis and gasification studies of biomass wood and peat," *Fundam. Thermochem Biomass Convers*, vol. 747, 1985.
- [122] J. Richard and M. J. Antal Jr, "Thermogravimetric studies of charcoal formation from cellulose at elevated pressures," *Adv Thermochem Biomass Convers*, vol. 784, 1994.
- [123] R. Narayan and M. J. Antal, "Thermal Lag, Fusion, and the Compensation Effect during Biomass Pyrolysis," *Ind. Eng. Chem. Res.*, vol. 35, no. 5, pp. 1711–1721, 1996.
- [124] M. G. Gronli, M. C. Melaaen, M. Grønli, and M. C. Melaaen, "Mathematical model for wood pyrolysis - Comparison of experimental measurements with model predictions," *Energy & Fuels*, vol. 14, no. 4, pp. 791–800, 2000.
- [125] J. Piskorz, P. Majerski, D. Radlein, and D. S. Scott, "Conversion of lignins to hydrocarbon fuels," *Energy Fuels*, vol. 3, no. 6, pp. 723–726, 1989.
- [126] T. Hosoya, H. Kawamoto, and S. Saka, "Cellulose-hemicellulose and cellulose-lignin interactions in wood pyrolysis at gasification temperature," *J. Anal. Appl. Pyrolysis*, vol. 80, no. 1, pp. 118–125, 2007.
- [127] M. J. Antal Jr, "Mathematical modelling of biomass pyrolysis phenomena.pdf," *Fuel*, vol. 64, pp. 1484–1486, 1985.
- [128] K. Słopiecka, P. Bartocci, and F. Fantozzi, "Thermogravimetric analysis and kinetic study of poplar wood pyrolysis," *Appl. Energy*, vol. 97, pp. 491–497, 2012.
- [129] B. F. C. Beal, "Differential Calometric Analysis of Wood and Wood Components," *Wood Sci. Technol.*, vol. 5, pp. 159–175, 1971.
- [130] T. Hosoya, H. Kawamoto, and S. Saka, "Different pyrolytic pathways of levoglucosan in vapor- and liquid/solid-phases," *J. Anal. Appl. Pyrolysis*, vol. 83, no. 1, pp. 64–70, 2008.
- [131] D. J. Nowakowski, a. V. Bridgwater, D. C. Elliott, D. Meier, and P. de Wild, "Lignin fast pyrolysis: Results from an international collaboration," *J. Anal. Appl. Pyrolysis*, vol. 88, no. 1, pp. 53–72, 2010.
- [132] M. P. Pandey and C. S. Kim, "Lignin Depolymerization and Conversion: A Review of Thermochemical Methods," *Chem. Eng. Technol.*, vol. 34, no. 1, pp. 29–41, 2011.
- [133] W. Mu, H. Ben, A. Ragauskas, and Y. Deng, "Lignin Pyrolysis Components and Upgrading—Technology Review," *BioEnergy Res.*, vol. 6, no. 4, pp. 1183–1204, 2013.
- [134] J. A. Caballero, R. Font, and A. Marcilla, "Pyrolysis of Kraft lignin: yields and correlations," *J. Anal. Appl. Pyrolysis*, vol. 39, no. 2, pp. 161–183, Feb. 1997.
- [135] D. Ferdous, a. K. Dalai, S. K. Bej, and R. W. Thring, "Pyrolysis of lignins: Experimental and kinetics studies," *Energy and Fuels*, vol. 16, no. 6, pp. 1405–1412, 2002.

- [136] T. R. Nunn, J. B. Howard, J. P. Longwell, and W. A. Peters, "Product compositions and kinetics in the rapid pyrolysis of milled wood lignin," *Ind. Eng. Chem. Process Des. Dev.*, vol. 24, no. 3, pp. 844–852, 1985.
- [137] K. G. Kalogiannis, S. D. Stefanidis, C. M. Michailof, A. a Lappas, and E. Sjöholm, "Pyrolysis of lignin with 2DGC quantification of lignin oil: Effect of lignin type, process temperature and ZSM-5 in situ upgrading," *J. Anal. Appl. Pyrolysis*, vol. 115, pp. 410–418, 2015.
- [138] J. M. Bouvier, M. Gelus, and S. Maugendre, "Wood liquefaction—An overview," *Appl. Energy*, vol. 30, no. 2, pp. 85–98, Jan. 1988.
- [139] F. Behrendt, Y. Neubauer, M. Oevermann, B. Wilmes, and N. Zobel, "Direct Liquefaction of Biomass," *Chem. Eng. Technol.*, vol. 31, no. 5, pp. 667–677, 2008.
- [140] Y. Solantausta, D. Beckman, A. V. Bridgwater, J. P. Diebold, and D. C. Elliott, "Assessment of liquefaction and pyrolysis systems," *Biomass and Bioenergy*, vol. 2, no. 1–6, pp. 279–297, 1992.
- [141] G. van Rossum, W. Zhao, M. Castellvi Barnes, J.-P. Lange, and S. R. a. Kersten, "Liquefaction of Lignocellulosic Biomass: Solvent, Process Parameter, and Recycle Oil Screening," *ChemSusChem*, vol. 7, no. 1, pp. 253–259, 2014.
- [142] S. Kumar, J. Lange, G. Van Rossum, and S. R. a Kersten, "Liquefaction of Lignocellulose: Process Parameter Study To Minimize Heavy Ends," *Ind. Eng. Chem. Res.*, vol. 53, p. 11668–11676, 2014.
- [143] T. Funazukuri, N. Wakao, and J. M. Smith, "Liquefaction of lignin sulphonate with subcritical and supercritical water," *Fuel*, vol. 69, no. 3, pp. 349–353, 1990.
- [144] U. Schuchardt, J. A. R. Rodrigues, A. Cotrim, and J. L. M. Costa, "Liquefaction of hydrolytic eucalyptus lignin with formate in water, using batch and continuous-flow reactors," *Bioresour. Technol.*, vol. 44, no. 2, pp. 123–129, 1993.
- [145] S. Kumar, J.-P. Lange, G. Van Rossum, and S. R. a. Kersten, "Liquefaction of lignocellulose: Do basic and acidic additives help out?," *Chem. Eng. J.*, vol. 278, pp. 99–104, 2015.